

2019

Scheduling for Cooperative Energy Harvesting Sensor Networks

Ahmed Ammar
aabuseta@mix.wvu.edu

Follow this and additional works at: <https://researchrepository.wvu.edu/etd>



Part of the [Systems and Communications Commons](#)

Recommended Citation

Ammar, Ahmed, "Scheduling for Cooperative Energy Harvesting Sensor Networks" (2019). *Graduate Theses, Dissertations, and Problem Reports*. 4074.
<https://researchrepository.wvu.edu/etd/4074>

This Dissertation is protected by copyright and/or related rights. It has been brought to you by the The Research Repository @ WVU with permission from the rights-holder(s). You are free to use this Dissertation in any way that is permitted by the copyright and related rights legislation that applies to your use. For other uses you must obtain permission from the rights-holder(s) directly, unless additional rights are indicated by a Creative Commons license in the record and/ or on the work itself. This Dissertation has been accepted for inclusion in WVU Graduate Theses, Dissertations, and Problem Reports collection by an authorized administrator of The Research Repository @ WVU. For more information, please contact researchrepository@mail.wvu.edu.

Scheduling for Cooperative Energy Harvesting Sensor Networks

Ahmed M. Abuseta Ammar

Dissertation submitted to the
Benjamin M. Statler College of Engineering and Mineral Resources
at West Virginia University
in partial fulfillment of the requirements
for the degree of

Doctor of Philosophy
in
Electrical Engineering

Daryl S. Reynolds, Ph.D., Chair
Matthew C. Valenti, Ph.D.
Natalia A. Schmid, Ph.D.
Vinod K. Kulathumani, Ph.D.
Erdogan Gunel, Ph.D.

Lane Department of Computer Science and Electrical Engineering

Morgantown, West Virginia
2017

Keywords: wireless sensor networks, energy harvesting, scheduling, throughput
maximization

Copyright 2017 Ahmed M. Abuseta Ammar

Abstract

Scheduling for Cooperative Energy Harvesting Sensor Networks

Ahmed M. Abuseta Ammar

In cooperative communication networks, the source node transmits its data to the destination either directly or cooperatively with a cooperating node. When using energy harvesting technology, where nodes collect their energy from the environment, the energy availability at the nodes becomes unpredictable due to the stochastic nature of energy harvesting processes. As a result, when the source has a transmission, it cannot immediately transmit its data cooperatively with the cooperating node. It first needs to determine whether the cooperating node has sufficient energy to forward its transmission or not. Otherwise, its transmitted data may get lost. Therefore, when using energy harvesting, the challenge is for the source to schedule its transmissions whether directly or cooperatively, such that the fraction of its events (sensed data) that are successfully reported to the destination is maximized.

Hence, in this dissertation, we address the problem of cooperating node scheduling in energy harvesting sensor networks. We consider the problem for the case of a single cooperating node and the case of multiple cooperating nodes, as well as the scenarios of one-way and two-way cooperative communications. We propose a simple scheduling scheme, called feedback scheme, which enables the source to optimally schedule its transmissions whether directly or cooperatively. We show that the feedback scheme maximizes the system performance, but does not require auxiliary parameter optimization as does the state-of-the-art scheme, i.e., the threshold-based scheme. However, the feedback scheme has the problem of overhead caused by transmitting the energy status of the cooperating node to the source. To overcome this burden, we introduce a statistical model that enables the source to estimate the energy status of the cooperating node. Because cooperation may result in the cooperating node performing worse than the source, we address this problem through fairness in the performance between the nodes in the network. In addition, we address the problem of scheduling for throughput maximization in a wireless energy harvesting uplink. We propose centralized and distributed algorithms that find the optimal solution, and we address complexity issues. Our algorithms are shown to have a linear or quadratic complexity compared to the exponential complexity of the brute force approach. Compared with cooperative transmission, our approach maximizes the network throughput such that no node's throughput is adversely affected.

Acknowledgments

My sincere gratitude to all those who participated and shared their ideas in this work to make it possible.

First of all, I offer my sincerest gratitude to my dissertation committee chairman and advisor, Dr. Daryl Reynolds, who gave me the opportunity to work under his supervision throughout my academic journey including my Masters and Ph.D. I would like to thank him for his patience, support, knowledge, encouragement, and effort that made this dissertation happen, and made me reach this level of my education. I would also like to thank him for all the skills that I gained and upgraded under his supervision.

I am very grateful to my committee members Dr. Matthew C. Valenti, Dr. Natalia A. Schmid, Dr. Vinod K. Kulathumani, and Dr. Erdogan Gunel. Special thanks go to Dr. Matthew C. Valenti and Dr. Natalia A. Schmid who were also members of my Masters committee, and I would like to thank them and Dr. Vinod K. Kulathumani for all the knowledge that I gained from their classes that helped me in my research. My sincere thanks to Dr. Erdogan Gunel who agreed to serve on my committee in our first meeting.

I would like to dedicate this work to my father and mother to whom I owe my success after Allah. I am thankful and grateful to them for their patience, love, compassion, and support throughout my life.

Contents

Acknowledgments	iii
List of Figures	vi
List of Tables	ix
1 Introduction	1
1.1 Overview	1
1.2 Literature Review	5
1.2.1 Energy Harvesting Sensor Networks	5
1.2.2 Cooperative Energy Harvesting Sensor Networks	6
2 Single Cooperating Node Scheduling	10
2.1 Introduction	10
2.2 System Model	11
2.3 Feedback Scheduling Scheme	14
2.4 Simulation Results	16
2.4.1 Performance Evaluation	17
2.4.2 Cooperating Node Priority Condition	18
2.4.3 Threshold-based Scheme Sensitivity	19
2.5 Conclusions	20
3 Multiple Cooperating Nodes Scheduling	22
3.1 Introduction	22
3.2 System Model	23
3.3 Scheduling Algorithm	25
3.4 Adaptive Scheme for Absolute Fairness	28
3.5 Simulation results	30
3.5.1 One-Way Cooperative Scenario	30
3.5.2 Two-Way Cooperative Scenario	31
3.5.3 Overhead Reduction	33
3.5.4 Fairness	34
3.6 Conclusions	35

4	Generalized Fairness and Optimal Scheduling	38
4.1	Introduction	38
4.2	System Model	39
4.3	Operating Modes	42
4.3.1	Noncooperation Mode	42
4.3.2	Cooperation Mode	43
4.3.3	Relay mode	47
4.3.4	Mixed mode	49
4.4	Scheduling Schemes	50
4.4.1	Fair Scheduling (FS) Scheme	50
4.4.2	Constrained Scheduling (CS) Scheme	55
4.5	Simulation Results	56
4.5.1	Fairness	57
4.5.2	Constrained Scheduling	59
4.6	Conclusions	59
5	Scheduling with Energy Status Estimation	61
5.1	Introduction	61
5.2	Cooperation Mode Statistical Model	62
5.3	Relay Mode Statistical Model	66
5.4	Simulation Results	66
5.4.1	Cooperation and relay modes (independent case)	67
5.4.2	Cooperation and relay modes (correlated case)	68
5.4.3	FS and CS schemes	69
5.5	Conclusions	71
6	Scheduling for Throughput Maximization	72
6.1	Introduction	72
6.2	System Model	74
6.3	Successful transmission probability Characterization	76
6.4	Problem Formulation	77
6.5	A brute force approach	79
6.6	Centralized Algorithm	80
6.7	Distributed Algorithm	84
6.8	Variable Transmit Power	88
6.9	Simulation Results	89
6.9.1	Fixed Transmit Power	92
6.9.2	Variable Transmit Power	92
6.9.3	Comparison with Cooperative Transmission	94
6.10	Conclusions	95
7	Summary and Future Work	96
7.1	Summary	96
7.2	Future Work	98
	References	101

List of Figures

2.1	A three-node network with an energy harvesting source N_1 , an energy harvesting cooperating node N_2 , and a destination. E_1 and E_2 are queues representing the energy harvested by N_1 and N_2 , respectively, in the n -th time block, $n \in \{1, 2, \dots, N\}$. A is the latest energy status of the cooperating node N_2	11
2.2	A state diagram of the two-state Markov process that models the event generation process of node $N_i, i \in \{1, 2\}$ with transition probabilities q_i^{on} and q_i^{off} . The energy generation process is modeled the same but with transition probabilities p_i^{on} and p_i^{off}	12
2.3	Two flowcharts illustrate the feedback and the threshold-based schemes to easily notice the difference between them.	16
2.4	The overall, the cooperating node, and the source packet delivery ratios of the feedback and the threshold-based schemes. Parameters used: $q_1^{\text{on}} = 0.9$, $q_1^{\text{off}} = 0.7$, $p_1^{\text{on}} = q_2^{\text{on}} = 0.85$, $p_1^{\text{off}} = q_2^{\text{off}} = 0.7$, $E_1 = E_2 = 1$, $\delta_1 = \delta_2 = 3$, $\tilde{\delta}_1 = \tilde{\delta}_2 = 1$, $K = 20$, $T_H = 10$	17
2.5	The overall, the cooperating node, and the source packet delivery ratios of the feedback scheme with both the source and the cooperating node priority conditions. Parameters used: $q_1^{\text{on}} = 0.9$, $q_1^{\text{off}} = 0.7$, $p_1^{\text{on}} = q_2^{\text{on}} = 0.85$, $p_1^{\text{off}} = q_2^{\text{off}} = 0.7$, $E_1 = E_2 = 1$, $\delta_1 = \delta_2 = 3$, $\tilde{\delta}_1 = \tilde{\delta}_2 = 1$, $K = 20$, $T_H = 10$	18
2.6	The overall, the cooperating node, and the source packet delivery ratios of the feedback and the threshold-based schemes when changing one of the parameters. Parameters used: $q_1^{\text{on}} = 0.9$, $q_1^{\text{off}} = 0.7$, $p_1^{\text{on}} = q_2^{\text{on}} = 0.85$, $p_1^{\text{off}} = q_2^{\text{off}} = 0.7$, $E_1 = E_2 = 1$, $\delta_1 = 3$, $\delta_2 = \tilde{\delta}_1 = \tilde{\delta}_2 = 1$, $K = 20$, $T_H = 10$	19
3.1	Energy harvesting sensor network of $M - 2$ cooperating nodes that assist cooperative communication between two sensors (N_1, N_2). Each node $N_m, m \in \{1, 2, \dots, M\}$ harvests E_m amount of energy if its energy generation process is “on”. Each node has a memory of $M - 2$ slots to save the latest status, $A_m, m \in \{3, 4, \dots, M\}$, of the cooperating node N_m as either 1 or 0 in the corresponding m -th slot.	23
3.2	A flowchart illustrates the feedback scheme for the case of multiple cooperating nodes when the cooperating node of the highest index is selected for relay transmission.	27

- 3.3 The packet delivery ratios of the one-way scenario when $M = 3$ and $M = 4$. Parameters used: $q_1^{\text{on}} = 0.9$, $q_1^{\text{off}} = 0.7$, $p_1^{\text{on}} = q_3^{\text{on}} = 0.85$, $p_1^{\text{off}} = q_3^{\text{off}} = 0.7$, $E_1 = E_3 = 1$, $\delta_1 = \delta_3 = 3$, $\tilde{\delta}_1 = \tilde{\delta}_3 = 1$, $K = 20$ 30
- 3.4 The packet delivery ratios of the one-way and two-way scenarios when $M = 3$. Parameters used: $q_1^{\text{on}} = 0.9$, $q_1^{\text{off}} = 0.7$, $p_1^{\text{on}} = q_3^{\text{on}} = 0.85$, $p_1^{\text{off}} = q_3^{\text{off}} = 0.7$, $E_1 = E_3 = 1$, $\delta_1 = \delta_3 = 3$, $\tilde{\delta}_1 = \tilde{\delta}_3 = 1$, $K = 20$ 31
- 3.5 The packet delivery ratios of the one-way and two-way scenarios when $M = 4$. Parameters used: $q_1^{\text{on}} = 0.9$, $q_1^{\text{off}} = 0.7$, $p_1^{\text{on}} = q_3^{\text{on}} = 0.85$, $p_1^{\text{off}} = q_3^{\text{off}} = 0.7$, $E_1 = E_3 = 1$, $\delta_1 = \delta_3 = 3$, $\tilde{\delta}_1 = \tilde{\delta}_3 = 1$, $K = 20$ 32
- 3.6 The number of status transmissions of the standard and adaptive status broadcastings for the one-way scenario when $M = 3$. Parameters used: $q_1^{\text{on}} = 0.9$, $q_1^{\text{off}} = 0.7$, $p_1^{\text{on}} = q_3^{\text{on}} = 0.85$, $p_1^{\text{off}} = q_3^{\text{off}} = 0.7$, $E_1 = E_3 = 1$, $\delta_1 = \delta_3 = 3$, $\tilde{\delta}_1 = \tilde{\delta}_3 = 1$, $K = 20$ 33
- 3.7 The packet delivery ratios of the two ways of cooperating nodes selection (selecting the node of the highest index and selecting the nodes sequentially) for the one-way scenario when $M = 4$. Parameters used: $q_1^{\text{on}} = 0.9$, $q_1^{\text{off}} = 0.7$, $p_1^{\text{on}} = q_3^{\text{on}} = 0.85$, $p_1^{\text{off}} = q_3^{\text{off}} = 0.7$, $E_1 = E_3 = 1$, $\delta_1 = \delta_3 = 3$, $\tilde{\delta}_1 = \tilde{\delta}_3 = 1$, $K = 20$ 35
- 3.8 The convergence of the packet delivery ratios for the one-way and two-way scenarios when $M = 3$. Parameters used: $q_1^{\text{on}} = q_3^{\text{on}} = 1$, $q_1^{\text{off}} = q_3^{\text{off}} = 0$, $p_1^{\text{on}} = 0.85$, $p_3^{\text{on}} = 0.95$, $p_3^{\text{off}} = 0.55$, $p_1^{\text{off}} = 0.7$, $E_1 = E_3 = 1$, $\delta_1 = 3$, $\tilde{\delta}_1 = \tilde{\delta}_3 = \delta_3 = 1$, $K = 20$ 36
- 4.1 A cooperative energy harvesting sensor network of two transmitting nodes (N_1 and N_2) and a destination. E_1 and E_2 are queues representing the energy harvested by N_1 and N_2 , respectively, in the n -th time block, $n \in \{1, 2, \dots, N\}$. 39
- 4.2 The figure illustrates the noncooperation, cooperation, and relay modes, which are used in appropriate combinations to build the FS and CS scheduling schemes. The solid line between S_1 , S_2 , or cooperating node and destination represents the direct transmission of the event of that node to the destination. The dashed path in the cooperation and relay modes represents the relay transmission of S_2 to the destination using cooperating and relay nodes, respectively. In the relay mode, there is no solid line between the relay node and the destination because the relay node has no own transmissions where it drops all its transmissions to help with S_2 transmissions. 40
- 4.3 The packet delivery ratios of N_1 and N_2 in noncooperation mode. Parameters used: $q_1 = 0.5$, $q_2 = 0.4$, $\tilde{\delta} = 1$, $\delta_1 = \delta_2 = 2$, $\tilde{K} = 1$, $K = 100$, $N = 5 \times 10^5$. . . 57
- 4.4 Figures (a) and (b) illustrate the optimal x and n provided by the FS scheme when $\alpha = 1$. Figure (c) shows the optimal performance of N_1 and N_2 by which fairness is considered achieved for the given penalty function. 58
- 4.5 Figures (a) and (b) illustrate the optimal x and n provided by the FS scheme when $\alpha = 3$. Figure (c) shows the optimal performance of N_1 and N_2 by which fairness is considered achieved for the given penalty function. 58

4.6	Figures (a) and (b) illustrate the optimal x and n provided by the FS scheme when $\alpha = 5$. Figure (c) shows the optimal performance of N_1 and N_2 by which fairness is considered achieved for the given penalty function.	59
4.7	Figures (a) and (b) illustrate the optimal x and n provided by the CS scheme in order for node N_1 to achieve the performance $\gamma = 0.7$. Figure (c) shows that node N_1 achieves the performance γ over the values $\overline{E_1}$ and $\overline{E_2}$ where the system is feasible.	60
5.1	Figures (a) and (b) show the performance of N_1 in the cooperation and relay modes using the statistical models compared with the feedback scheme. Figure (c) shows the number of energy status transmissions of N_2 over the N time blocks.	67
5.2	Figures (a) and (b) show the packet delivery ratio of N_1 versus correlation coefficient ρ for the cooperation and relay modes, respectively, using the statistical models compared with the feedback scheme.	68
5.3	Figures (a) and (b) show the packet delivery ratios of N_1 and N_2 , respectively, for the FS scheme when using the statistical models compared with the feedback scheme. We used the same penalty function in Section VI (A) with $\alpha = 3$	69
5.4	Figures (a) and (b) illustrate the optimal x and n provided by the CS scheme using the statistical models in order for node N_1 to achieve the performance $\gamma = 0.7$. Figure (c) shows that node N_1 achieves the performance γ over the values $\overline{E_1}$ and $\overline{E_2}$ where the system is feasible.	70
6.1	A network consists three categories of sensor nodes; type S_1 node which transmits directly to the base station, type S_2 node which transmits to the base station through another node called cooperating node, and cooperating node which transmits its own events as well as it forwards some type S_2 nodes' events to the base station.	73
6.2	Successful transmission probability $\tau_i(q_i, \delta_i, \mathbf{p}_i)$ of node $i \in \mathcal{N}$ versus q_i for different values of δ_i and K , and for $\mathbf{p}_i = [0.3 \ 0.7]$	76
6.3	The number of all possible combinations increases exponentially with M	80
6.4	Figure (a) shows the network throughput for all the scenarios shown in Table 6.1. Figure (b) shows the successful transmission probability of N_1 , N_2 , and N_3 . Parameters used: $q_1 = q_2 = q_3 = 0.2$, $\mathbf{p}_1 = \mathbf{p}_2 = [0.2 \ 0.8]$, $\mathbf{p}_3 = [0.8 \ 0.2]$, $\tilde{K} = 1$, $K = 100$, $N = 10^5$, $\delta_1 = \delta_2 = \delta_3 = 2$, $\tilde{\delta} = 1$	91
6.5	Figure (a) shows the network throughput for all the scenarios shown in Table 6.1. Figure (b) shows the successful transmission probability of N_1 , N_2 , and N_3 . Parameters used: $q_1 = q_2 = q_3 = 0.2$, $\mathbf{p}_1 = \mathbf{p}_2 = \mathbf{p}_3 = [0.2 \ 0.8]$, $\tilde{K} = 1$, $K = 100$, $N = 10^5$, $\delta_1 = \delta_2 = \delta_3 = 2$, $\tilde{\delta} = 1$	91
6.6	The network throughput for each scenario shown in Table 6.1 when the transmit power is variable and fixed. Parameters used: $q_1 = 0.2$, $q_2 = 0.8$, $q_3 = 0.2$, $\mathbf{p}_1 = [0.025 \ 0.025 \ 0.025 \ 0.025 \ 0.1 \ 0.8]$, $\mathbf{p}_2 = [0.2 \ 0.3 \ 0.3 \ 0.2 \ 0 \ 0]$, $\mathbf{p}_3 = [0.1 \ 0.1 \ 0.2 \ 0.3 \ 0.3 \ 0]$, $\tilde{K} = 5$, $K = 100$, $N = 10^5$, $\delta_1 = \delta_2 = \delta_3 = 6$, $\delta_{1,2} = 2$, $\delta_{1,3} = 4$, $\delta_{2,3} = 1$	93

List of Tables

6.1 All Possible Scenarios of the Network	90
---	----

Chapter 1

Introduction

1.1 Overview

Wireless sensor networks have been widely used for different applications including surveillance and monitoring, medical, and emergency applications [1]. Commonly, these applications use sensors that are powered by small size batteries so that they become energy-limited. One general approach to improving energy efficiency in sensor network applications is cooperative communications, in which source node's packets are sent to the destination through direct paths and through relays/cooperating nodes [2]-[6]. Existing research has shown that cooperative communications can achieve the same bit error rate with a lower transmission energy as compared to direct transmissions [7].

Importantly, the limited size of the batteries causes the demand of periodic batteries replacement or recharging, which is costly, inconvenient, or sometimes impossible, especially in networks of a high number of sensors that are deployed in a hostile environment. One solution to this problem, energy harvesting, has recently generated a great deal of research interest for wireless sensor networks [8, 9]. Energy harvesting can provide essentially limitless energy without the hassle of manual recharging, battery replacement, and the dangers associated with battery leakage (environmentally-friendly). Moreover, energy harvesting can be used in emergencies when a conventional power supply is unavailable or human intervention is impractical.

These advantages of energy harvesting and the low power transmission property of co-

operative communications have motivated researchers to combine these two technologies in wireless sensor networks. Thus, their energy efficiency increases, and they become well suited in some applications where human intervention or battery replacement/recharging is impractical. However, the stochastic nature of the energy harvesting processes imposes more challenges on the system design [10]. One of the challenges is cooperating node usage scheduling for cooperative communication. Due to the stochastic energy availability at the nodes, the source cannot immediately transmit cooperatively with the cooperating node. It has first to determine whether the cooperating node has sufficient energy to forward its transmission or not. Otherwise, its transmission may get lost. Under this energy constraint, the challenge here is how to design an efficient scheduling algorithm that enables the source to optimally schedule its transmission whether on its own or by using the cooperating node, such that the packet delivery ratio of the system is maximized. In this dissertation, we focus on this problem.

First, in Chapter 2, we address the problem of single cooperating node scheduling. We consider a network of three nodes; a source, a cooperating node, and a destination, where the source transmits its events either directly or cooperatively using the cooperating node to the destination, and the cooperating node helps with the source's transmissions as well as it transmits its own events to the destination. For such a network model, we propose a scheduling algorithm, called feedback algorithm, that enables the source to optimally decide whether to transmit directly or cooperatively such that the packet delivery ratio of the network is maximized, which is the ratio of the total events that are successfully delivered, to the total events that are generated. In the proposed algorithm, the cooperating node usage is scheduled based on a feedback that is frequently sent to the source carrying the energy status of the cooperating node as either 1 or 0, i.e., *energized* or *unenergized*, where *energized* means that the cooperating node has sufficient energy to forward the source's transmission to the destination. When the source has a transmission and the cooperating node status is *energized*, cooperating node usage is scheduled; otherwise the source is scheduled to transmit on its own if it has sufficient energy for direct transmission. The results show that our algorithm maximizes the system performance, but does not require auxiliary parameter optimization as does the-state-of-the-art scheme, which is the threshold-based scheme [53].

In the threshold-based scheme, the decision on the cooperating node usage is made based on a threshold level. When the source has a transmission and its energy battery level is less than that threshold level, the cooperating node is scheduled to assist with the source's transmission. Otherwise, the source is scheduled to transmit on its own. To maximize the system performance, the threshold level must be tuned for any given set of system parameters or for any change in the system parameters. Tuning the threshold level requires simulating the system at different energy levels of the source's battery. This might not be easy or even possible to implement especially in networks of unstable parameters or in networks with sensors of a huge battery capacity.

Next, in Chapter 3 we upgrade the feedback algorithm for the scenario of multiple cooperating nodes and two-way cooperative communications. In this scenario, we assume that the system has multiple cooperating nodes between two transmitting nodes, which communicate with each other either directly or cooperatively using one of the cooperating nodes. In the algorithm, the cooperating nodes are indexed increasingly, and each node is assumed to broadcast its energy status to the network as either *energized* or *unenergized* whenever it changes. Hence, when any of the transmitting nodes has a transmission and there is at least one energized cooperating node, the transmitting node transmits cooperatively. Otherwise, it transmits directly if it has sufficient energy for direct transmission. If there is more than one energized cooperating node, the transmitting node uses the cooperating node of the highest index, or in another scenario, it uses the energized cooperating nodes sequentially. Because of the overhead problem caused by broadcasting the energy status of each cooperating node to the network, we propose an adaptive method to decrease this burden. That is, when the energy harvesting rate of a cooperating node is low, the other nodes in the network will set the energy status of that node to *unenergized* after each time it transmits as it will be more likely to be so. If the node is still energized after transmission, the node will broadcast 1 to the network so that the other nodes will set its status back to *energized*. Thus, the cooperating node does not need to always broadcast its energy status to the network, which will reduce the overhead when the energy harvesting rate is low. In addition, we propose an adaptive scheduling algorithm that incorporates fairness constraints to ensure the same performance between the nodes. The algorithm optimally

switches between two conditions, where one prioritizes the source's transmission while the other prioritizes the cooperating node's transmission, such that the two nodes achieve the same performance. However, in the adaptive scheme, the penalty on the cooperating node performance sometimes has to be high in order to achieve the same performance of the source node. In addition, because in the system model each node is fixed and categorized a priori as either a source or a cooperating node, in the adaptive scheme fairness cannot be achieved if the source has higher performance than the cooperating node. Therefore, in Chapter 4, we first generalize the system model of the three nodes network, where each node can be either a source, a cooperating, or a relay node depending on the system parameters. Then, We propose a fairness scheduling (FS) scheme that achieves fairness based on a given penalty function, which fairly determines how much a node should cooperate with the other. We also propose a constrained scheduling (CS) scheme that constrains one of the nodes to achieve a certain performance.

Although the adaptive method proposed in Chapter 3 decreases the burden of overhead, it is still relatively high and could consume a significant amount of energy, especially when using protocols of fixed packet/frame format, as in IEEE 802.11. Thus, to solve the problem of overhead, we introduce in Chapter 5 a statistical model that estimates the cooperating node's energy status at the source. The simulation results show that over some values of the energy harvesting rates of the transmitting nodes, it is more energy efficient to use the statistical model than the feedback scheme with the adaptive method. Lastly, we address in Chapter 6 the problem of scheduling for throughput maximization in a wireless energy harvesting uplink. In most of the existing works, throughput is maximized at the expense of some nodes that are either close to the sink or that discard their own transmissions in favor of relaying. For fairness, we maximize the network throughput such that each node's throughput cannot drop below what it achieves by direct transmission to the base station. The throughput is maximized using data relaying, and by optimally assigning a role to each node, i.e., cooperating node, source (direct transmission), or user (of a cooperating node). Both centralized and decentralized algorithms that find the optimal assignment of each node are proposed and studied. We consider both fixed and variable transmit power scenarios, and address complexity issues. Our algorithms are shown to have a linear or

quadratic complexity compared to the exponential complexity of the brute force approach. Compared with cooperative transmission, our approach maximizes the overall throughput of the network such that no node's throughput is adversely affected.

Throughout this dissertation, we assume a real-time monitoring scenario, where no packets/events are buffered for later transmission. In other words, we assume that there is no buffer for storing sensed data as in [71]. We also assume that the transmission energy required for reliably transmitting an event from a sensor node to another or from a sensor node to a destination is constant, i.e., the transmission rate is constant. Moreover, unlike [63], we assume that if a node has an event to transmit to the destination, the node transmits only if its current residual energy is sufficient for reliable transmission. Thus, if the transmission occurs, the transmitted event is considered successfully delivered to the destination, with no retransmissions required. We do not consider the energy consumption of signal processing including receive signal processing. However, it can easily be subsumed under the transmit energy.

1.2 Literature Review

In this section, we present literature related to the problems addressed in this dissertation. We first start with the research work related to the area of energy harvesting sensor networks, where we briefly discuss the technology of energy harvesting and mention some research work that consider this technology in wireless sensor networks. Then, we present the research work in the area of using cooperative communication in energy harvesting sensor networks. In this area, we first talk about cooperative communication technology, and then we present some research work that combine this technology with energy harvesting in wireless sensor networks.

1.2.1 Energy Harvesting Sensor Networks

Energy harvesting technology has been widely addressed in the literature. Some of its sources have been studied and investigated including but not limited to wind, solar, thermal, and mechanical vibration [11]. Depending on the energy source, it has been shown that the

power that can be harvested is in the range between several μW to several hundred mW [12, 13, 14]. Because the power consumption of a sensor node is usually in the range between 1 to 100 μW [15, 16, 17], in the past few years some sensor nodes that can be powered by energy harvesting sources have been introduced to the research communities. Some of the existing energy harvesting sensor nodes are listed in [18]. Such sensor nodes can provide many unique features that cannot be provided by conventional sensors, including, 1) no need for battery replacement/recharging when it runs out, which reduces labor and new batteries' costs, 2) easy and fast deployment in hostile or inaccessible environments, and 3) reduction of carbon effects associated with batteries leakage. These attributes have motivated researchers to study and consider the idea of using energy harvesting technology in wireless sensor networks. Due to the new imposed energy constraints, some fundamental issues and standard designs of wireless sensor networks have been revisited and reanalyzed in the literature. In [19] and [20], the authors analyzed the performance of various MAC schemes for a multi-sink and a single-sink networks. In [21], the authors analyzed the power consumption of a ZigBee-Based energy harvesting sensor network. The authors in [22] investigated the feasibility of using IEEE 802.11 in energy harvesting sensor networks of low-power sensing applications. In [23], the authors characterized the transmission capacity of an ad hoc wireless network with ALOHA and CSMA protocols. Some sleep and wakeup strategies have been proposed for solar-powered wireless sensor networks in [24]. Finally, the authors in [25]-[30] have revisited the issues of power transmission and allocation as well as the issue of throughput maximization for different models of energy harvesting sensor networks. More research work and challenges can be found in [10].

1.2.2 Cooperative Energy Harvesting Sensor Networks

The idea of cooperative communication was first introduced by van der Meulen in the 1970s, where he introduced the three-terminal relay channel and derived the inner bounds for capacity using a timesharing approach [5]. The results in this paper showed that cooperative communication can be a promising solution for communication systems. Therefore, after that, cooperative communication has been addressed extensively in the literature. Different

issues were investigated and analyzed including diversity gain, outage probability, capacity, energy and bandwidth utilization. In [6], the authors analyzed the capacity for the three-terminal relay channel assuming that all the nodes operate in the same band. In [31] and [32], the authors explored the idea of some general cooperative communication scenarios including decode-and-forward, amplify-and-forward, and selection relaying. The idea of cooperative communication was extended further to a more generic sense of cognitive radio in [33]. In [34]-[36], the authors focused on achieving diversity gains in coded cooperation systems. Cooperative communication using collaborative MIMO has also been investigated in the literature. Some recent developments and challenges about using cooperative MIMO in sensor networks can be found in [37].

Cooperative communication has been used in wireless sensor networks for more energy efficiency and longer lifetime. However, some fundamental issues have been revisited and considered. In [38]-[41], some MAC layer issues have been considered and cooperative MAC protocols have been proposed under different assumptions. A cross-layer strategy and a cooperation algorithm were proposed in [42] and [43], respectively. Cooperative communication has also been used in wireless sensor networks with energy harvesting to maximize the data collected from their sensor nodes. Data collection can also be maximized using a mobile sink [44]-[46] or multihop transmission [47]-[52]. However, using a mobile sink may not be suitable for small networks or for hostile environments, where optimizing the trajectory may be impossible. On the other hand, using multihop transmission results in data delivery latency that may be intolerated in some applications. These two problems are avoided when using cooperative communication.

In the literature, there has been a substantial research effort on using cooperative communication to maximize data collection in energy harvesting sensor networks. In [53], the authors considered a three-node relay network, and developed a scheduling scheme to maximize the data collected from the source node. In [54]-[58], the problem was considered for the scenario when the network has multiple relays, and relay selection protocols were proposed. The authors in [59] and [60] considered the problem for a three-node network of an energy harvesting relay node that harvests its energy from the RF radiation of the source. The authors proposed relaying protocols that enable the relay to switch between

energy harvesting and data processing. A relaying protocol was also proposed in [61] for a different setup of three-node relay network. In [62], the problem was considered for a Gaussian three-node relay network. The authors in [63] improved data throughput for a network of a set of nodes over low energy harvesting rates. The network throughput is improved by assigning a cooperative repeater role to some nodes, which drop all their transmissions over a period of time and retransmit the sources' transmissions only if they are not successfully received at the base station. Lastly, in order to maximize the data collected from the source at the destination, the authors in [64] proposed schemes that enable the source to optimally schedule the relays' energy harvesting and data transmission for a multiple-relay network.

As in [53], in this dissertation, we also consider the problem of relay/cooperating node usage scheduling for cooperative communication at source. Using partially observable Markov decision process, the authors in [53] derived an optimal policy which maximizes the system performance in terms of the packet delivery ratio, which is the ratio of the data that is successfully delivered, to the total data that is generated. This optimal policy is quite sensitive to system parameters, which makes it impractical. Therefore, the authors designed a simple and practical threshold-based relay scheduling scheme that is sensitive only to one system parameter. The scheme achieves performance close to the optimal policy, and thus we consider it as the state-of-the-art scheme to evaluate our proposed schemes. Because cooperative communication can maximize data collection at the expense of relay or cooperating nodes, we also use the approach of data relaying in the last chapter to maximize the network throughput such that no node's throughput is adversely affected. In this approach, each node is assumed to transmit to the base station either direct or in two hops.

The rest of the dissertation is organized as follows. Chapter 2 addresses the problem of single cooperating node scheduling, and proposes a practical relay scheduling scheme to maximize the system performance. In Chapter 3, the proposed scheme in Chapter 2 is upgraded to include the scenarios of multiple cooperating nodes and sources, and to accommodate fairness constraints. Chapter 4 generalizes fairness and provides analytical-based approach fair and constraint scheduling schemes for optimal scheduling. In Chapter 5, a statistical model is proposed to estimate the energy status of the relay or the cooperating node, considering the same system model in Chapter 4. Chapter 6 considers the problem of

data collection throughput maximization for an uplink wireless network. Chapter 7 concludes the dissertation and presents some directions for future work.

Chapter 2

Single Cooperating Node Scheduling

2.1 Introduction

In this chapter, we consider a network of a single cooperating node that assists cooperative communication between a source and a destination. We propose a simple practical scheduling scheme, called feedback scheme, that enables the source to optimally decide whether to transmit on its own or by using the cooperating node in order to maximize the packet delivery ratio of the network, which is the ratio of the data that is successfully delivered, to the total data that is generated. In the feedback scheme, the decision on the cooperating node usage is made based on its actual energy status that is sent to the source in a feedback message as either 1 or 0, i.e., *energized* or *unenergized*, where *energized* means that the cooperating node has sufficient energy to forward the source's transmission. The results show that the feedback scheme provides almost the same performance of the threshold-based scheme, which performs close to the optimal policy derived in [53]. The threshold-based scheme is sensitive to one of the system parameters, threshold level. In order to maximize the system performance, the threshold level has to be tuned for each given set of parameters or for any change in the parameters, and tuning the threshold level requires simulating the system at different levels of the source battery. Therefore, as the feedback scheme does not require auxiliary parameter optimization to maximize the system performance, it becomes more practical especially in networks with unstable parameters or with sensors of large battery capacity.

Portion of this chapter appears in: A. Ammar and D. Reynolds, "A practical relay scheduling scheme for wireless sensor networks with energy harvesting," 47th Annual Conference on Information Sciences and Systems (CISS), vol. 1, no. 6, pp. 20-22, March 2013.

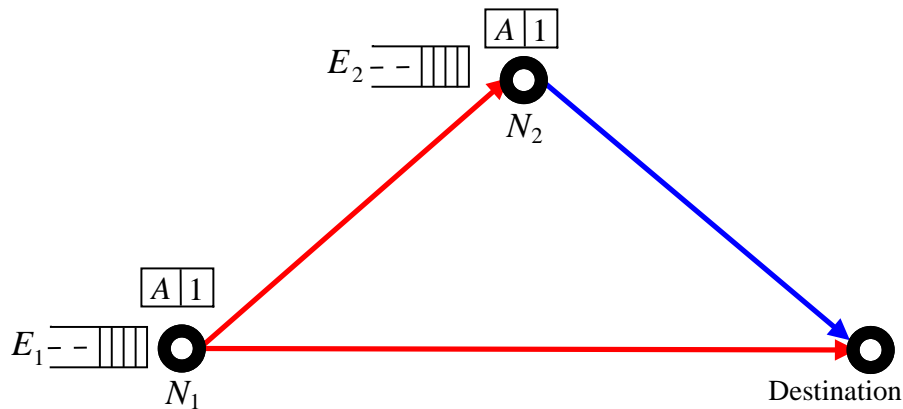


Figure 2.1: A three-node network with an energy harvesting source N_1 , an energy harvesting cooperating node N_2 , and a destination. E_1 and E_2 are queues representing the energy harvested by N_1 and N_2 , respectively, in the n -th time block, $n \in \{1, 2, \dots, N\}$. A is the latest energy status of the cooperating node N_2 .

2.2 System Model

We consider a three-node network with a source node N_1 , a cooperating node N_2 , and a destination, as depicted in Figure 2.1, where each node is equipped with energy harvesting devices and has a rechargeable battery with capacity K . We assume a discrete-time model, where time is divided into N time blocks. To avoid collision, we use a TDMA protocol where each block is divided into three time slots. The first time slot is for the source's transmission, the second is for the cooperating node to forward the source's transmission, and the third is for the cooperating node's transmission. The energy available at node $N_i, i \in \{1, 2\}$ in the time block $n, n \in \{1, 2, \dots, N\}$ is denoted by $L_i[n] \in \{0, 1, 2, \dots, K\}$.

We assume that there is at most one event generated per each transmitting node N_1 and N_2 per time block. As in [53] and [65], the event generation process at node $N_i, i \in \{1, 2\}$ is modeled by a temporally correlated, two-state Markov process (“on”, “off”) with transition probabilities q_i^{on} and q_i^{off} , as illustrated in Figure 2.2. In the time block $n, n \in \{1, 2, \dots, N\}$, the “on” state means that there is an event generated at that block, i.e., $\mathcal{E}_i[n] = 1$, while the “off” state means that there is no event generated, i.e., $\mathcal{E}_i[n] = 0$. The energy generation process of $N_i, i \in \{1, 2\}$ is assumed to be modeled by the same process, but with transition probabilities p_i^{on} and p_i^{off} . The “on” state at the n -th time block means that the sensor

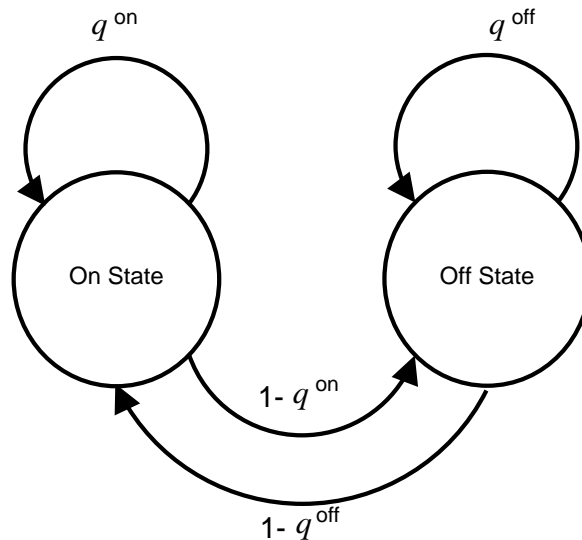


Figure 2.2: A state diagram of the two-state Markov process that models the event generation process of node $N_i, i \in \{1, 2\}$ with transition probabilities q_i^{on} and q_i^{off} . The energy generation process is modeled the same but with transition probabilities p_i^{on} and p_i^{off} .

harvests E_i amount of energy at that block while the “off ” state means that there is no energy harvested.

During each time block in which there is an event to report, the source node N_1 operates in one of two transmission modes; *direct transmission* or *relay transmission*. In direct transmission, the source transmits its event directly to the destination using δ_1 amount of energy. In relay transmission, the source transmits its event to the destination using $\tilde{\delta}_1$ amount of energy, and it also makes use of the cooperating node N_2 to forward its transmission to the destination in the next time slot. The cooperating node N_2 also operates in one of two transmission modes; *own-traffic transmission* or *relay transmission*. In the own-traffic transmission, the cooperating node transmits its own packet to the destination using δ_2 amount of energy. While in the relay transmission, the cooperating node forwards N_1 's transmission to the destination using $\tilde{\delta}_2$ amount of energy. As in [53], we assume no packet/event transmission losses occurred. We also assume that sensors are deployed in a real-time monitoring scenario where no packets/events are buffered for later transmissions.

We assume that the cooperating node transmits its energy status A to the source node as either 1 or 0, representing whether the cooperating is *energized* or *unenergized*, respectively.

Algorithm 2.1 Feedback Scheduling Scheme

(a) Source node N_1	(b) Cooperation Node N_2
1: Inputs: $\mathcal{E}_1[n], L_1[n], A[n], \delta_1, \tilde{\delta}_1$;	1: Inputs: $\mathcal{E}_2[n], L_2[n], \delta_1, \tilde{\delta}_2$;
2: Outputs: Transmission action of N_1 ;	2: Outputs: Transmission action of N_2 ;
3: if $\mathcal{E}_1[n] = 1$ then in time slot 1	3: if $L_2[n] \geq \tilde{\delta}_2$ then
4: if $L_1[n] \geq \delta_1$ AND $A[n] = 0$ then	4: Sense the link N_1 - N_2 for N_1 action;
5: N_1 action = <i>direct transmission</i> ;	5: if N_1 action = <i>relay transmission</i> then
6: elseif $L_1[n] \geq \tilde{\delta}_1$ AND $A[n] = 1$ then	6: In time slot 2,
7: N_1 action = <i>relay transmission</i> ;	7: N_2 action = <i>relay transmission</i> ;
8: else	8: In time slot 3, Go to step 10:
9: N_1 action = <i>no transmission</i> ;	9: elseif N_1 action = <i>no transmission</i> then
10: endif ;	10: In time slot 3,
11: else	11: if $\mathcal{E}_2[n] = 1$ AND $L_2[n] \geq \delta_1$ then
12: N_1 action = <i>no transmission</i> ;	12: N_2 action = <i>own-traffic transmission</i> ;
13: endif	13: else
	14: N_2 action = <i>no transmission</i> ;
	15: endif
	16: endif
	17: else
	18: N_2 action = <i>no transmission</i> ;
	19: endif

In the n -th time block, the cooperating node N_2 is said to be *energized* if it has sufficient energy to forward at least one event for the source, i.e., $L_2[n] \geq \tilde{\delta}_2$. Otherwise, it is said to be *unenergized*. We assume that the cooperating node status is transmitted only whenever it changes, i.e., if the cooperating node transmits its own packet or forwards the source packet and its status is still the same as before transmitting or forwarding, the cooperating node will not transmit its status.

2.3 Feedback Scheduling Scheme

The feedback scheduling scheme proposed in this chapter is summarized in Algorithm 2.1. At the beginning of the time block $n \in \{1, 2, \dots, N\}$, the source node N_1 generates an event with probability modeled by the two-state process described earlier. And based on the event status $\mathcal{E}_1[n]$, the source in the first time slot takes one of the three transmission actions; *direct transmission*, *relay transmission*, or *no transmission*, as illustrated in part (a) of the algorithm. If $\mathcal{E}_1[n] = 1$, the source takes *direct transmission* action if $A[n] = 0$ and $L_1[n] \geq \delta_1$, i.e., if the cooperating node is *unenergized* and the source has sufficient energy to transmit directly. On the other hand, if $\mathcal{E}_1[n] = 1$, the source takes *relay transmission* action if $A[n] = 1$ and $L_1[n] \geq \tilde{\delta}_1$, i.e., if the cooperating node is *energized* and the source has sufficient energy to transmit cooperatively. In these two scenarios, the source's event is considered successfully delivered to the destination. If $\mathcal{E}_1[n] = 1$ and the transmission action can neither be *direct transmission* nor *relay transmission*, the source takes the transmission action *no transmission*, and in this scenario the source's event is considered lost or not successfully reported to the destination. If $\mathcal{E}_1[n] = 0$, the source takes the transmission action *no transmission* regardless of the energy availability at both the source and the cooperating node.

As for the cooperating node N_2 , it takes a transmission action that is either *own-traffic transmission*, *relay transmission*, or *no transmission*, as illustrated in part (b) of the algorithm. In the first slot of the n -th time block, the cooperating node N_2 senses the N_1 - N_2 link only if its latest energy status is *energized*. If there is a transmission coming from the source in that slot, which means that the transmission action taken at the source is a *relay transmission*, then the transmission action at the cooperating node will be taken as a *relay transmission* to forward the source's transmission in the second time slot. Otherwise, the transmission action will be taken as *no transmission* in the first two time slots. In the third time slot, the cooperating node takes the transmission action *own-traffic* to transmit its own event if $\mathcal{E}_2[n] = 1$ and if $L_2[n] \geq \delta_2$. In these two scenarios, the event of the source and the event of the cooperating node are considered to be reported successfully to the destination. In the first two time slots, if the latest energy status of the cooperating node is *unenergized*,

then the cooperating node will not sense the N_1 - N_2 link since the transmission action at the source will not be taken as a *relay transmission* at that status. Hence, the transmission action will be taken as *no transmission* in the first two time slots. The transmission action will be taken as *no transmission* in the third time slot as well if the cooperating node has no event generated, or has no sufficient energy to transmit its event, i.e., $L_2[n] < \delta_2$. In this scenario, the cooperating node's event is considered lost. Note that in the algorithm, the default transmission action of each node is *no transmission*. If a node takes a transmission action that is not a *no transmission* in some time slot, the node will set its transmission action back to *no transmission* at the end of that time slot.

The feedback scheme is a distributed algorithm because each node performs some analysis and takes a decision on its transmission action by itself. As we will see later in the simulation results, the feedback algorithm maximizes the overall packet delivery ratio of the system, which is the ratio of the number of events that are successfully delivered for both the source and the cooperating node over the total number of events that are generated for both the source and the cooperating node over the N time blocks. In the algorithm, however, the cooperating node prioritizes the source's transmission over its own, i.e., when both the source and the cooperating nodes have an event generated in the same time block, the cooperating node cooperates with the source first and then it transmits its own event if sufficient energy remained. If no sufficient energy remained, the cooperating node's event would be dropped. Consequently, the packet delivery ratio of the source will improve at the expense of the cooperating node. The problem can be reversed if the source priority condition ($A[n] = 1$ if $L_2[n] \geq \tilde{\delta}_2$) is changed to the cooperating node priority condition ($A[n] = 1$ if $L_2[n] \geq \tilde{\delta}_2$ & $\mathcal{E}_2[n] = 0$). Under the cooperating node priority condition, the cooperating node will prioritize its transmission over the source's transmission which will improve its performance. Note that, the packet delivery ratio of a node is the ratio of the total events that are successfully delivered for that node to the total number of its generated events over the N time blocks.

The flowcharts in Figure 2.3 illustrate the feedback and the threshold-based schemes. It can easily be noticed that the difference between them is only in the condition where the cooperating node is decided whether to be used or not. Our scheme bases its decision on

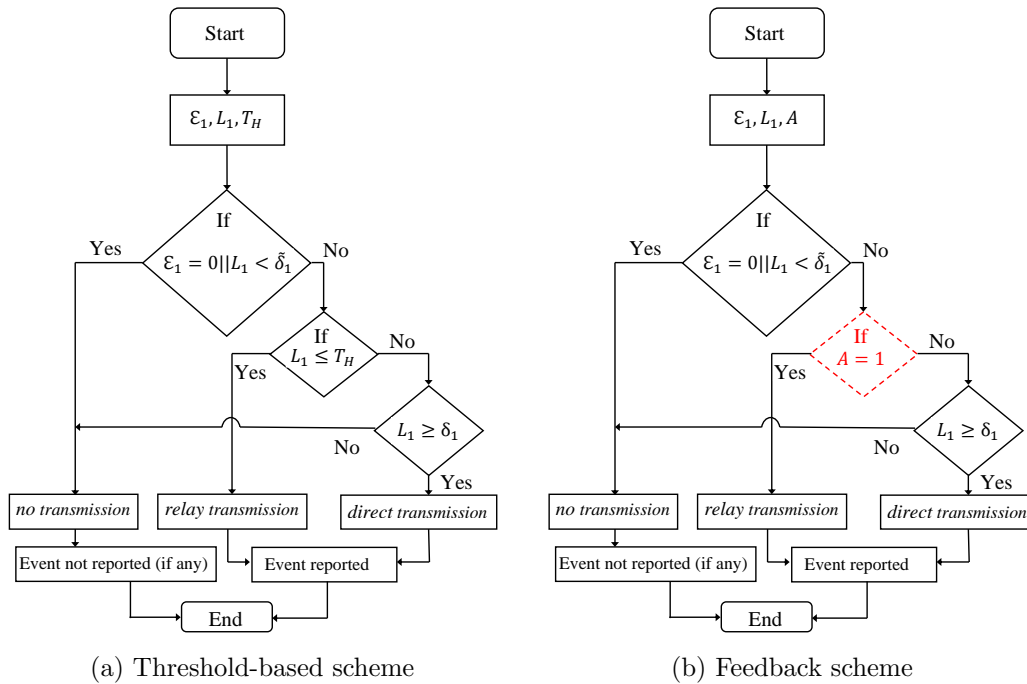


Figure 2.3: Two flowcharts illustrate the feedback and the threshold-based schemes to easily notice the difference between them.

the actual energy status of the cooperating node while the threshold-based scheme bases its decision on the threshold value T_H . As stated before, the threshold value needs to be tuned for any given set of system parameters in order to maximize the system performance, and tuning it requires simulating the system at different energy battery levels of the source node, which is impractical in networks of unstable parameters or in networks of sensors with batteries of huge capacity.

2.4 Simulation Results

In this section, we evaluate the performance of the feedback scheme by comparing it with the performance of the threshold-based scheme. We simulate the two schemes using the same set of parameters that was used to simulate the threshold-based scheme in [53]. We simulate the feedback scheme for the two priority conditions to evaluate the performance of each node under each condition. In addition, we simulate the two schemes when one of the system parameters changes in order to show the sensitivity of the threshold-based scheme to

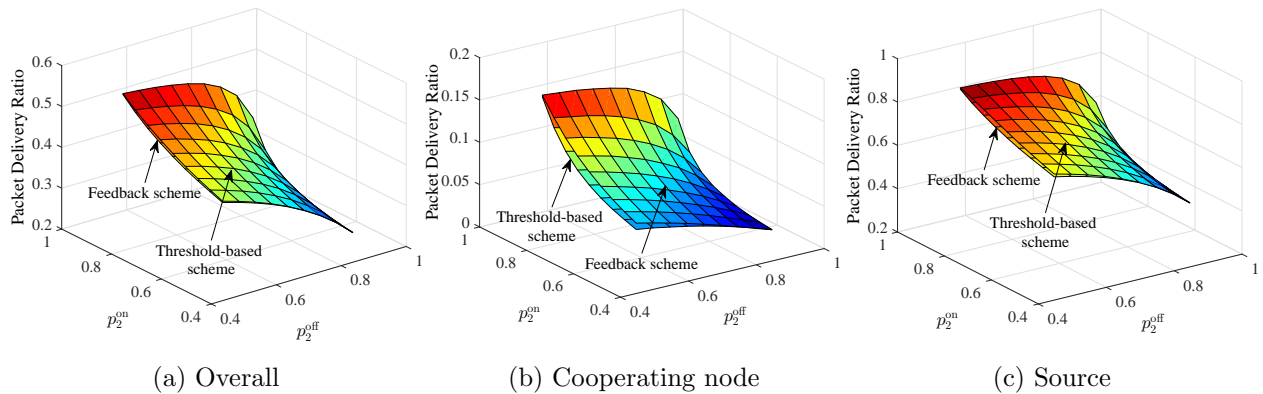


Figure 2.4: The overall, the cooperating node, and the source packet delivery ratios of the feedback and the threshold-based schemes. Parameters used: $q_1^{\text{on}} = 0.9$, $q_1^{\text{off}} = 0.7$, $p_1^{\text{on}} = q_2^{\text{on}} = 0.85$, $p_1^{\text{off}} = q_2^{\text{off}} = 0.7$, $E_1 = E_2 = 1$, $\delta_1 = \delta_2 = 3$, $\tilde{\delta}_1 = \tilde{\delta}_2 = 1$, $K = 20$, $T_H = 10$.

the system parameters, and how our scheme stands in this case. The simulations were done using *Matlab* and they were run for a duration of $N = 5 \times 10^6$ time blocks.

The performance is represented in terms of the packet delivery ratio versus energy harvesting probabilities of the cooperating node p_2^{on} and p_2^{off} . Therefore, in the simulations, these two parameters are changing from 0.55 to 0.95 while the rest of the parameters are fixed. As in [53], the threshold value in the threshold-based scheme is set to the half of the battery capacity, i.e., $T_H = 10$, which is the tunable value for the system parameters given in Figure 2.4 that maximizes the performance. The energy harvesting rate for both the source and the cooperating node E_1 and E_2 are set to 1, where the source and the cooperating node each harvests 1 unit of energy in a time block if its energy harvesting state is “on” at that block. All the used parameters are given in the caption of the figures.

2.4.1 Performance Evaluation

Figure 2.4 illustrates the simulation results for the feedback and threshold-based schemes using the system parameters shown in the figure. The figure shows that the overall, the cooperating node, and the source packet delivery ratios for the two schemes are almost the same. In [53], it has been shown that the threshold-based scheme performs close to the optimum policy, meaning that, the feedback scheme performs also close to the optimum

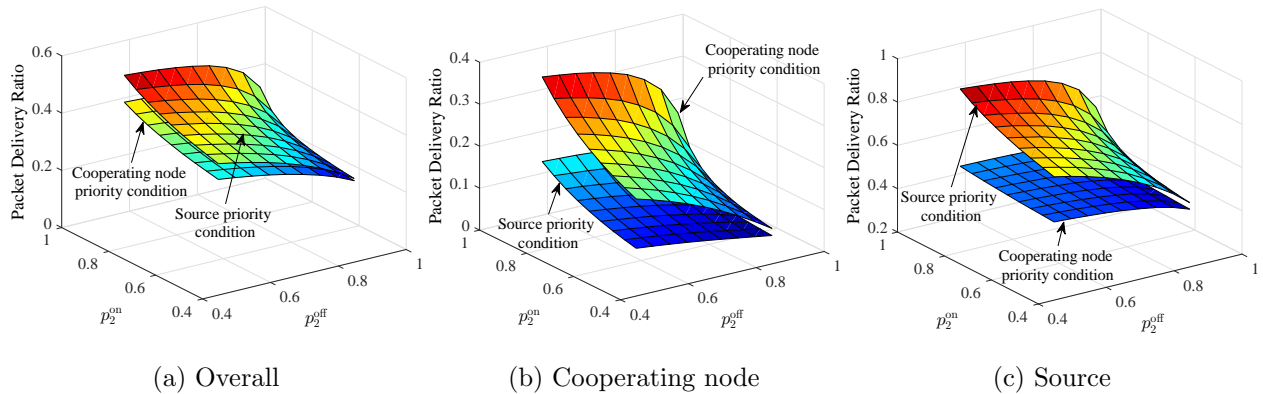


Figure 2.5: The overall, the cooperating node, and the source packet delivery ratios of the feedback scheme with both the source and the cooperating node priority conditions. Parameters used: $q_1^{\text{on}} = 0.9$, $q_1^{\text{off}} = 0.7$, $p_1^{\text{on}} = q_2^{\text{on}} = 0.85$, $p_1^{\text{off}} = q_2^{\text{off}} = 0.7$, $E_1 = E_2 = 1$, $\delta_1 = \delta_2 = 3$, $\tilde{\delta}_1 = \tilde{\delta}_2 = 1$, $K = 20$, $T_H = 10$.

policy. However, the close performance to the optimum in the feedback scheme is achieved without requiring the optimization of system parameters.

From Figures 2.4 (a) and (b), it can be observed that the packet delivery ratio of the cooperating node is significantly lower than the source. In the two schemes, the cooperating node gives priority to the source's transmission over its own. Thus, the cooperating node spends most of its harvested energy on forwarding the source's packets instead of transmitting its own, which affects its packet delivery ratio. As we will see in the next simulation, the packet delivery ratio of the cooperating node can be improved in the feedback scheme by using the cooperating node priority condition mentioned in Section 2.3.

2.4.2 Cooperating Node Priority Condition

In this simulation, we simulate the feedback scheme using the cooperating node priority condition ($A = 1$ if $L_2 \geq \tilde{\delta}_2$ & $\mathcal{E}_2 = 0$) and compare it with the case when the source priority condition ($A = 1$ if $L_2 \geq \tilde{\delta}_2$) is used. Figure 2.5 (b) shows that the packet delivery ratio of the cooperating node improves when using the cooperating node priority condition compared to the source priority condition. However, the overall and the source packet delivery ratios decrease as can be noticed from Figures 2.5 (a) and (c). The packet delivery

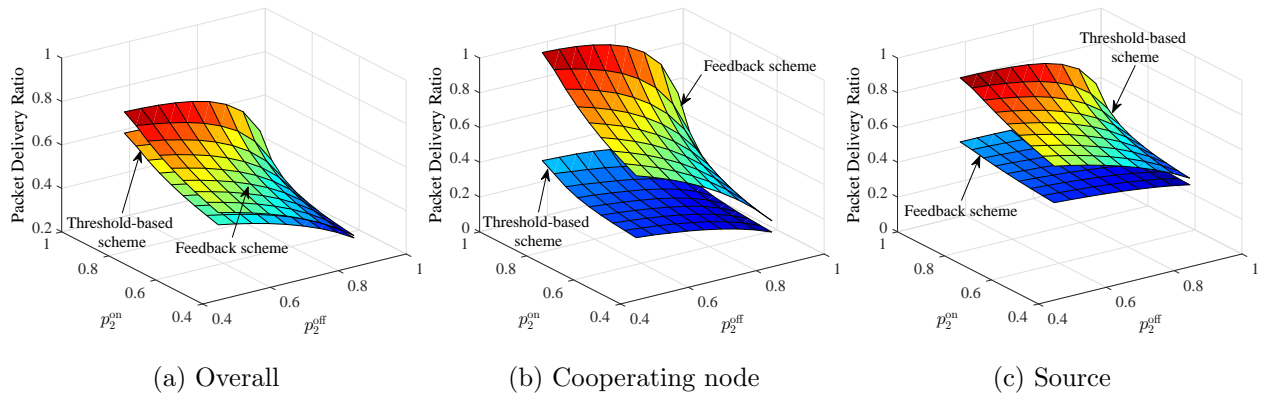


Figure 2.6: The overall, the cooperating node, and the source packet delivery ratios of the feedback and the threshold-based schemes when changing one of the parameters. Parameters used: $q_1^{\text{on}} = 0.9$, $q_1^{\text{off}} = 0.7$, $p_1^{\text{on}} = q_2^{\text{on}} = 0.85$, $p_1^{\text{off}} = q_2^{\text{off}} = 0.7$, $E_1 = E_2 = 1$, $\delta_1 = 3$, $\delta_2 = \tilde{\delta}_1 = \tilde{\delta}_2 = 1$, $K = 20$, $T_H = 10$.

ratio of the source decreases because the cooperating node cooperates less with it when using the cooperating node priority condition. From Figures 2.5 (b) and (c), we can notice that the gap between the cooperating node and the source node packet delivery ratios decreases when using the cooperating node priority condition, which is more fair than when using the source priority condition.

2.4.3 Threshold-based Scheme Sensitivity

To show its sensitivity to the system parameters, we simulate the threshold-based scheme when δ_2 changes from 3 to 1 while the threshold value T_H is still the same, not tuned. We compare its performance with the feedback scheme. The simulation results in Figure 2.6 (a) show that the overall packet delivery ratio of the feedback scheme is better than the threshold-based scheme. This is because the performance in the threshold-based scheme is not maximized due to the fact that the threshold value $T_H = 10$ is not the tunable value for the new set of parameters. Hence, we conclude that using the threshold-based scheme in networks of unstable parameters is impractical when the maximum packet delivery ratio of the system needs to be maintained. Finally, Figure 2.6 (c) illustrates that the packet delivery ratio of the source in the threshold-based scheme is better than the feedback scheme. This is

because in the threshold-based scheme, the cooperating node in this new set of parameters cooperates more with the source, which results in better packet delivery ratio for the source, and worse packet delivery ratio for the cooperating node as can be seen from Figure 2.6 (b).

2.5 Conclusions

This chapter considers an energy harvesting three-node network of a source, a cooperating node, and a destination, and it proposes a simple practical scheme, called feedback scheme, that maximizes the packet delivery ratio of the system. The feedback scheme can be generalized to any network of many sensor nodes when each group of three nodes in the network can form a three-node relay channel. In the opposite to the threshold-based scheme, the feedback scheme does not require auxiliary parameter optimization in order to maximize the system performance. This advantage makes the feedback scheme easier and more practical to be used, especially in networks with unstable parameters or with sensors of huge battery capacity.

The feedback scheme can easily switch between two different conditions on the cooperating node energy status, cooperating node priority condition and source priority condition, in order to prioritize the transmissions of either the source or the cooperating node. Hence, if the energy harvesting rate of the cooperating node is higher than its event occurrence rate and the opposite holds true for the source, then the feedback scheme should use the source priority condition. Thus, the cooperating node cooperates more and more events will be delivered for the source. While if the energy harvesting rate of the cooperating node is lower than its event occurrence rate and the opposite holds true for the source, the feedback scheme should use the cooperating node priority condition. Thus, the cooperating node cooperates less and more events will be delivered for the cooperating node. The switch between these two conditions can easily be done by the cooperating node, assuming that the event occurrence probability and the energy harvesting rate of the source are known at the cooperating node. In the threshold based scheme, prioritizing the transmissions of either the source or the cooperating node is not easy. It requires tuning the threshold level at the optimal value, which requires simulating the system at different levels of the source's energy

battery. Lastly, the feedback scheme is distributed as each node performs some analysis and makes a decision on its transmission action by itself.

Chapter 3

Multiple Cooperating Nodes Scheduling

3.1 Introduction

In this chapter, the feedback scheme is upgraded to include the scenario of multiple cooperating nodes in one-way or two-way cooperative communications. In this scenario, we assume that the system has multiple cooperating nodes that assist cooperative communication between two transmitting nodes, as well as they transmit their own events to one of the transmitting nodes in the network. In the algorithm, the cooperating nodes are indexed increasingly, and each node is assumed to broadcast its energy status to the network as either *energized* or *unenergized*. When any of the two transmitting nodes has a transmission and there is more than one energized cooperating node, then the transmitting node uses the cooperating node of the highest index. In another scenario, the transmitting node uses the cooperating nodes sequentially in order to be fair between the cooperating nodes. Using a cooperating node definitely improves the performance of the transmitting nodes. However, it increases the power consumed by the cooperating node, which affects its packet delivery ratio. Therefore, we propose an adaptive scheduling algorithm that incorporates fairness constraints to ensure the same performance between the nodes.

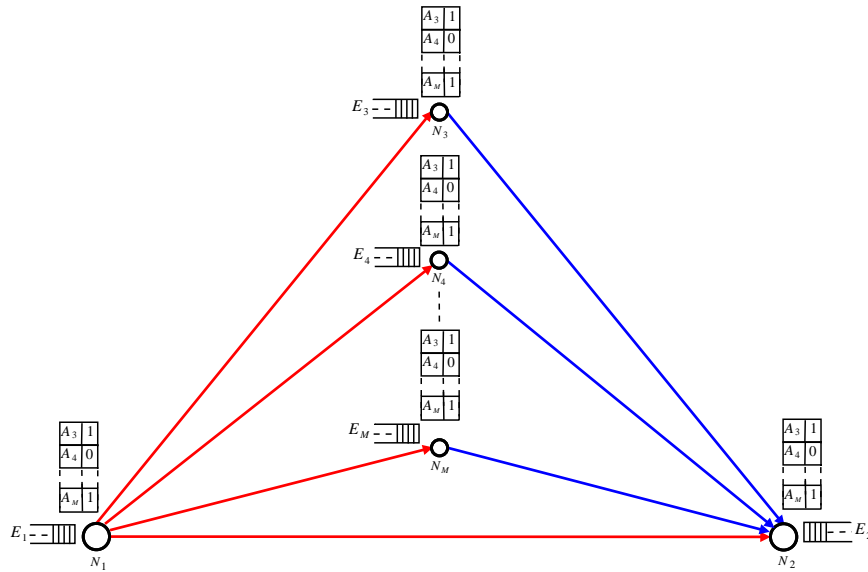


Figure 3.1: Energy harvesting sensor network of $M - 2$ cooperating nodes that assist cooperative communication between two sensors (N_1, N_2). Each node $N_m, m \in \{1, 2, \dots, M\}$ harvests E_m amount of energy if its energy generation process is “on”. Each node has a memory of $M - 2$ slots to save the latest status, $A_m, m \in \{3, 4, \dots, M\}$, of the cooperating node N_m as either 1 or 0 in the corresponding m -th slot.

3.2 System Model

We consider a wireless sensor network with M sensor nodes, including $M - 2$ cooperating nodes that assist cooperative communications between two nodes (N_1 and N_2), as depicted in Figure 3.1. We allow for one-way or two-way cooperative scenarios. In the one-way scenario, N_1 and N_2 serve as a source and destination, respectively, and each cooperating node $N_m, m \in \{3, 4, \dots, M\}$ serves as a relay for N_1 and as a source to transmit its own packets to the destination. In the two-way scenario, N_1 and N_2 serve as both a source and a destination, and each cooperating node N_m serves as a source and also as a relay for both N_1 and N_2 . Each sensor node is equipped with energy harvesting devices and has a rechargeable battery with capacity K . The energy available at node $N_m, m \in \{1, 2, \dots, M\}$, is $L_m \in \{0, 1, 2, \dots, K\}$. As in the previous chapter, we assume no errors or packet losses occurred and that sensors are deployed in real-time monitoring scenarios where no packets are buffered. Based on these assumptions, there is no need to use more than one cooperating

node per transmission.

As in the previous chapter, we assume a discrete-time model, where time is divided into blocks. We also use a TDMA protocol to avoid collision, however, here each block is divided into a number of time slots that depends on the scenario. In the one-way scenario, there are M time slots where the first slot is assigned for node N_1 , the second is assigned for a cooperating node to forward N_1 's transmission, and the rest are assigned for the cooperating nodes sequentially for their own transmissions. In the two-way scenario, there is $M + 2$ time slots, i.e., two extra time slots. One of these extra slots is the third time slot, which is assigned for N_2 , and the second extra slot is the fourth time slot, which is used for forwarding N_2 's transmission.

During each time slot in which there is an event to report, the sensor node N_i , $i \in \{1, 2\}$ operates in one of two transmission modes; *direct transmission* or *relay transmission*. In direct transmission, the sensor node N_i transmits its packet directly to the destination using δ_i amount of energy. In relay transmission, the sensor node N_i transmits its packet to the destination using $\tilde{\delta}_i$ amount of energy, and it also makes use of a cooperating node N_m , $m \in \{3, \dots, M\}$ to forward its transmission in the next time slot. The cooperating node N_m also operates in one of two transmission modes; *own-traffic transmission* or *relay transmission*. In the own-traffic transmission, the cooperating node transmits its own packet to the destination using δ_m amount of energy. While in the relay transmission, the cooperating node forwards the event of node N_i to the destination using $\tilde{\delta}_m$ amount of energy.

As in Chapter 2, we assume that there is at most one event generated per transmitting sensor per block. Both the event generation and the energy harvesting processes at each node are modeled by a temporally correlated, two-state Markov process (“on”, “off”). For node N_i , $i \in \{1, 2, \dots, M\}$, the transition probabilities of the event generation process are q_i^{on} and q_i^{off} while the transition probabilities of the energy generation process are p_i^{on} and p_i^{off} . The event generation status in the n -th time block for node N_i is denoted by $\mathcal{E}_i[n] \in \{1, 2\}$, and the amount of harvested energy in a time block when the state is “on” is denoted by E_i .

The cooperating node N_m , $m \in \{3, 4, \dots, M\}$ is assumed to broadcast its energy status $A_m \in \{0, 1\}$ to the network whenever it changes, and all the M nodes are assumed to have

a memory of $M - 2$ slots, indexed as S_3, S_4, \dots, S_M , where the most recent status of each cooperating node is stored. As stated in Chapter 2, the status of 1 corresponds to the cooperating node status *energized*, and the status of 0 corresponds to the cooperating node status *unenergized*. In the n -th time block, the cooperating node N_m is said to be *energized* if it has sufficient energy to forward at least one event, i.e., it satisfies $L_m[n] \geq \tilde{\delta}_m$. Otherwise, it is said to be *unenergized*. In the n -th time block, we assume that $\mathcal{A}[n]$ is a set that includes all the energized cooperating nodes.

Broadcasting a cooperating node status whenever it changes increases the overhead of the energy statuses' transmissions, which could consume a significant amount of energy and increase the computational complexity modestly (linearly) with the number of cooperating nodes. This burden can be reduced when p_m^{on} , the energy harvesting probability of the cooperating node N_m , is low by adapting the energy status broadcasting of that node. Such that, if the cooperating node N_m transmits, then all the M sensors will automatically set the energy status of that node to *unenergized*. This is because node N_m is more likely to be *unenergized* after transmitting due to its low rate of energy harvesting. If node N_m is still *energized* after transmitting, the node will broadcast 1 to the network so that all the nodes set its status back to *energized*.

3.3 Scheduling Algorithm

Algorithm 3.1 describes the scheduling algorithm for the one-way scenario. As illustrated in part (a) of the algorithm, in the n -th time block, $n \in \{1, 2, \dots, N\}$, node N_1 generates an event \mathcal{E}_1 using the Markov process described earlier. If $\mathcal{E}_1[n] = 1$, then the transmission action will be *direct transmission* if all the cooperating nodes are *unenergized* and $L_1[n] \geq \delta_1$. If $\mathcal{E}_1[n] = 1$, then the transmission action will be *relay transmission* if there is at least one energized cooperating node and $L_1[n] \geq \tilde{\delta}_1$. In these two scenarios, the event of N_1 is considered successfully reported. If $\mathcal{E}_1[n] = 1$ and the transmission action can neither be *direct transmission* nor *relay transmission*, then the transmission action will be *no transmission*. In this scenario, the event of N_1 is considered not successfully reported or lost. If $\mathcal{E}_1[n] = 0$, then the transmission action will also be *no transmission*. When

Algorithm 3.1 Feedback Scheduling Scheme

(a) Source node N_1	(b) Cooperation Node
	$N_m, m \in \{3, 4, \dots, M\}$
1: Inputs: $\mathcal{E}_1[n], L_1[n], \mathcal{A}[n], \delta_1, \tilde{\delta}_1$; 2: Outputs: Transmission action of N_1 ; 3: if $\mathcal{E}_1[n] = 1$ then 4: In time slot 1, 5: if $L_1[n] \geq \delta_1$ AND $ \mathcal{A}[n] = 0$ then 6: N_1 action= <i>direct transmission</i> ; 7: elseif $L_1[n] \geq \tilde{\delta}_1$ AND $ \mathcal{A}[n] > 0$ then 8: N_1 action= <i>relay transmission</i> ; 9: The node of the highest index is scheduled; 10: else 11: N_1 action= <i>no transmission</i> ; 12: endif ; 13: else 14: N_1 action = <i>no transmission</i> ; 15: endif	1: Inputs: $\mathcal{E}_m[n], L_m[n], \mathcal{A}[n], \delta_m, \tilde{\delta}_m$; 2: Outputs: Transmission action of N_m ; 3: if $A_m[n] = 1$ then 4: if m is the highest index in $\mathcal{A}[n]$ then 5: Sense the link N_1 - N_m for N_1 action; 6: if N_1 action = <i>relay transmission</i> then 7: In time slot 2, 8: N_m action = <i>relay transmission</i> ; 9: In time slot 3, Go to step 11: 10: elseif N_1 action = <i>no transmission</i> then 11: In time slot $m+1$, 12: if $\mathcal{E}_m[n] = 1$ AND $L_m[n] \geq \delta_m$ then 13: N_m action = <i>own-traffic transmission</i> ; 14: else 15: N_m action = <i>no transmission</i> ; 16: endif 17: endif 18: else 19: Go to step 11; 20: endif 21: else 22: N_m action = <i>no transmission</i> ; 23: endif

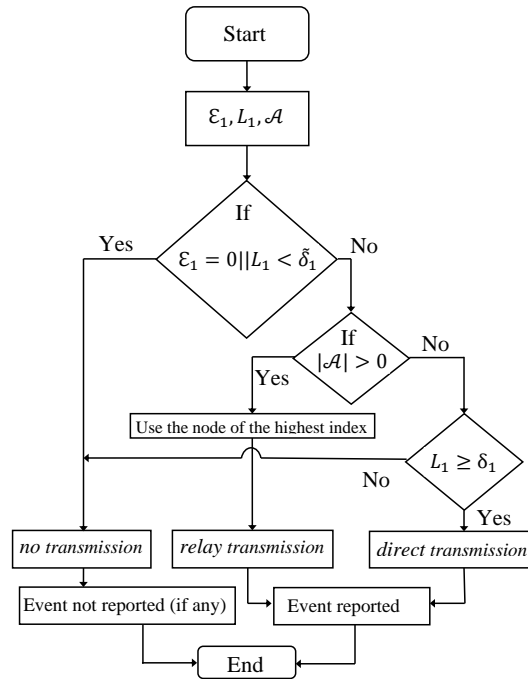


Figure 3.2: A flowchart illustrates the feedback scheme for the case of multiple cooperating nodes when the cooperating node of the highest index is selected for relay transmission.

the transmission action is *relay transmission*, there is no advantage to using more than one cooperating node because we assume no errors or packet losses occurred. If there is more than one energized cooperating node, the algorithm will arbitrarily choose the cooperating node with the highest index number. Note that, choosing the cooperating node with the highest index causes the cooperating node of the highest index to be scheduled more than the others, which is unfair. This problem could be solved, for example, by choosing the cooperating nodes sequentially instead of always choosing the cooperating node of the highest index, i.e., replace line 9 of part (a) of Algorithm 3.1 with “Schedule the cooperating nodes sequentially”. However, scheduling the cooperating nodes sequentially may require the cooperating nodes to track the most recently used cooperating node to decide which cooperating node should cooperate next. The flowchart in Figure 3.2 illustrates how the decision is taken at the source node N_1 given the set of the energized cooperating nodes $\mathcal{A}[n]$ as well as its current energy battery level and event status.

With regard to the cooperating nodes, in the first time slot of the block, the energized cooperating node with the highest index number, say node N_m , $m \in \{3, 4, \dots, M\}$, will sense

the N_1 - N_m link. If N_1 has transmitted, this means that the transmission action taken at N_1 is a *relay transmission*. Therefore, the transmission action at that cooperating node will be taken as a *relay transmission* to forward N_1 's transmission in the next time slot. If not, the cooperating node will take no action and there will be no transmission in the first two slots. In the rest of the time slots, each cooperating node generates an event \mathcal{E}_m with independent realizations of the same Markov process, and it takes a transmission action in its corresponding time slot based on its $\mathcal{E}_m[n]$ and $L_m[n]$. If $\mathcal{E}_m[n] = 0$ or $L_m[n] < \delta_m$, then the transmission action will be taken as *no transmission*. If $\mathcal{E}_m[n] = 1$ and $L_m[n] \geq \delta_m$, then the transmission action will be taken as an *own-traffic transmission*, and the event will be reported successfully. If $\mathcal{E}_m[n] = 1$ and $L_m[n] < \delta_m$, the transmission action will be taken as a *no transmission*, and the event will be dropped.

For the two-way scenario, node N_2 can use part (a) of the algorithm to schedule one of the cooperating nodes if slot 1 in line 4 is changed to slot 3. And the cooperating node of the highest index that will cooperate with N_2 can use part (b) of the algorithm if slot 2 in line 7 is changed to slot 4, slot 3 in line 9 is changed to slot 5, and slot $m+1$ is changed to slot $m+2$. As in Algorithm 2.1, the default transmission action of each node is *no transmission*. Thus, if a node takes a transmission action that is not a *no transmission* in some time slot, the node will set its transmission action back to *no transmission* at the end of that time slot.

3.4 Adaptive Scheme for Absolute Fairness

In Chapter 2, we saw that the feedback scheme can easily switch between the two conditions, source priority condition and cooperating node priority condition, in order to prioritize the transmissions of either the source or the cooperating node. Hence, the packet delivery ratio of the prioritized node over the N time blocks becomes higher than the other, which may not be desired in some applications when the same performance needs to be achieved by the nodes. Therefore, we here propose an adaptive scheme that automatically switches between the two priority conditions such that the nodes achieve the same performance over the N time blocks. Again, for the cooperating node N_m , $m \in \{3, 4, \dots, M\}$, the source prior-

ity condition is ($A_m[n] = 1$ if $L_m[n] \geq \tilde{\delta}_m$), which prioritizes the transmissions of N_1 and N_2 , and the cooperating node priority condition is ($A_m[n] = 1$ if $L_m[n] \geq \tilde{\delta}_m$ and $E_m[n] = 0$), which prioritizes the cooperating nodes' transmissions. The algorithm switches adaptively between these two conditions based on the current relative performance of N_1 , N_2 , and the cooperating nodes. More specifically, we assume that the packet delivery ratio of, say N_1 , is sent to the cooperating nodes after each interval of T blocks. In the first interval, the decision on the cooperating nodes' energy status is made by the source priority condition for the first half of the blocks, and by the cooperating node priority condition for the second half. After the first interval, the cooperating nodes will change the number of blocks of each condition after receiving the packet delivery ratio of N_1 . If the packet delivery ratio of N_1 is higher than the cooperating nodes, the cooperating nodes will increase the number of blocks of the cooperating node priority condition at the expense of the source priority condition time blocks, so that the cooperating nodes cooperate less with N_1 in the next interval which improves their performance. In the case of the opposite, however, the cooperating nodes will increase the number of the time blocks of the source priority condition at the expense of the cooperating node priority condition time blocks, so that the cooperating nodes cooperate more with N_1 in the next interval which improves N_1 's performance. Changing the number of time blocks of the two conditions is done gradually, with a step size that can be chosen depending upon the divergence gap between N_1 and the cooperating nodes' packet delivery ratios and T .

As we will see in Section 3.5.4.2, the system will converge and ensure fairness for a fixed set of parameters. However, changing any of the parameters relatively changes the packet delivery ratio of N_1 and the cooperating nodes. Therefore, after converging, if any of the parameters changes, the system will diverge and the fairness problem will occur again. This indicates that changing any of the system parameters influences fairness, and as we will see in Section 3.5.4.2, the system will adapt as parameters change. With respect to the threshold-based scheme and to the best of our knowledge, there is no straightforward way to adapt the scheme for fairness.

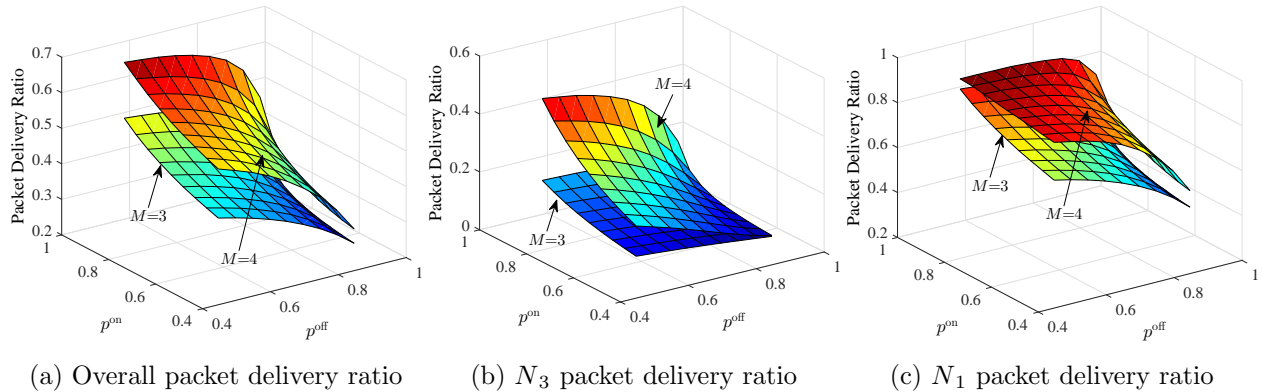


Figure 3.3: The packet delivery ratios of the one-way scenario when $M = 3$ and $M = 4$. Parameters used: $q_1^{\text{on}} = 0.9$, $q_1^{\text{off}} = 0.7$, $p_1^{\text{on}} = q_3^{\text{on}} = 0.85$, $p_1^{\text{off}} = q_3^{\text{off}} = 0.7$, $E_1 = E_3 = 1$, $\delta_1 = \delta_3 = 3$, $\tilde{\delta}_1 = \tilde{\delta}_3 = 1$, $K = 20$.

3.5 Simulation results

We simulate the proposed scheme in Section 3.3 for one-way and two-way scenarios when $M = 3$ and $M = 4$. We use the same set of parameters used in the previous chapter, which is shown in the figures. We also simulate the adaptive way of broadcasting the energy status described at the end of Section 3.2. Moreover, we simulate the adaptive scheduling scheme described in Section 3.4. In the simulations, the event occurrence parameters (q_i^{on} , q_i^{off}) for $N_i, i \in \{1, 2, \dots, M\}$, and the energy harvesting process parameters (p_i^{on} , p_i^{off}) for $N_i, i \in \{1, 2\}$ are fixed while the energy harvesting process parameters (p_m^{on} , p_m^{off}) for $N_m, m \in \{3, 4, \dots, M\}$ are allowed to vary. We set q_i^{on} , q_i^{off} , p_i^{on} , and p_i^{off} to be the same for all $i \in \{1, 2\}$, and we also set q_m^{on} and q_m^{off} to be the same for all $m \in \{3, 4, \dots, M\}$. In order to plot the results, we set $p_m^{\text{on}} = p^{\text{on}}$ and $p_m^{\text{off}} = p^{\text{off}}$ for all $m \in \{3, 4, \dots, M\}$, and they both vary from 0.55 to 0.95.

3.5.1 One-Way Cooperative Scenario

As stated in Section 3.2, in the one-way scenario node N_1 operates as a source while node N_2 operates as a destination, and the remaining $M - 2$ nodes operate as cooperating nodes to relay for N_1 and as sources to transmit their own events to N_2 . So, in this scenario, all the transmitted packets will flow only in one direction, from N_1 and $\{N_m\}_{m=3}^M$ towards N_2 .

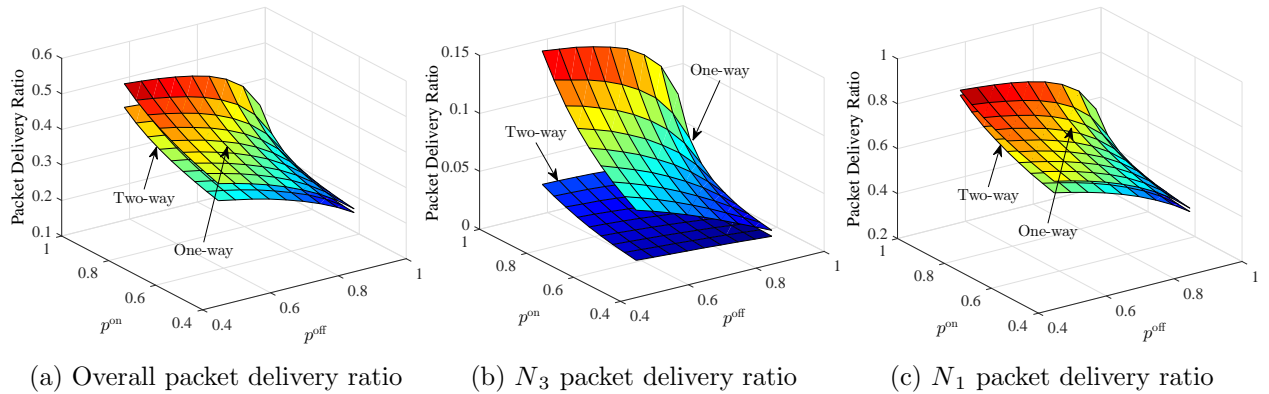


Figure 3.4: The packet delivery ratios of the one-way and two-way scenarios when $M = 3$. Parameters used: $q_1^{\text{on}} = 0.9$, $q_1^{\text{off}} = 0.7$, $p_1^{\text{on}} = q_3^{\text{on}} = 0.85$, $p_1^{\text{off}} = q_3^{\text{off}} = 0.7$, $E_1 = E_3 = 1$, $\delta_1 = \delta_3 = 3$, $\tilde{\delta}_1 = \tilde{\delta}_3 = 1$, $K = 20$.

Based on $\{A_m\}_{m=3}^M$, L_1 , and \mathcal{E}_1 , N_1 schedules a cooperating node N_m for usage in its time slot using Algorithm 3.1.

Using the parameters given in Figure 3.3, the scenario was simulated using Algorithm 3.1 for the case when the system has only one cooperating node N_3 , i.e., $M = 3$, and for the case when the system has two cooperating nodes N_3 and N_4 , i.e., $M = 4$. The simulation results in Figure 3.3 compare the performance of the two cases. To make a fair comparison, the overall performance in the case when $M = 4$ was represented by the packet delivery ratio of N_1 and N_3 . The results show that the performance of N_3 and the performance of N_1 improve when $M = 4$. When $M = 4$, N_1 has a better chance to transmit cooperatively than when $M = 3$, so that more energy will be saved and more packets will be delivered for N_1 . Also, when $M = 4$, each cooperating node cooperates less with N_1 since the nodes share the cooperation between them. Less cooperation with N_1 means more packets delivered for N_3 . Of course, increasing the number of delivered packets for N_1 and N_3 improves their performance, and the overall performance of the system.

3.5.2 Two-Way Cooperative Scenario

In the two-way scenario, N_1 and N_2 both operate as a source and destination, and the remaining $M - 2$ nodes operate as cooperating nodes to relay for N_1 and N_2 , and

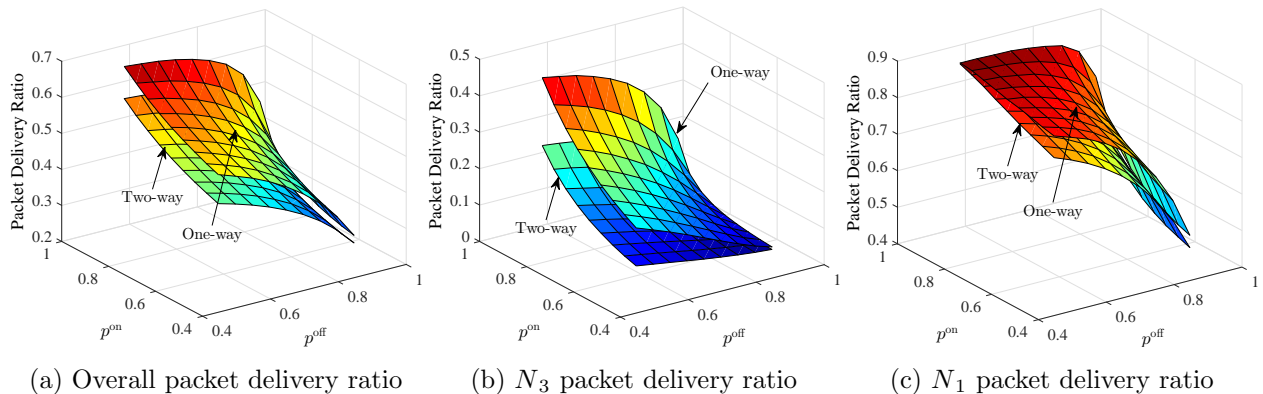


Figure 3.5: The packet delivery ratios of the one-way and two-way scenarios when $M = 4$. Parameters used: $q_1^{\text{on}} = 0.9$, $q_1^{\text{off}} = 0.7$, $p_1^{\text{on}} = q_3^{\text{on}} = 0.85$, $p_1^{\text{off}} = q_3^{\text{off}} = 0.7$, $E_1 = E_3 = 1$, $\delta_1 = \delta_3 = 3$, $\tilde{\delta}_1 = \tilde{\delta}_3 = 1$, $K = 20$.

operate as sources as well. So, in this scenario, all the transmitted packets will flow in two directions, from N_1 and $\{N_m\}_{m=3}^M$ towards N_2 , and from N_2 and $\{N_m\}_{m=3}^M$ towards N_1 . Using Algorithm 3.1, N_1 and N_2 both schedule a node N_m for cooperation using their parameters L_i , \mathcal{E}_i , $i \in \{1, 2\}$, and the cooperating nodes energy statuses $\{A_m\}_{m=3}^M$ as described earlier.

The simulation results in Figure 3.4 illustrate the performance of the algorithm for the two-way scenario when $M = 3$. The results also compare the performance of the two-way scenario with the one-way scenario when $M = 3$. To make the overall performance of the two scenarios fairly comparable, the overall performance of the two-way scenario was represented by the packet delivery ratios of N_1 and N_3 , meaning that the performance of N_2 was not included. The results show that the performance of the two-way scenario is worse than the one-way scenario. This is reasonable since N_3 cooperates with two nodes in the two-way scenario instead of one. Cooperating with two nodes increases the cooperation load on N_3 and thus affects its performance. Also, it decreases the cooperation chance of N_3 with N_1 which affects the performance of N_1 . As a result, the overall performance of the system decreases due to the decrease in the performance of N_1 and N_3 .

The algorithm was also simulated for the two-way scenario with two cooperating nodes N_3 and N_4 , i.e., $M = 4$. Figure 3.5 shows the simulation results for the two-way scenario compared with the one-way scenario when $M = 4$. The overall performance of the two

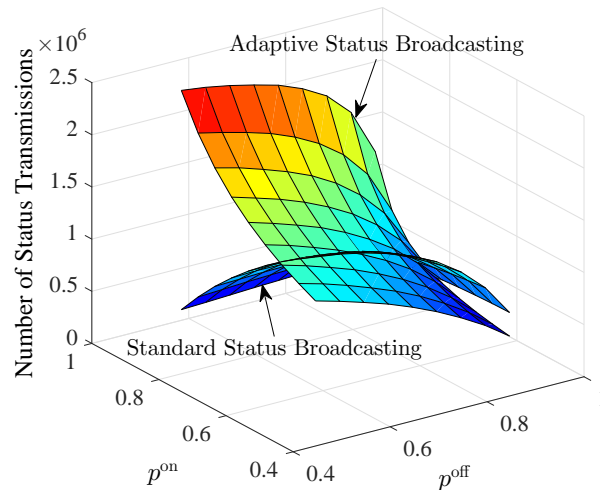


Figure 3.6: The number of status transmissions of the standard and adaptive status broadcastings for the one-way scenario when $M = 3$. Parameters used: $q_1^{\text{on}} = 0.9$, $q_1^{\text{off}} = 0.7$, $p_1^{\text{on}} = q_3^{\text{on}} = 0.85$, $p_1^{\text{off}} = q_3^{\text{off}} = 0.7$, $E_1 = E_3 = 1$, $\delta_1 = \delta_3 = 3$, $\tilde{\delta}_1 = \tilde{\delta}_3 = 1$, $K = 20$.

scenarios is represented by the packet delivery ratio of N_1 and N_3 .

3.5.3 Overhead Reduction

In Section 3.2, we mentioned that broadcasting a cooperating node status in the standard way (whenever it changes) increases status transmissions overhead, and we suggested an adaptive way of a cooperating node status broadcasting that could reduce this burden for low values of p^{on} . Here, we simulate the system when $M = 3$ for the standard and adaptive ways of status broadcasting. Figure 3.6 illustrates the number of status transmissions of N_3 for the two ways. It can be noticed that the number of status transmissions is reduced when $p^{\text{on}} \leq 0.75$, where the energy harvesting probability of N_3 is considered low. Although this burden is reduced for some values of p^{on} , the burden is still relatively high. Therefore, in Chapter 5 we develop a statistical model that enables the source to estimate the energy status of the cooperating nodes.

3.5.4 Fairness

3.5.4.1 Between Cooperating Nodes

In Algorithm 3.1, if there is more than one active cooperating node, the algorithm will arbitrarily select the node with the highest index number. As mentioned earlier in Section 3.3, this selection causes an unfairness problem between the cooperating nodes, and this problem could be solved by selecting the cooperating nodes sequentially instead of always selecting the cooperating node of the highest index. The algorithm was simulated for the two ways of selection for the one-way system when $M = 4$. Figure 3.7 illustrates the simulation results, where Figure 3.7 (a) illustrates the overall packet delivery ratio which is represented by N_1 and N_3 , Figure 3.7 (b) illustrates the packet delivery ratios of the cooperating nodes N_3 and N_4 , and Figure 3.7 (c) illustrates the packet delivery ratio of node N_1 .

It can be noticed from Figure 3.7 (b) that N_3 and N_4 have the same packet delivery ratio when the nodes are selected sequentially. This ensures fairness between the cooperating nodes in contrast to the highest node selection case where the packet delivery ratio of N_4 is less than N_3 . Figure 3.7 (c) shows that the packet delivery ratio of N_1 is virtually the same for the two ways of selection. This is expected since the only difference between the two ways of selection is deciding which node should cooperate with N_1 . Figure 3.7 (a) shows that the overall packet delivery ratio when the highest cooperating node is always selected is better than it when the cooperating nodes are selected sequentially. This is also expected since the cooperating node N_3 is used more often when the cooperating nodes are selected sequentially than when the highest cooperating node is always selected.

3.5.4.2 Between Cooperating Nodes and N_1 and/or N_2

The adaptive scheduling scheme described in Section 3.4 is simulated for the one and two-way scenarios with one cooperating node N_3 , i.e., $M = 3$. In the two scenarios and for the given set of parameters shown in Figure 3.8, the step size of adjusting the number of blocks of the two conditions is set to 900 for an interval length $T = 5000$ blocks. When the divergence gap becomes less than 0.1, the step size is changed to 200, where the gap stays in the range between 0.005 to about 0.05. At this small range, the performance of N_1 and

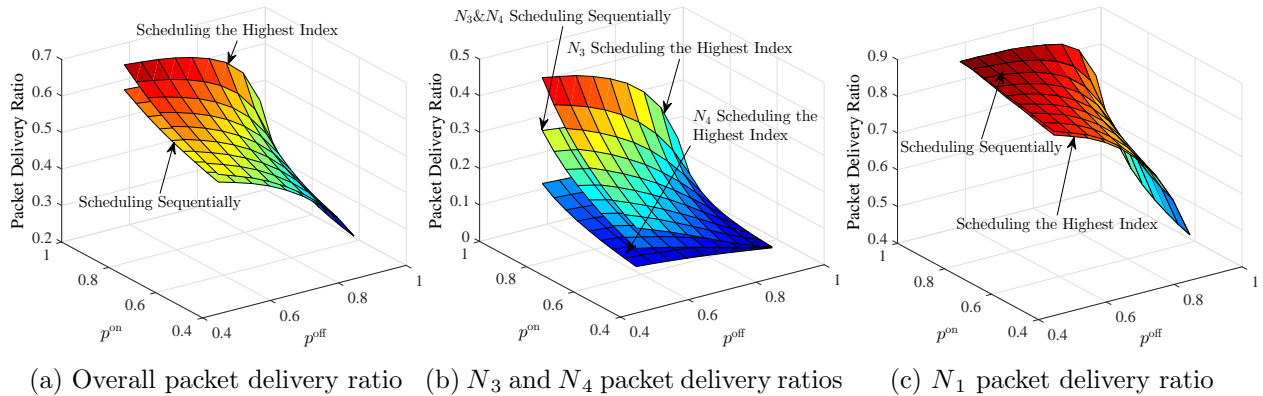


Figure 3.7: The packet delivery ratios of the two ways of cooperating nodes selection (selecting the node of the highest index and selecting the nodes sequentially) for the one-way scenario when $M = 4$. Parameters used: $q_1^{\text{on}} = 0.9$, $q_1^{\text{off}} = 0.7$, $p_1^{\text{on}} = q_3^{\text{on}} = 0.85$, $p_1^{\text{off}} = q_3^{\text{off}} = 0.7$, $E_1 = E_3 = 1$, $\delta_1 = \delta_3 = 3$, $\tilde{\delta}_1 = \tilde{\delta}_3 = 1$, $K = 20$.

the performance N_3 are considered to be converged.

Figure 3.8 (a) illustrates the convergence between N_1 and N_3 performances of the one-way scenario. It can be noticed that the performance of the two nodes converges in the second interval. At interval 41, the performance diverges again due to the change in one of the system parameters, $\tilde{\delta}_1$ is changed to 3. After two intervals, i.e., at interval 43, the performance gets converged again by repeating the same procedures. Before the parameter change, the performance converges one block faster than after the parameter change. This is because the divergence gap between N_1 and N_3 performances in the first interval before the parameter change is smaller than it after the parameter change.

As for the two-way scenario, Figure 3.8 (b) shows the convergence in the performance between the three nodes N_1 , N_2 , and N_3 . The figure shows that the performance converges twice, before and after the change of $\tilde{\delta}_1$. Because of the same reason in the one-way system, the convergence before the parameter change is faster than after the parameter change.

3.6 Conclusions

We upgrade the feedback scheme proposed in Chapter 2 for the scenarios of multiple cooperating nodes, and for one-way and two-way cooperative communications. The upgraded

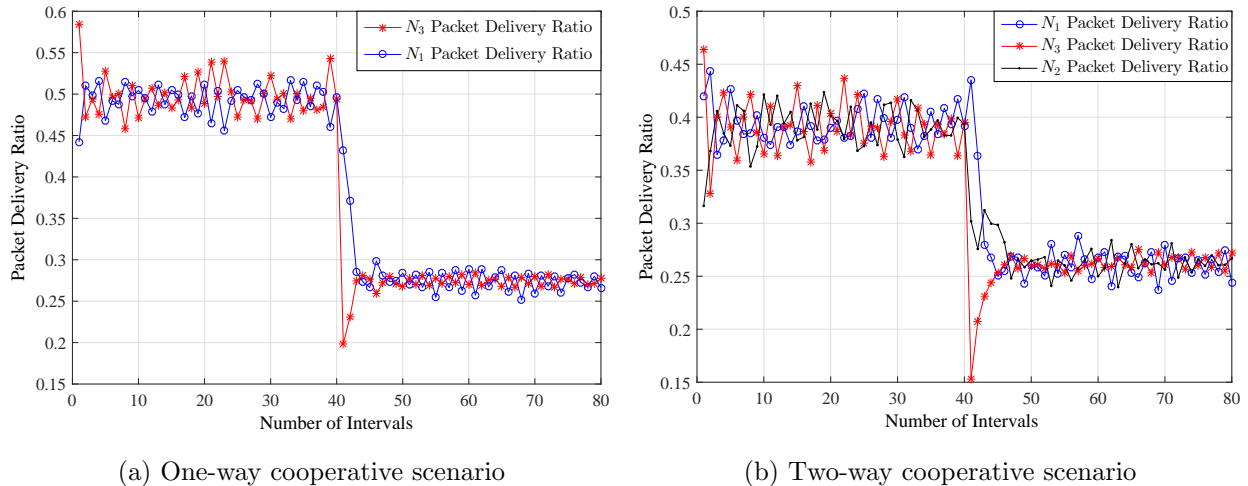


Figure 3.8: The convergence of the packet delivery ratios for the one-way and two-way scenarios when $M = 3$. Parameters used: $q_1^{\text{on}} = q_3^{\text{on}} = 1$, $q_1^{\text{off}} = q_3^{\text{off}} = 0$, $p_1^{\text{on}} = 0.85$, $p_3^{\text{on}} = 0.95$, $p_3^{\text{off}} = 0.55$, $p_1^{\text{off}} = 0.7$, $E_1 = E_3 = 1$, $\delta_1 = 3$, $\tilde{\delta}_1 = \tilde{\delta}_3 = \delta_3 = 1$, $K = 20$.

algorithm communicates in one or two hops, maximizing the packet delivery ratio of the system. It can be extended to three or more hops where in each hop the transmitting node selects a cooperating node from the next hop using the same algorithm. However, this requires some changes in the system model. For example, the number of time slots per a time block would need to be adjusted. In this chapter, we also propose an adaptive scheme that ensures fairness between the nodes and adapts as the parameters change. In addition, we propose a method to decrease the overhead caused by energy statuses broadcasting. Although this method reduces the overhead, it is still relatively high and might be intolerated in some applications. As a solution, in Chapter 5 we develop a statistical model that enables the source in the network to estimate the cooperating node energy status. Lastly, in the adaptive scheme, fairness is considered ensured when the nodes achieve the same performance. This might be unfair in some scenarios, for example, when the penalty on the cooperating node's performance has to be high in order to achieve the same performance as the other node. Moreover, since each transmitting node in the system is fixed and categorized a priori as either a source or a cooperating node, the adaptive scheme will not achieve fairness if the source node achieves higher performance than the cooperating node. Therefore, in the next chapter, we generalize the system model and we propose an analytical-based scheme

that ensures fairness depending on a given penalty function while maximizing the overall performance of the system.

Chapter 4

Generalized Fairness and Optimal Scheduling

4.1 Introduction

In Chapter 2, we proposed a scheduling scheme, called feedback scheme, for a network of a single cooperating node. We then upgraded this scheme in Chapter 3 to include the scenario of multiple cooperating nodes as well as the scenarios of one-way and two-way cooperative communications. In Chapter 3, we also proposed an adaptive scheduling scheme that incorporates fairness in the performance between the transmitting nodes. However, the adaptive scheme considers only the case of absolute fairness, which might be unfair in the scenarios when the penalty on the cooperating node performance has to be high in order to achieve the same performance of the source. Also, because each transmitting node in the system is fixed and categorized a priori as either a source or a cooperating node, the adaptive scheme cannot achieve fairness if the source node achieves higher performance than the cooperating node. Therefore, in this chapter, we first generalize the system model of the three-node network, where each transmitting node can be either a source, a cooperating, or a relay node depending on the system parameters. And then we propose an analytical-based approach scheme, called fair scheduling (FS), that 1) ensures fairness between the performance of the transmitting nodes while maximizing the sum of their packet delivery ratios, and 2) considers not only the case of absolute fairness, but also the case when fairness

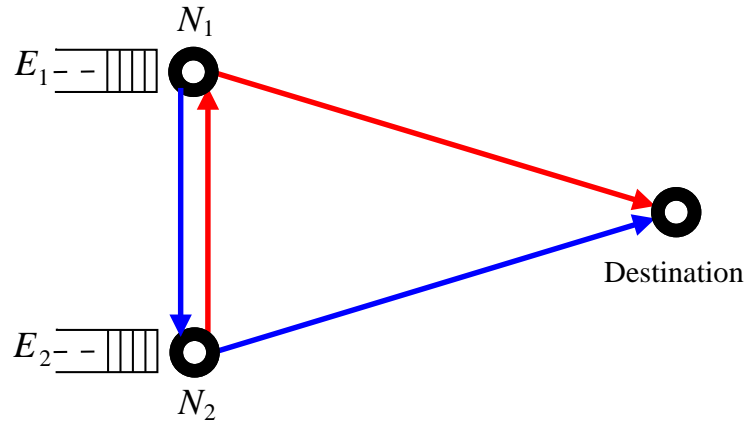


Figure 4.1: A cooperative energy harvesting sensor network of two transmitting nodes (N_1 and N_2) and a destination. E_1 and E_2 are queues representing the energy harvested by N_1 and N_2 , respectively, in the n -th time block, $n \in \{1, 2, \dots, N\}$.

is ensured when the transmitting nodes achieve performance with some difference that is determined by a given penalty function. We also propose a constraint scheduling (CS) scheme that constrains one of the transmitting nodes to achieve a certain performance.

To build the FS and CS schemes, we optimally design the system to operate in a mixed mode which is a combination of two of the three operating modes: noncooperation, cooperation, and relay. For a given penalty function, the simulation results show that the FS scheme provides the optimal operating mode for the system such that fairness is ensured for the transmitting nodes while maximizing the sum of their performances. In addition, the results show that the CS scheme provides the optimal operating mode for the system in order for a transmitting node to achieve a certain performance, if possible.

4.2 System Model

We consider a network of three nodes: two transmitting nodes (N_1 and N_2) and a destination, as depicted in Figure 4.1. Depending on the scheduling purpose, the system operates in a mixed mode which is optimally combined of two of the three operating modes: noncooperation, cooperation, and relay, that are illustrated in Figure 4.2. In noncooperation mode, each transmitting node operates as a Source type 1 (S_1) node, which transmits on its own

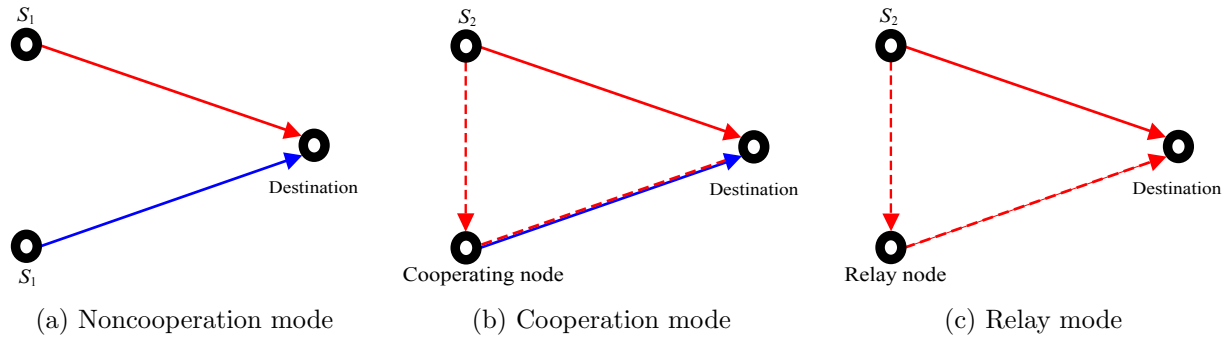


Figure 4.2: The figure illustrates the noncooperation, cooperation, and relay modes, which are used in appropriate combinations to build the FS and CS scheduling schemes. The solid line between S_1 , S_2 , or cooperating node and destination represents the direct transmission of the event of that node to the destination. The dashed path in the cooperation and relay modes represents the relay transmission of S_2 to the destination using cooperating and relay nodes, respectively. In the relay mode, there is no solid line between the relay node and the destination because the relay node has no own transmissions where it drops all its transmissions to help with S_2 transmissions.

directly to the destination. In cooperation mode, one of the transmitting nodes operates as a Source type 2 (S_2) node while the other operates as a cooperating node. The S_2 node transmits its events to destination either directly or through the cooperating node, and the cooperating node assists cooperative communication between S_2 and destination, as well as it transmits its own events directly to the destination. In relay mode, one of the transmitting nodes operates as an S_2 node similar to the cooperation mode. In the relay mode, however, the S_2 node transmits cooperatively using the other transmitting node that operates as a relay node, which discards all of its own events to help with the transmissions of the S_2 node to the destination.

The main assumptions and notations that are used for the system model throughout this chapter are:

1. Each transmitting node is equipped with energy harvesting devices and a rechargeable battery with capacity K .
2. We use a discrete-time model where time is divided into N blocks.

3. There is at most one event generated per transmitting node per block. We assume that sensors are monitoring different events so that their event generation processes are independent. As in [65], the event generation process of each node is modeled as a Bernoulli process, where in the time block n , $n \in \{1, 2, \dots, N\}$, node N_i , $i \in \{1, 2\}$ generates an event $\mathcal{E}_i[n] = 1$ with probability q_i .
4. The energy arrival process is modeled as a discrete random process. In the n -th block, N_i , $i \in \{1, 2\}$, harvests E_i amount of energy, respectively, where $E_i \in \{0, 1, \dots, \tilde{K}\}$ and $\tilde{K} \leq K$ is the maximum amount of energy that can be harvested in one block. Because a cooperation scenario is considered meaning that sensors locate close to each other and thus experience a similar environment, the energy harvesting processes of the two nodes are assumed to be correlated, where the joint probability of any two energy arrivals E_1 and E_2 is $p(E_1, E_2)$. The marginal probability of E_i , $i \in \{1, 2\}$ is denoted by $p^{(i)}(E_i)$.
5. The energy harvested in the n -th block can be used only in a later time block.
6. We consider a real-time monitoring deployment scenario where no packets are buffered.
7. We assume that the length of each time block is enough to transmit only one event. So that in the cooperation mode, if S_2 and the cooperating node both have an event generated and sufficient energy for transmission in the same time block, the cooperating node will cooperate with S_2 and drop its transmission.
8. As in [13] and [14], the battery of a transmitting node is modeled as a buffer, and that each slot in the buffer can hold one energy unit. The maximum number of quanta that can be stored is K so that the set of possible energy levels of node N_i is $L_i^x = \{0, 1, \dots, K\}$, $x \in \{n, c, r\}$, where the superscript n is to indicate the noncooperation mode, the superscript c is to indicate the cooperation mode, and the superscript r is to indicate the relay mode.
9. We assume that δ_i is the energy required to reliably transmit information about the event \mathcal{E}_i from the transmitting node N_i to the destination, and $\tilde{\delta}$ is the energy required

for reliable transmission between N_1 and N_2 in the cooperation and relay modes, where $\tilde{\delta} < \delta_i$ and $\tilde{\delta}, \delta_i \in \{0, 1, \dots, K\}$.

10. We denote the achieved packet delivery ratio of node N_i , $i \in \{1, 2\}$ by $\Delta_i \in \{\Delta_i^n, \Delta_i^c, \Delta_i^r, \Delta_i^m\}$, where the superscripts n, c, and r are as defined in Assumption 9 and the superscript m is to indicate the mixed mode.

4.3 Operating Modes

As stated earlier, the system operates in a mixed mode which is a combination of two of the three operating modes; noncooperation, cooperation, and relay. In order to design the appropriate mixed mode, depending on the scheduling purpose, we first need to study these three modes and calculate the packet delivery ratio achieved by each transmitting node in each mode.

4.3.1 Noncooperation Mode

In this operating mode, the transmitting node N_i , $i \in \{1, 2\}$ operates as an S_1 node which transmits its generated event $\mathcal{E}_i[n]$, $n \in \{1, 2, \dots, N\}$ on its own to the destination over the N time blocks. The event $\mathcal{E}_i[n]$ is considered to be successfully delivered to the destination if N_i is energized in the n -th time block, i.e., its energy battery level $L_i^n[n] \geq \delta_i$. Thus, the packet delivery ratio Δ_i^n of node N_i over the N time blocks is

$$\Delta_i^n = \frac{P(\mathcal{E}_i[n] = 1) \Pr(L_i^n[n] \geq \delta_i)N}{\Pr(\mathcal{E}_i[n] = 1)N} = \Pr(L_i^n[n] \geq \delta_i), \quad (4.1)$$

and the energy battery level of the node is

$$L_i^n[n] = \min \{L_i^n[n-1] + E_i[n-1] - \mathbb{1}_{\{L_i^n[n-1] \geq \delta_i\}} \mathcal{E}_i[n-1], K\}, \quad (4.2)$$

where $\mathbb{1}_{\{\cdot\}}$ is the indicator function. $L_i^n[n]$ is set to equal to the minimum between the two terms shown in (4.2) because of battery overflow, which might occur due to the assumption that the battery capacity of the transmitting nodes is finite. Because $L_i^n[n]$ depends only on the previous energy battery level $L_i^n[n-1]$, $L_i^n[n]$ is modeled as a Markov chain with

state space $\{0, 1, \dots, K\}$, where the transition between any two states depends on $E_i[n-1]$ and $\mathcal{E}_i[n-1]$. Let m and n be the current and the previous states of energy battery level, respectively, and let $z = m - n$ and $w = m - n + \delta_i$. Then given q_i and $p^{(i)}(E_i)$, $E_i \in \{0, 1, \dots, \tilde{K}\}$, the transition probability $P_{n,m}^{(i)} = \Pr(L_i[n] = m | L_i[n-1] = n)$ of node N_i , $i \in \{1, 2\}$ between any two states $n, m \in \{0, 1, \dots, K\}$ is

$$P_{n,m}^{(i)} = \begin{cases} p^{(i)}(z) & n < \delta_i, m < K \\ p^{(i)}(w)q_i + p^{(i)}(z)(1-q_i) & n \geq \delta_i, m < K \\ \sum_{k=z}^{\tilde{K}} p^{(i)}(k)I_1 & n < \delta_i, m = K \\ \sum_{k=z}^{w-1} p^{(i)}(k)(1-q_i)I_2 + \sum_{k=w}^{\tilde{K}} p^{(i)}(k)I_3 & n \geq \delta_i, m = K, \end{cases} \quad (4.3)$$

where $I_1 = \mathbb{1}_{\{z \leq \tilde{K}\}}$, $I_2 = \mathbb{1}_{\{z \leq w-1\}}$, and $I_3 = \mathbb{1}_{\{w \leq \tilde{K}\}}$ are the indicator functions. Let $\mathbf{P}^{(i)}$ be the transition matrix of the Markov chain where its (n, m) -th element is given by $P_{n,m}^{(i)}$. Since this Markov chain is finite, irreducible, and aperiodic, it has average (steady state) probabilities for all states, energy battery levels. As in [65], we can obtain these average probabilities using the eigen decomposition of the matrix $\mathbf{P}^{(i)}$. Such that, the eigen vector $\boldsymbol{\pi}^{(i)} = [\pi_0^{(i)}, \pi_1^{(i)}, \dots, \pi_K^{(i)}]^\top$ of $\mathbf{P}^{(i)}$ that corresponds to its unity eigen value represents the average state probabilities, where $\pi_{i,k}$, $k = \{0, \dots, K\}$ is the average probability of the k -th energy battery level of node N_i , $i \in \{1, 2\}$. Using the average probabilities, the packet delivery ratio of N_i in (4.1) becomes

$$\Delta_i^n = \Pr(L_i^n \geq \delta_i) = \sum_{k=\delta_i}^K \pi_k^{(i)}. \quad (4.4)$$

4.3.2 Cooperation Mode

In cooperation mode, one of the transmitting nodes, say N_i , $i \in \{1, 2\}$, operates as an S_2 while the other transmitting node N_j , $j \in \{1, 2\}$, $i \neq j$, operates as a cooperating node. As stated in Section 4.2, the S_2 node transmits its events to destination either directly or through the cooperating node, and the cooperating node assists cooperative communication between S_2 and destination, as well as it transmits its own events to the destination. Algorithm 4.1 explains the cooperation scenario of N_j with N_i . It is similar to Algorithm 2.1, however,

Algorithm 4.1 Cooperation Mode

(a) S_2 node $N_i, i \in \{1, 2\}$	(b) Cooperating node $N_j, j \in \{1, 2\}, i \neq j$
1: Inputs: $\mathcal{E}_i[n], L_i^c[n], A_j^c[n], \tilde{\delta}, \delta_i$; 2: Outputs: Transmission action of N_i ; 3: if $\mathcal{E}_i[n] = 1$ then 4: if $L_i^c[n] \geq \delta_i$ AND $A_j^c[n] = 0$ then 5: N_i action = <i>direct transmission</i> ; 6: elseif $L_i^c[n] \geq \tilde{\delta}$ AND $A_j^c[n] = 1$ then 7: N_i action = <i>relay transmission</i> ; 8: else 9: N_i action = <i>no transmission</i> ; 10: endif ; 11: else 12: N_i action = <i>no transmission</i> ; 13: endif	1: Inputs: $\mathcal{E}_j[n], L_j^c[n], \delta_j$; 2: Outputs: Transmission action of N_j ; 3: if $L_j^c[n] \geq \delta_j$ then 4: Sense the link N_i - N_j for N_i action; 5: if N_i action = <i>relay transmission</i> then 6: N_j action = <i>relay transmission</i> ; 7: N_j 's event will be discarded, if any; 8: elseif N_i action = <i>no transmission</i> then 9: if $\mathcal{E}_j[n] = 1$ then 10: N_j action = <i>own-traffic transmission</i> ; 11: else 12: N_j action = <i>no transmission</i> ; 13: endif 14: endif 15: else 16: N_j action = <i>no transmission</i> ; 17: endif

here there is no need for using a TDMA protocol because of the assumption that only one event is reported per time block. As can be seen in Algorithm 4.1, the decision on the S_2 transmission action in the n -th time block is made based on the energy status A_j^c of the cooperating node N_j , which is given by

$$A_j^c[n] = \begin{cases} 1 & \text{if } L_j^c[n] \geq \delta_j \\ 0 & \text{otherwise.} \end{cases} \quad (4.5)$$

Using $A_j^c[n]$ as shown in part (a) of the algorithm, the S_2 node N_i in each time block takes one of three transmission actions: *direct transmission*, *relay transmission*, or *no transmission*. In direct transmission action, S_2 transmits its event directly to the destination if it has an event generated $\mathcal{E}_i[n] = 1$, it is energized $L_i^c[n] \geq \delta_i$, and the cooperating node N_j is not energized $A_j^c[n] = 0$. In relay transmission action, S_2 transmits its event to the destination using the cooperating node if it has an event generated $\mathcal{E}_i[n] = 1$, it is energized for relay transmission $L_i^c[n] \geq \tilde{\delta}$, and the cooperating node N_j is energized $A_j^c[n] = 1$. In both of these two transmission actions, the event of S_2 is reported successfully to the destination. If none of these two transmission actions is taken, the transmission action of S_2 will be *no transmission* where no event will be reported for S_2 .

As shown in part (b) of the algorithm, the cooperating node N_j also takes one of three transmission actions: *own-traffic transmission*, *relay transmission*, or *no transmission*. In each time block, if $L_j^c[n] \geq \delta_j$, the cooperating node senses the transmission link N_i - N_j . If there is a transmission, i.e., S_2 has a relay transmission, the cooperating node takes *relay transmission* action to forward the transmission of S_2 . In this scenario, if the cooperating node has an event generated, its event will be discarded due to the assumption that only one event is reported per time block. If there is no transmission, the cooperating node takes *own-traffic transmission* action if it has an event generated $\mathcal{E}_j[n] = 1$, or *no transmission* action if it has no event generated $\mathcal{E}_j[n] = 0$. If the own-traffic transmission action is taken, the event of the cooperating node is reported successfully to the basestation. If $L_j^c[n] < \delta_j$, the cooperating node does not need to sense the transmission link N_i - N_j and takes *no transmission* action, where no event will be reported for the cooperating node.

Let d_1^c and d_2^c be the events of the direct and relay transmission actions of the S_2 node

N_i , respectively, and let d_3^c and d_4^c be the events of the own-traffic and relay transmission actions of the cooperating node N_j , where from Algorithm 4.1

$$d_1^c[n] = \begin{cases} 1 & \text{if } (\mathcal{E}_i[n] = 1 \cap L_i^c[n] \geq \delta_i \cap A_j^c[n] = 0) \\ 0 & \text{otherwise,} \end{cases} \quad (4.6)$$

$$d_2^c[n] = \begin{cases} 1 & \text{if } (\mathcal{E}_i[n] = 1 \cap L_i^c[n] \geq \tilde{\delta} \cap A_j^c[n] = 1) \\ 0 & \text{otherwise,} \end{cases} \quad (4.7)$$

$$d_3^c[n] = \begin{cases} 1 & \text{if } (\mathcal{E}_j[n] = 1 \cap L_j^c[n] \geq \delta_j) \cap (\mathcal{E}_i[n] = 0 \cup L_i^c[n] < \tilde{\delta}) \\ 0 & \text{otherwise,} \end{cases} \quad (4.8)$$

and $d_4^c = d_2^c$. Then, the energy battery level L_i^c of N_i is

$$L_i^c[n] = \min \{L_i^c[n-1] + E_i[n-1] - \tilde{\delta}d_2^c[n-1] - \delta_id_1^c[n-1], K\}, \quad (4.9)$$

and the energy battery level L_j^c of N_j is

$$L_j^c[n] = \min \{L_j^c[n-1] + E_j[n-1] - \delta_jd_4^c[n-1] - \delta_jd_3^c[n-1], K\}. \quad (4.10)$$

The current energy battery levels $L_i^c[n]$ and $L_j^c[n]$ in (4.9) and (4.10), respectively, are dependent, and each depends only on the energy battery levels of the previous time block $L_i^c[n-1]$ and $L_j^c[n-1]$, so that their joint distribution is modeled as a Markov chain with a state space $\{(0, 0), (0, 1), \dots, (0, K), (1, 0), \dots, (1, K), \dots, (K, 0), \dots, (K, K)\}$. Let m and n , $m, n \in \{0, 1, \dots, K\}$ be the previous energy battery levels of the source and cooperating nodes $L_i^c[n-1]$ and $L_j^c[n-1]$, respectively, and let u and v , $u, v \in \{0, 1, \dots, K\}$ be their current energy battery levels $L_i^c[n]$ and $L_j^c[n]$, respectively. Define $w = u - m$ and $z = v - n$. Then from (4.9) and (4.10), the transition probability $P_{s_1, s_2} = \Pr(s_1 = (u, v) | s_2 = (m, n))$ from state (m, n) to state (u, v) if $u < K$ and $v < K$ is

$$P_{s_1, s_2} = \begin{cases} p(w, z) & m < \delta_i, n < \delta_j, \\ p(w, z + \delta_j)q^r + p(w, z)(1 - q^r) & m < \tilde{\delta}, n \geq \delta_j, \\ p(w + \tilde{\delta}, z + \delta_j)q^s + (p(w, z + \delta_j)q^r + p(w, z)(1 - q^r))(1 - q^s) & m \geq \tilde{\delta}, n \geq \delta_j, \\ p(w + \delta_i, z)q^s + p(w, z)(1 - q^s) & m \geq \delta_i, n < \delta_j, \end{cases} \quad (4.11)$$

where the first case is for the scenario when none of the nodes has sufficient energy for any transmission; the second case is for the scenario when the source node has no sufficient energy for any transmission while the cooperating node does; the third case is for the scenario when the source node and cooperating node both have sufficient energy for cooperative transmission, and the fourth case is for the scenario when the source has sufficient energy for direct transmission and the cooperating node has no sufficient energy for any transmission. In each of these four cases, if $u = K$ and/or $v = K$, the transition from state (m,n) to state (u,v) will include all events that energy arrival in the previous time block can cause battery overflow. For example, in the first case when $m < \delta_i$ and $n < \delta_j$, $P_{s_1,s_2} = \sum_{x=z}^{\tilde{K}} p_{(w,x)}$ if $u < K$ and $v = K$, $P_{s_1,s_2} = \sum_{y=w}^{\tilde{K}} p_{(y,z)}$ if $u = K$ and $v < K$, and $P_{s_1,s_2} = \sum_{y=w}^{\tilde{K}} \sum_{x=z}^{\tilde{K}} p_{(y,x)}$ if $u = K$ and $v = K$.

Let \mathbf{P} be the transition matrix of the Markov chain where its elements are given by P_{s_1,s_2} . Then, we can obtain the marginal probabilities $\Pr(L_i^c)$ and $\Pr(L_j^c)$ as well as the joint probability $\Pr(L_i^c, L_j^c)$ using eigen decomposition of \mathbf{P} . Using these probabilities, the packet delivery ratio Δ_i^c of S_2 is

$$\Delta_i^c = \frac{[\Pr(d_1^c = 1) + \Pr(d_2^c = 1)]N}{\Pr(\mathcal{E}_i = 1)N}, \quad (4.12)$$

$$\Delta_i^c = \Pr(L_i^c \geq \delta_i \cap L_j^c < \delta_j) + \Pr(L_i^c \geq \tilde{\delta} \cap L_j^c \geq \delta_j), \quad (4.13)$$

and the packet delivery ratio Δ_j^c of the cooperating node is

$$\Delta_j^c = \frac{\Pr(d_3^c = 1)N}{\Pr(\mathcal{E}_i = 1)N}, \quad (4.14)$$

$$\begin{aligned} \Delta_j^c &= (1 - q_i) \Pr(L_j^c \geq \delta_j) + \Pr(L_i^c < \tilde{\delta} \cap L_j^c \geq \delta_j) - \\ &\quad (1 - q_i) \Pr(L_i^c < \tilde{\delta} \cap L_j^c \geq \delta_j). \end{aligned} \quad (4.15)$$

4.3.3 Relay mode

The relay mode is similar to the cooperation mode. However, instead of operating as a cooperating node, node N_j in the relay mode operates as a relay node, which drops all its own transmissions to help with the transmissions of node N_i , the S_2 node. Algorithm

4.1 can represent the relay mode if the lines (9-13) in part (b) are replaced by the line: N_j action = *no transmission*, and superscript c is replaced by r in the two parts. Consequently, the S_2 node N_i will still have the same three transmission actions, while the relay node N_j will have two transmission actions instead of the three that are *relay transmission* and *no transmission*.

Let A_j^r be the energy status of the relay node, then the events of the direct and relay transmission actions d_1^r and d_2^r , respectively, of the S_2 node N_i in the n -th time block are

$$d_1^r[n] = \begin{cases} 1 & \text{if } (\mathcal{E}_i[n] = 1 \cap L_i^r[n] \geq \delta_i \cap A_j^r[n] = 0) \\ 0 & \text{otherwise,} \end{cases} \quad (4.16)$$

$$d_2^r[n] = \begin{cases} 1 & \text{if } (\mathcal{E}_i[n] = 1 \cap L_i^r[n] \geq \tilde{\delta} \cap A_j^r[n] = 1) \\ 0 & \text{otherwise,} \end{cases} \quad (4.17)$$

and the event of the relay transmission action of the relay node N_j $d_4^r[n] = d_2^r[n]$. As a result, the energy battery level L_i^r of N_i is

$$L_i^r[n] = \min \{ L_i^r[n-1] + E_i[n-1] - \tilde{\delta} d_2^r[n-1] - \delta_i d_1^r[n-1], K \}, \quad (4.18)$$

and the energy battery level L_j^r of N_j is

$$L_j^r[n] = \min \{ L_j^r[n-1] + E_j[n-1] - \delta_j d_4^r[n-1], K \}, \quad (4.19)$$

As in cooperation mode, the joint distribution of $L_i^r[n]$ and $L_j^r[n]$ is modeled as a Markov chain with the same state space. The transition matrix of L_i^c and L_j^c described in (4.11) can represent the transition matrix of L_i^r and L_j^r if we set $q^r = 1$ and replace $z + \delta_j$ by z only in the terms that have q^r . From the transition matrix, we can find the probabilities $\Pr(L_i^r)$, $\Pr(L_j^r)$, and $\Pr(L_i^r, L_j^r)$. Using these probabilities, the packet delivery ratio Δ_i^r of S_2 is

$$\Delta_i^r = \frac{[\Pr(d_1^r = 1) + \Pr(d_2^r = 1)]N}{\Pr(\mathcal{E}_i = 1)N}, \quad (4.20)$$

$$\Delta_i^r = \Pr(L_i^r \geq \delta_i \cap L_j^r < \delta_j) + \Pr(L_i^r \geq \tilde{\delta} \cap L_j^r \geq \delta_j), \quad (4.21)$$

and the packet delivery ratio of the relay node $\Delta_j^r = 0$, which is due to the fact that the relay node drops all its own transmissions to help with the transmissions of S_2 .

To compare the packet delivery ratios achieved by each transmitting node in the three previous modes, assume that the transmitting node $N_i, i \in \{1, 2\}$ and the transmitting node $N_j, j \in \{1, 2\}, j \neq i$, each operates as an S_1 node in the noncooperation mode, and N_i operates as an S_2 node in cooperation and relay modes and N_j operates as a cooperating node and as a relay node in cooperation and relay modes, respectively. Then for any given set of parameters, the performance of node N_i in relay mode is higher than or equal to its performance in cooperation mode, and this is higher than or equal to its performance in noncooperation mode, i.e., $\Delta_i^r \geq \Delta_i^c \geq \Delta_i^n$. This holds the opposite in the case of node N_j where its performance in noncooperation mode is higher than or equal to its performance in cooperation mode, and this is higher than or equal to its performance in relay mode, i.e., $\Delta_j^n \geq \Delta_j^c \geq \Delta_j^r = 0$. This is because in cooperation mode S_2 sometimes transmits with lower energy via node N_j , which saves S_2 some amount of energy that can be used to transmit more events than in noncooperation mode. In relay mode, S_2 transmits more frequently via node N_j than in cooperation mode. Thus, more energy will be saved and more events will be transmitted. As for node N_j , it achieves lower performance in cooperation mode than in noncooperation mode for two reasons. First, some of its harvested energy will rather be used to forward some events of S_2 than transmitting its own. Second, some events of N_j will be dropped even when enough energy is available due to Assumption 8. In relay mode, node N_j spends all its harvested energy to forward the events of S_2 by dropping all its generated events. Therefore, its performance in relay mode is lower than cooperation and noncooperation modes.

4.3.4 Mixed mode

In mixed mode, the system operates in two of the three previous modes over the N time blocks. Such that, the system operates in the first mode in the first n time blocks. After that, i.e., in the remaining $N - n$ blocks, the system operates in the second mode, so that the packet delivery ratio of each node will be the summation of its successfully delivered events in the two modes over its total generated events in the N time blocks. For any mixed mode, let $x, y \in \{n, c, r\}, x \neq y$, be the first and the second operating modes, respectively,

where n, c , and r are as defined in Assumption 9. Then, the packet delivery ratio of the transmitting node $N_i, i \in \{1, 2\}$ of that mixed mode will be

$$\Delta_i^m(x, y, n) = \frac{\Delta_i^x n + (N - n)\Delta_i^y}{N}. \quad (4.22)$$

From (4.22) if $n = N$, the system will operate in x mode regardless of y , and the node will achieve the packet delivery ratio Δ_i^x . In contrast, if $n = 0$, the system will operate in y mode regardless of x , and the node will achieve the packet delivery ratio Δ_i^y . In the first case y is considered do not care while in the second case x is considered do not care.

4.4 Scheduling Schemes

4.4.1 Fair Scheduling (FS) Scheme

In noncooperation mode, one of the transmitting nodes may achieve lower packet delivery ratio than the other. Thus, it will successfully deliver lower percentage of its total generated events to the destination over the N time blocks. Therefore, here we address the issue of event delivering with fairness from the transmitting nodes to the destination while providing the optimal sum of their packet delivery ratios. The optimal or fair packet delivery ratios can be achieved by providing the optimal scheduling or the optimal operating mode for the system.

Assume that in noncooperation mode, node $N_j, j \in \{1, 2\}$ achieves a packet delivery ratio that is higher than or equal to node $N_i, i \in \{1, 2\}, i \neq j$. Then for fairness, intuitively node N_j should cooperate with or relay for node N_i , but by how much? Let the system operate in mixed x - n mode, where $x \in \{c, r\}$, and let node N_i operate as an S_2 in x mode as it achieves lower performance in noncooperation mode. Using (4.22), the packet delivery ratios Δ_i and Δ_j of N_i and N_j , respectively, achieved in the mixed x - n mode over the N time blocks can be expressed as

$$\Delta_i = \Delta_i^n + \frac{n(\Delta_i^x - \Delta_i^n)}{N}, \quad (4.23)$$

$$\Delta_j = \Delta_j^n + \frac{n(\Delta_j^x - \Delta_j^n)}{N}. \quad (4.24)$$

Because in x mode node N_i operates as an S_2 and node N_j operates as a cooperating or relay node depending on x , we have that $\Delta_i^r \geq \Delta_i^c \geq \Delta_i^n$ and $\Delta_j^n \geq \Delta_j^c \geq \Delta_j^r$ as explained in Section 4.3.3. Thus, from (4.23) and (4.24), as n increases for a given $x \in \{c, r\}$, the packet delivery ratio of node N_i increases linearly while the packet delivery ratio of N_j decreases linearly. This implies that as n increases, the difference between the performance of the two nodes decreases until it reaches to its minimum at the value of n where Δ_i and Δ_j intersect. After that, the difference will start increasing because the performance of N_j becomes lower than N_i . Hence, before the difference is minimized, the more node N_j cooperates with or relays for node N_i , the better fairness is achieved in the performance of the two nodes. However, the higher penalty is in the decrease of node N_j 's performance. Therefore, in order to compromise, we achieve fairness based on a given penalty function while maximizing the sum of the packet delivery ratios of the nodes. Define the penalty function $\Gamma(|\Delta_j - \Delta_i|)$ as a monotonic increasing function in the absolute difference between the performance of the two nodes, where as $\Gamma(|\Delta_j - \Delta_i|)$ decreases, the better fairness is achieved and the higher penalty is in the decrease of node N_j 's performance. For a given $\Gamma(|\Delta_j - \Delta_i|)$, the problem of fairness under the constraints that $x \in \{c, r\}$ and $0 \leq n \leq N$ is formulated as

$$\begin{aligned} & \max_{\Delta_j, \Delta_i} \quad \max_{n, x} \quad \Delta_j + \Delta_i - \Gamma(|\Delta_j - \Delta_i|), \\ & \text{subject to} \quad x \in \{c, r\}, \\ & \quad \quad \quad 0 \leq n \leq N. \end{aligned} \tag{4.25}$$

For a given $x \in \{c, r\}$, we have from (4.23) and (4.24) that $(\Delta_j + \Delta_i)$ is a linear function that decays as n increases. Therefore, because $\Gamma(|\Delta_j - \Delta_i|)$ is a convex function that monotonically increases from both sides of its minimum, the cost function in (4.25) will be concave over n for a given x , and its maximum is at some value of n that is less than the value of n at which Δ_i and Δ_j intersect. Note that because the cost function is concave in both when $x = c$ and $x = r$, it is also maximized over Δ_i and Δ_j as can be seen from (4.25).

Define n^c and n^r as the values of n that maximizes the cost function when $x = c$ and when $x = r$, respectively, and these values can be solved for by taking the derivative of the cost function and setting it to 0. For some penalty functions, n^c can be a value that is higher than N . This happens when node N_i harvests energy with a rate that is much lower than its

Algorithm 4.2 FS Scheme

- 1: **Goal:** Achieving fairness while maximizing the sum $(\Delta_1 + \Delta_2)$ for a given $\Gamma(|\Delta_1 - \Delta_2|)$;
 - 2: **Inputs:** $q_1, q_2, \tilde{\delta}, \delta_1, \delta_2, \tilde{K}, K, p(E_1, E_2), \Gamma(|\Delta_1 - \Delta_2|)$;
 - 3: **Outputs:** $n^*, x^*, \Delta_1^*, \Delta_2^*$;
 - 4: Derive n^x , which is the value of n that makes the derivative of (4.25) w.r.t n equal to 0;
 - 5: Generate the distributions $\Pr(L_1^n)$ and $\Pr(L_2^n)$ as described in Section 4.3.1;
 - 6: Calculate Δ_1^n and Δ_2^n using (6.3);
 - 7: **if** $\Delta_1^n \geq \Delta_2^n$ **then**
 - 8: $i = 2, j = 1$;
 - 9: **else**
 - 10: $i = 1, j = 2$;
 - 11: **endif**
 - 12: Let $N_j =$ Cooperating node, $N_i = S_2$ node, and form $\Pr(L_1^c, L_2^c)$ as in Section 4.3.2;
 - 13: Let $N_j =$ Relay node, $N_i = S_2$ node, and form $\Pr(L_1^r, L_2^r)$ as in Section 4.3.3;
 - 14: Calculate Δ_i^c, Δ_j^c , and Δ_i^r using (4.13), (4.15), and (4.21), respectively, and set $\Delta_j^r = 0$;
 - 15: Calculate n^c and n^r using $\Delta_i^c, \Delta_j^c, \Delta_i^r, \Delta_j^r$, and the equation derived in step 4;
 - 16: **if** $0 \leq n^c \leq N$, then
 - 17: $x^* = c, n^* = n^c, \Delta_i^* = \Delta_i^m(c, n, n^c)$, and $\Delta_j^* = \Delta_j^m(c, n, n^c)$;
 - 18: **elseif** $0 \leq n^r \leq N$
 - 19: $x^* = r, n^* = n^r, \Delta_i^* = \Delta_i^m(r, n, n^r)$, and $\Delta_j^* = \Delta_j^m(r, n, n^r)$;
 - 20: **else**
 - 21: $x^* =$ do not care, $n^* = 0, \Delta_i^* = \Delta_i^n$, and $\Delta_j^* = \Delta_j^n$;
 - 22: **endif**
-

event generation rate, where Δ_i will still be lower than Δ_j even when N_j cooperates with N_i the all N time blocks. In this case, Δ_i and Δ_j will intersect at a value of $n > N$, which results in n^c to be higher than N . This holds the opposite for n^r , which is always a value that is less than N , and this is because Δ_i and Δ_j will always intersect at some value of $0 \leq n \leq N$ due to the fact that in relay mode $\Delta_j^r = 0$. On the other hand, for some penalty functions, n^x , $x \in \{c, r\}$ can be a value that is less than 0, which occurs when fairness for the given penalty function needs to be achieved when the difference between Δ_j and Δ_i is higher than $\Delta_j^n - \Delta_i^n$. Because $\Delta_j^n - \Delta_i^n$, which occurs when $n = 0$, is the maximum difference over the range that is less than the value of n at which Δ_i and Δ_j intersect, achieving a difference that is higher than $\Delta_j^n - \Delta_i^n$ can happen only if n^x is less than 0.

The optimal solution n^* and x^* for the cost function in (4.25) is determined based on the location of its maximum when $x = c$ and its maximum when $x = r$, i.e., n^c and n^r . If $n^c \in [0, N]$, then $x^* = c$ and $n^* = n^c$ regardless of where the cost function is maximized at when $x = r$. This is because when $x = c$, $(\Delta_j + \Delta_i)$ decays slower than when $x = r$ due the fact that in relay mode $\Delta_j^r = 0$. Thus, the maximum of the cost function when $x = c$ will be higher than when $x = r$ for the same penalty function, so that the optimal solution is when $x^* = c$ and $n^* = n^c$. If $n^r \in [0, N]$ and $n^c \notin [0, N]$, then $x^* = r$ and $n^* = n^r$. If $n^c, n^r < 0$, then $n^* = 0$ and x^* is do not care. In this case, the system will operate in noncooperation mode where the closest performance to the optimal will be achieved. The values x^* and n^* provide the optimal mixed mode of the system for the given penalty function, and by using them, the optimal performance of the two nodes Δ_i^* and Δ_j^* can be calculated using (4.23) and (4.24), respectively. Algorithm 4.2 summarizes the process of how to find the optimal solution for the cost function in (4.25).

As a simple example, we can set $\Gamma = |\Delta_j - \Delta_i|^\alpha$, where $\alpha > 1$. By taking the derivative of the cost function in (4.25) containing this monotonic increasing penalty function, the value of n that maximizes the cost function for a given $x \in \{c, r\}$ is

$$n^x = \frac{N}{(\Delta_j^x - \Delta_j^n) - (\Delta_i^x - \Delta_i^n)} \left[\left(\frac{(\Delta_j^x - \Delta_j^n) + (\Delta_i^x - \Delta_i^n)}{\alpha [(\Delta_j^x - \Delta_j^n) - (\Delta_i^x - \Delta_i^n)]} \right)^{\alpha-1} - (\Delta_j^n - \Delta_i^n) \right]. \quad (4.26)$$

By following Algorithm 4.2, the optimal value of x and the optimal value of n can be found for any given set of system parameters as we will see later in the simulation results.

Algorithm 4.3 CS Scheme

- 1: **Goal:** If possible, node N_1 achieves the performance γ , i.e., $\Delta_1 = \gamma$;
 - 2: **Inputs:** $q_1, q_2, \tilde{\delta}, \delta_1, \delta_2, \tilde{K}, K, p(E_1, E_2), \gamma$;
 - 3: **Outputs:** $n^*, x^*, \Delta_1^*, \Delta_2^*$;
 - 4: Generate $\Pr(L_1^n)$ and $\Pr(L_2^n)$ as in Section 4.3.1, then calculate Δ_1^n, Δ_2^n using (6.3);
 - 5: **If** $\gamma \leq \Delta_1^n$
 - 6: Let $N_1 =$ Relay node, $N_2 = S_2$, and form $\Pr(L_1^r, L_2^r)$ as described in Section 4.3.3;
 - 7: Calculate Δ_2^r using (4.13) and set $\Delta_1^r = 0$, and calculate n^r using (4.28);
 - 8: $x^* = r, n^* = n^r, \Delta_1^* = \gamma, \Delta_2^* = \Delta_2^m(r, n, n^*)$;
 - 9: **else**
 - 10: Let $N_2 =$ Cooperating node, $N_1 = S_2$, and form $\Pr(L_1^c, L_2^c)$ as in Section 4.3.2;
 - 11: Let $N_2 =$ Relay node, $N_1 = S_2$, and reform $\Pr(L_1^r, L_2^r)$;
 - 12: Calculate Δ_1^c, Δ_2^c , and Δ_1^r using (4.13), (4.15), and (4.21), respectively, and set $\Delta_2^r = 0$;
 - 13: Calculate $n^x, x \in \{c, r\}$ using (4.28);
 - 14: **If** $0 < n^c \leq N$, **then**
 - 15: $x^* = c, n^* = n^c, \Delta_1^* = \gamma, \Delta_2^* = \Delta_2^m(c, n, n^*)$;
 - 16: **elseif** $0 < n^r \leq N$ **then**
 - 17: $x^* = r, n^* = n^r, \Delta_1^* = \gamma, \Delta_2^* = \Delta_2^m(r, n, n^*)$;
 - 19: **else**
 - 20: γ cannot be achieved, optimal solution is unfeasible;
 - 21: **endif**
 - 22: **endif**
-

4.4.2 Constrained Scheduling (CS) Scheme

In some applications, one of the transmitting nodes, say node $N_i, i \in \{1, 2\}$ may need to successfully report the average $0 \leq \gamma \leq 1$ of its total generated events to the destination over the N time blocks, which can happen only if node N_i achieves the packet delivery ratio $\Delta_i = \gamma$. Depending on its energy harvesting rate, node N_i might be able to achieve the performance γ either by its own or by the help of the other node $N_j, j \in \{1, 2\}, i \neq j$, or node N_i might not be able to achieve the performance γ neither by its own nor by the help of node N_j . Therefore, if γ is achievable, we provide the optimal operating mode of the system. If not, we consider that the optimal operating mode of the system is unfeasible.

Assume that the system operates in mixed x -n mode, where $x \in \{c, r\}$. As node N_i may need the help of node N_j to achieve γ , in x mode node N_i will operate as an S_2 while $N_j, j \neq i$ will operate as a cooperating or relay node depending on x . As stated earlier, when node N_i operates as an S_2 in x mode, its performance Δ_i will increase linearly over n . Therefore, because γ is a value from 0 to 1, the absolute difference between γ and Δ_i will be convex over n that increases linearly from both sides of its minimum, which is 0. Finding the optimal n and x that minimize the absolute difference between γ and Δ_i will provide the optimal operating mode of the system in which node N_i achieves the performance γ . Under the constraints that $0 \leq n \leq N$ and $x \in \{c, r\}$, the problem can be formulated as

$$\begin{aligned} \min_{n,x} \quad & \left| \gamma - \left(\Delta_i^n + \frac{n(\Delta_i^x - \Delta_i^n)}{N} \right) \right|, \\ \text{subject to} \quad & x \in \{c, r\}, \\ & 0 \leq n \leq N. \end{aligned} \tag{4.27}$$

Define n^c and n^r as the values of n that minimizes the cost function in (4.27) when $x = c$ and when $x = r$, respectively. Then by setting (4.27) equal to 0 and solving for n , the value of n^x is

$$n^x = \frac{(\gamma - \Delta_i^n)N}{\Delta_i^x - \Delta_i^n}. \tag{4.28}$$

From (4.28), n^x will be in the range from $(0, N]$ if $\Delta_i^n < \gamma \leq \Delta_i^x$, i.e., if node N_i can achieve the performance γ only with the help of node N_j either by cooperation or relaying depending on x . n^x will be higher than N if $\gamma > \Delta_i^x$, i.e., N_i cannot achieve the performance

γ neither by its own nor by the help of node N_j . Thus, due to the fact that Δ_i increases faster when $x = r$ than when $x = c$ over n , we imply that n^r will definitely be in the range from $[0, N]$ if n^c is in the range from $[0, N]$, and not necessarily vice versa. In addition, we imply that n^c will definitely be higher than N if n^r is higher than N , and not necessarily vice versa. This can be interpreted as that γ will definitely be achieved when $x = r$ if it is achieved when $x = c$, and γ will definitely not be achieved when $x = c$ if it is not achieved when $x = r$. Lastly, n^x will be less than or equal to 0 if $\gamma \leq \Delta_i^n$, which means that node N_i can achieve the performance γ on its own.

Based on Δ_i^n and $n^x, x \in \{c, r\}$, we find the optimal solution x^* and n^* for (4.27). For a given γ , we first calculate Δ_i^n . If $\gamma \leq \Delta_i^n$, i.e., node N_i can achieve γ by its own and $n^r, n^c \leq 0$, then the optimal solution is when $x^* = r$ and $n^* = n^r$. However, here node N_i will operate as a relay to improve N_j 's performance while achieving the performance γ . If $\gamma > \Delta_i^n$, then we first calculate n^c and n^r using (4.28). If $n^c, n^r \in (0, N]$, i.e., γ can be achieved when $x = c$ and when $x = r$, then there will be two optimal solutions. First is when $x^* = c$ and $n^* = n^c$ and second is when $x^* = r$ and $n^* = n^r$. We select the first solution because N_j will achieve higher performance due to the fact that in relay mode $\Delta_j^r = 0$. If $n^r \in (0, N]$ and $n^c \notin (0, N]$, i.e., γ can be achieved only when $x = r$, then $x^* = r$ and $n^* = n^r$. If $n^r, n^c > N$, the optimal solution is considered unfeasible because γ cannot be achieved even if node N_j cooperates with or relays for node N_i all the time blocks. The CS scheme, illustrated in Algorithm 4.3, summarizes the process of how to find the optimal solution for (4.27) when node N_1 needs to achieve the performance γ .

4.5 Simulation Results

We evaluate the performance of the proposed scheduling schemes in terms of the packet delivery ratio, assuming that the energy status in Algorithm 4.1 is known by feedback. For the simulations, we choose the system parameters shown in Figure 4.3, which shows the packet delivery ratios of N_1 and N_2 in noncooperation mode. We plot the packet delivery ratio versus energy harvesting rates \overline{E}_1 and \overline{E}_2 of N_1 and N_2 , respectively. For better representation and analysis of the results, we consider that the energy harvesting processes

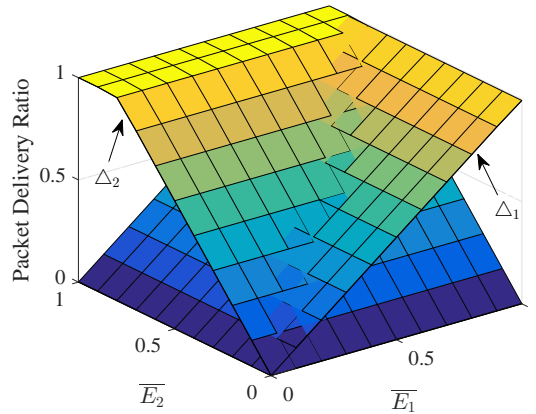


Figure 4.3: The packet delivery ratios of N_1 and N_2 in noncooperation mode. Parameters used: $q_1 = 0.5, q_2 = 0.4, \tilde{\delta} = 1, \delta_1 = \delta_2 = 2, \tilde{K} = 1, K = 100, N = 5 \times 10^5$.

E_1 and E_2 are independent (uncorrelated) and $\tilde{K} = 1$. So, $\overline{E}_1 = p^{(1)}(1)$ and $\overline{E}_2 = p^{(2)}(1)$, which are the probabilities of harvesting one unit of energy per time block by N_1 and N_2 , respectively.

4.5.1 Fairness

We simulate the FS scheme summarized in Algorithm 4.2 using the penalty function given in Section 4.4.1 with three different values of α . Figures (4.4), (4.5), and (4.6) illustrate the simulation results when $\alpha = 1, \alpha = 3$, and $\alpha = 5$, respectively. $\alpha = 1$ represents the case of absolute fairness, i.e., the case when the two nodes have to achieve the same performance. In this case, n^x is not given by (4.26) because the cost function is not differentiable. So, we solve for it by setting the cost function to 0 without taking the derivative.

For each value of α as can be seen from Figures 4.4, 4.5, and 4.6, the FS scheme provides the optimal x and n that achieve fairness in the performance between the transmitting nodes. In the case of absolute fairness, we can notice from Figure 4.4 (c) that the two transmitting nodes achieve the same performance as expected. From Figures 4.4 (c), 4.5 (c), and 4.6 (c), it can be noticed that as α increases, the performance of each transmitting node gets closer to its performance in noncooperation mode shown in Figure 4.3. This implies that as α increases, the cooperation or relaying between the transmitting nodes decreases over the time blocks. Therefore, when one of the transmitting nodes achieves very high packet

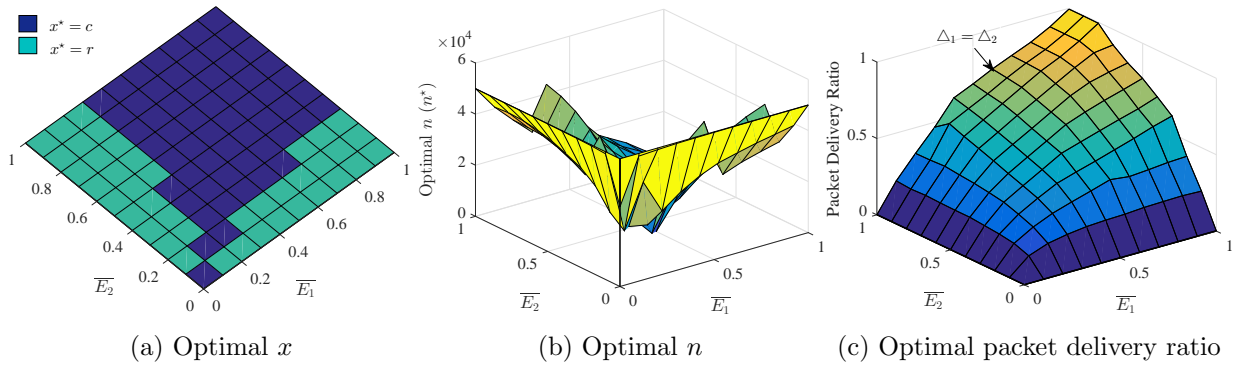


Figure 4.4: Figures (a) and (b) illustrate the optimal x and n provided by the FS scheme when $\alpha = 1$. Figure (c) shows the optimal performance of N_1 and N_2 by which fairness is considered achieved for the given penalty function.

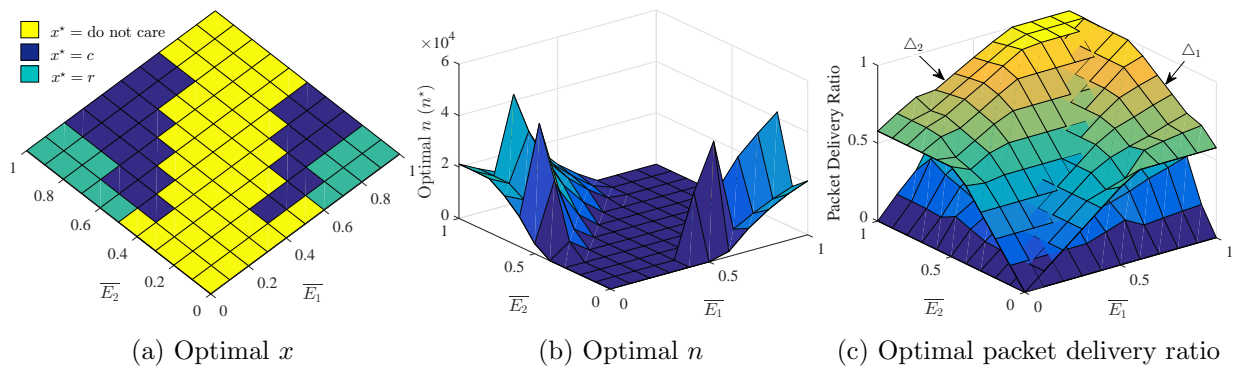


Figure 4.5: Figures (a) and (b) illustrate the optimal x and n provided by the FS scheme when $\alpha = 3$. Figure (c) shows the optimal performance of N_1 and N_2 by which fairness is considered achieved for the given penalty function.

delivery ratio than the other in noncooperation mode, the value of α is recommended to be high. Hence, the node of higher performance does not cooperate with or relay for the other node over a long time, and thus it does not lose high performance for a slight improvement in the other node's performance, which is not considered in the adaptive scheme proposed in Chapter 3.

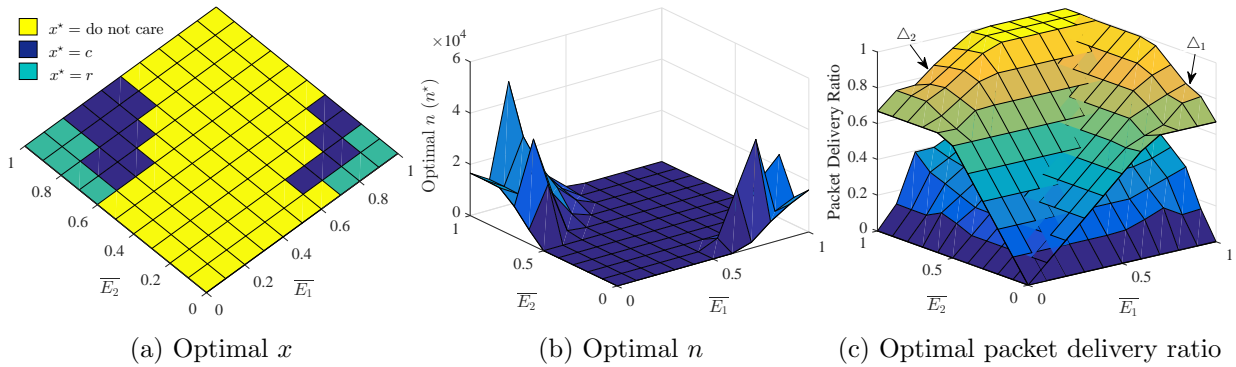


Figure 4.6: Figures (a) and (b) illustrate the optimal x and n provided by the FS scheme when $\alpha = 5$. Figure (c) shows the optimal performance of N_1 and N_2 by which fairness is considered achieved for the given penalty function.

4.5.2 Constrained Scheduling

We simulate the CS scheme summarized in Algorithm 4.3 for the scenario when N_1 needs to report 70% of its total generated events to the destination, i.e., when $\gamma = 0.7$. From the simulation results shown in Figure 4.7, we can see that the CS scheme provides the optimal x and n by which node N_1 achieves the performance γ . When $\overline{E}_1 \geq 0.7$, node N_1 can achieve γ by its own. Therefore, over this range, it operates as a relay for N_2 while achieving γ . When $\overline{E}_1 < 0.7$, node N_1 can achieve γ over some values of \overline{E}_2 only by the help of node N_2 that is either by cooperating or relaying. So, over these values of \overline{E}_2 , node N_1 operates as an S_2 to achieve γ by the help of node N_2 . For the remaining values of \overline{E}_2 when $\overline{E}_1 < 0.7$, node N_1 cannot achieve γ neither by its own nor by the help of node N_2 . Therefore, the optimal solution is unfeasible and the packet delivery ratios of the transmitting nodes are not plotted.

4.6 Conclusions

In this chapter, we consider a network of three nodes, two transmitting nodes and destination. We define three operating modes for the network that are combined appropriately to build two scheduling schemes. The first scheme is to ensure fairness in the performance between the two transmitting nodes while maximizing the sum of their packet delivery ra-

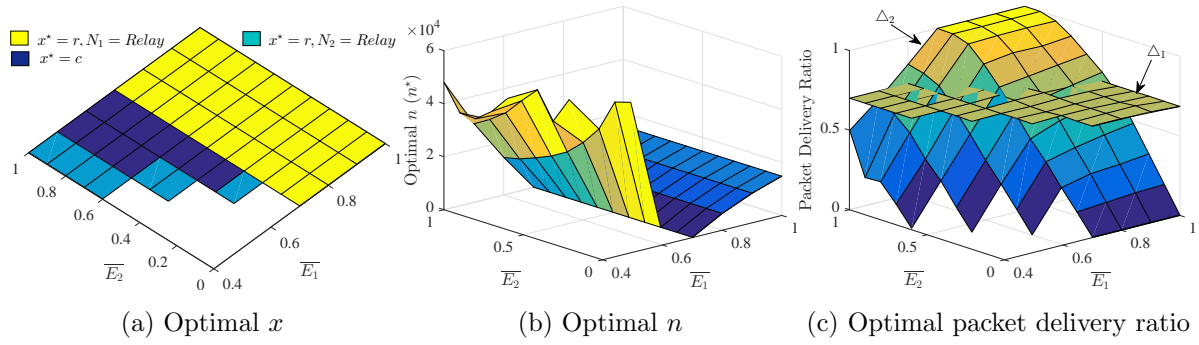


Figure 4.7: Figures (a) and (b) illustrate the optimal x and n provided by the CS scheme in order for node N_1 to achieve the performance $\gamma = 0.7$. Figure (c) shows that node N_1 achieves the performance γ over the values \overline{E}_1 and \overline{E}_2 where the system is feasible.

tios, and the second scheme is to constrain one of the transmitting nodes to achieve a certain performance. The FS scheme ensures fairness in the performance of the transmitting nodes based on a given penalty function that determines how much reduction in the performance of the cooperating or relay node can be tolerated.

Chapter 5

Scheduling with Energy Status Estimation

5.1 Introduction

In the previous chapter, in part (a) of Algorithm 4.1 (Line 4 and Line 6), node S_2 needs the knowledge of the cooperating/relay node's energy status to make the decision on its usage. In this chapter, we introduce a statistical model to estimate the energy status of the cooperating/relay node at node S_2 . As discussed in the previous chapters, the energy status of cooperating/relay node can be obtained by exchanging a few bits of information between nodes as in the the feedback scheme, or by comparing the energy battery level of the source by a threshold value as in the threshold-based scheme. However, in a practical fixed packet/frame format, as in IEEE 802.11, or in large networks with dynamic parameters, the overhead incurred or optimization of parameters may make estimation a better alternative.

In the proposed statistical model, node S_2 makes the decision on the energy status of the cooperating/relay node using a state information, which depends on the instantaneous transmission status of the cooperating/relay node. When the cooperating/relay node has a transmission, the state information includes the transmission status of the cooperating/relay node and its current energy battery level. As in [53], we assume that the current energy battery level of the cooperating/relay node is included in the header of its packet. So, whenever the cooperating/relay node has a transmission, the S_2 node receives only the

header and reads the current energy battery level. When the cooperating/relay node has no transmission, the state information includes the transmission status of the cooperating/relay node and the relay transmission status of the S_2 node. We evaluate the performance of the statistical model by comparing it with the feedback scheme, which performs close to the optimal policy [53], as shown in Chapter 2.

5.2 Cooperation Mode Statistical Model

The cooperation mode scenario using the statistical model is similar to the cooperation mode scenario summarized in Algorithm 4.1 and Section 4.3.2. However, in the cooperation mode scenario using the statistical model, the S_2 node $N_i, i \in \{1, 2\}$ in each time block makes the decision on its transmission action using the estimate energy status \hat{A}_j^c of the cooperating node $N_j, j \in \{1, 2\}, j \neq i$. Thus, in the n -th time block, the direct transmission event \tilde{d}_1^c and the relay transmission event \tilde{d}_2^c of node N_i become

$$\tilde{d}_1^c[n] = \begin{cases} 1 & \text{if } (\mathcal{E}_i[n] = 1 \cap L_i^c[n] \geq \delta_i \cap \hat{A}_j^c[n] = 0) \\ 0 & \text{otherwise,} \end{cases} \quad (5.1)$$

$$\tilde{d}_2^c[n] = \begin{cases} 1 & \text{if } (\mathcal{E}_i[n] = 1 \cap L_i^c[n] \geq \tilde{\delta} \cap \hat{A}_j^c[n] = 1) \\ 0 & \text{otherwise.} \end{cases} \quad (5.2)$$

In each time block, the cooperating node N_j senses the transmission action of the S_2 node $\tilde{d}_1^c[n]$ and $\tilde{d}_2^c[n]$ to decide on its transmission action. If $\tilde{d}_2^c[n] = 1$ is taken at S_2 based on a correct estimate of $A_j^c[n]$, the transmission action at the cooperating node will be *relay transmission*. While if $\tilde{d}_2^c[n] = 1$ is taken based on a wrong estimate of $A_j^c[n]$, the transmission action at the cooperating node will be *no transmission*, where in this case the S_2 event will be lost. If $\tilde{d}_1^c[n] = 1$, the cooperation node will take *no transmission* action regardless of its event and energy statuses due to Assumption 8, and to avoid interference. If $\tilde{d}_2^c[n] = 0$ and $\tilde{d}_1^c[n] = 0$, the transmission action at the cooperating node will be *own-traffic* if it has an event generated and it is energized. Consequently, in the n -th time block, the own-traffic transmission event $\tilde{d}_3^c[n]$ and the relay transmission event $\tilde{d}_4^c[n]$ of the cooperating

node are

$$\tilde{d}_3^c[n] = \begin{cases} 1 & \text{if } (\tilde{d}_1^c[n] = 0 \cap \tilde{d}_2^c[n] = 0 \cap \mathcal{E}_j[n] = 1 \cap L_j^c[n] \geq \delta_j) \\ 0 & \text{otherwise,} \end{cases} \quad (5.3)$$

$$\tilde{d}_4^c[n] = \begin{cases} 1 & \text{if } (\tilde{d}_2^c[n] = 1 \cap L_j^c[n] \geq \delta_j) \\ 0 & \text{otherwise.} \end{cases} \quad (5.4)$$

Using $\tilde{d}_1^c[n]$, $\tilde{d}_2^c[n]$, $\tilde{d}_3^c[n]$, and $\tilde{d}_4^c[n]$, in the next time block the energy battery level L_i^c of the S_2 node N_i is

$$L_i^c[n+1] = \min \{L_i^c[n] + E_i[n] - \delta \tilde{d}_2^c[n] - \delta_i \tilde{d}_1^c[n], K\}, \quad (5.5)$$

and the energy battery level L_j^c of the cooperating node N_j in the next time block is

$$L_j^c[n+1] = \min \{L_j^c[n] + E_j[n] - \delta_j \tilde{d}^c[n], K\}, \quad (5.6)$$

where $\tilde{d}^c[n] = \tilde{d}_4^c[n] + \tilde{d}_3^c[n]$ is either 0 or 1 since $(\tilde{d}_4^c[n] = 1 \cap \tilde{d}_3^c[n] = 1) = \emptyset$. $\tilde{d}^c[n] = 1$ means that the cooperating node has either a relay or an own traffic transmission in the n -th time block, and $\tilde{d}^c[n] = 0$ means that the cooperating node has no transmission.

Now after deriving its model in (5.6), the energy battery level $L_j^c[n+1]$ is estimated at S_2 using the state information of the current time block $\mathcal{X}[n]$. One of the pieces of information included in $\mathcal{X}[n]$ is $E_i[n]$ which is correlated with $E_j[n]$. The rest of the information depends on the transmission status $\tilde{d}^c[n]$ of node N_j , which is considered known at the S_2 node by sensing the link between N_j and the destination in each time block. If $\tilde{d}^c[n] = 1$, the rest of the information includes: a) the transmission status of the cooperating node $\tilde{d}^c[n] = 1$, and b) the current energy battery level of the cooperating node $L_j^c[n] = u, u \in \{0, 1, \dots, K\}$, $u \geq \delta_j$. As stated earlier, we assume that $L_j^c[n]$ is included in the header of the transmitted packet. Whenever the cooperating node transmits, the S_2 node receives only the header and reads $L_j^c[n]$. If $\tilde{d}^c[n] = 0$, the rest of the information includes: a) the transmission status of the cooperating node $\tilde{d}^c[n] = 0$, and b) the relay transmission action of the S_2 node $\tilde{d}_2^c[n] = b \in \{0, 1\}$. The state information can be summarized as

$$\mathcal{X}[n] = \begin{cases} \{E_i[n], \tilde{d}^c[n] = 1, L_j^c[n] = u\} & \text{if } (\tilde{d}^c[n] = 1) \quad \text{Case 1} \\ \{E_i[n], \tilde{d}^c[n] = 0, \tilde{d}_2^c[n] = b\} & \text{if } (\tilde{d}^c[n] = 0) \quad \text{Case 2} \end{cases} \quad (5.7)$$

Given the state information $\mathcal{X}[n-1]$, the maximum likelihood estimator of $L_j^c[n]$ at S_2 is

$$\hat{L}_j^c[n] = \arg \max_{0 \leq k \leq K} \Pr(L_j^c[n] = k | \mathcal{X}[n-1]). \quad (5.8)$$

Using $\hat{L}_j^c[n]$, the estimate energy status of the n -th time block is

$$\hat{A}_j[n] = \begin{cases} 1 & \text{if } \hat{L}_j^c[n] \geq \delta_j \\ 0 & \text{otherwise.} \end{cases} \quad (5.9)$$

Depending on the state information $\mathcal{X}[n-1]$, the probability $\Pr(L_j^c[n] = k | \mathcal{X}[n-1])$ in (5.8) is calculated as follows.

Case 1: when $\mathcal{X}[n-1] = \{E_i[n-1], \tilde{d}^c[n-1] = 1, L_j^c[n-1] = u\}$. Let $\mathcal{L}_j^c[n]$ be a variable that is defined as

$$\mathcal{L}_j^c[n] = L_j^c[n-1] + E_j[n-1] - \delta_j \tilde{d}^c[n-1]. \quad (5.10)$$

Because $\tilde{d}^c[n-1] = 1$, $\mathcal{L}_j^c[n]$ can be a value from 0 to $K + \tilde{K} - \delta_j$. Using (5.10) and because E_j and E_i are correlated, $\Pr(\mathcal{L}_j^c[n] = v | \mathcal{X}[n-1])$, $v \in \{0, 1, \dots, K + \tilde{K} - \delta_j\}$ is

$$\Pr(\mathcal{L}_j^c[n] = v | \mathcal{X}[n-1]) = \Pr(E_j[n-1] = \tilde{k} | E_i[n-1]) = \frac{\Pr(\tilde{k}, E_i[n-1])}{p^{(i)}(E_i[n-1])}, \quad (5.11)$$

where $\tilde{k} = v - u + \delta_j$ and $\Pr(\tilde{k}, E_i[n]) = 0 \forall \tilde{k} \notin [0, \tilde{K}]$. Using $\Pr(\mathcal{L}_j^c[n] = v | \mathcal{X}[n-1])$, we can calculate $\Pr(L_j^c[n] = k | \mathcal{X}[n-1]) \forall 0 \leq k \leq K$ as follows. If $\tilde{K} < \delta_j$,

$$\Pr(L_j^c[n] = k | \mathcal{X}[n-1]) = \begin{cases} \Pr(\mathcal{L}_j^c[n] = k | \mathcal{X}[n-1]) & \text{if } 0 \leq k \leq K + \tilde{K} - \delta_j, \\ 0 & \text{otherwise,} \end{cases}$$

and if $\tilde{K} \geq \delta_j$

$$\Pr(L_j^c[n] = k | \mathcal{X}[n-1]) = \begin{cases} \Pr(\mathcal{L}_j^c[n] = k | \mathcal{X}[n-1]) & \text{if } 0 \leq k \leq K-1, \\ \sum_{\ell=K}^{K+\tilde{K}-\delta_j} \Pr(\mathcal{L}_j^c[n] = \ell | \mathcal{X}[n-1]) & \text{otherwise.} \end{cases}$$

Case 2: when $\mathcal{X}[n-1] = \{E_i[n-1], \tilde{d}^c[n-1] = 0, \tilde{d}_2^c[n-1] = b\}$. Because $\tilde{d}^c[n-1] = 0$, $\mathcal{L}_j^c[n]$ in (5.10) becomes

$$\mathcal{L}_j^c[n] = L_j^c[n-1] + E_j[n-1]. \quad (5.12)$$

Here, $\mathcal{L}_j^c[n]$ can be a value from 0 to $K + \tilde{K}$. Because E_j and E_i are correlated and L_j^c and E_j in the same time block are independent, the distribution of $(\mathcal{L}_j^c[n]|\mathcal{X}[n-1])$ is the convolution of $\Pr(L_j^c[n-1])$ and $\Pr(E_j[n-1]|E_i[n-1])$. Thus, $\Pr(\mathcal{L}_j^c[n] = v|\mathcal{X}[n-1])$, $v \in \{0, 1, \dots, K + \tilde{K}\}$ is calculated as

$$\Pr(\mathcal{L}_j^c[n] = v|\mathcal{X}[n-1]) = \sum_{\tilde{k}=0}^{\tilde{K}} \Pr(L_j^c[n-1] = v - \tilde{k}) \frac{\Pr(\tilde{k}, E_i[n-1])}{p^{(i)}(E_i[n-1])}. \quad (5.13)$$

The distribution of $L_j^c[n-1]$ in (5.13) is the same as the distribution of $L_j^c[n-1]$ that was calculated in the previous time block given the state information $\mathcal{X}(n-2)$, i.e., $\Pr(L_j^c[n-1] = u) = \Pr(L_j^c[n-1] = u|\mathcal{X}(n-2))$, $u \in \{0, 1, \dots, K\}$. However, if $b = 1$, i.e., $A^c[n-1]$ was estimated wrong and $L_j^c[n-1]$ should be a value that is less than δ_j since $\tilde{d}^c[n-1] = 0$, then we weight the probabilities $\Pr(L_j^c[n-1] = u|\mathcal{X}(n-2))$, $\delta_j \leq u \leq K$ on the probabilities $\Pr(L_j^c[n-1] = u|\mathcal{X}(n-2))$, $0 \leq u < \delta_j$ as

$$\Pr(L_j^c[n-1]=u) = \begin{cases} \Pr(L_j^c[n-1]=u|\mathcal{X}(n-2)) + \left(\sum_{l=\delta_j}^K \Pr(L_j^c[n-1]=l|\mathcal{X}(n-2))\right)/\delta_j & \text{if } 0 \leq u \leq \delta_j-1, \\ 0 & \text{otherwise.} \end{cases}$$

Using $\Pr(\mathcal{L}_j^c[n] = v|\mathcal{X}[n-1])$, we can calculate $\Pr(L_j^c[n] = k|\mathcal{X}[n-1]) \forall 0 \leq k \leq K$ as follows.

$$\Pr(L_j^c[n]=k|\mathcal{X}[n-1]) = \begin{cases} \Pr(\mathcal{L}_j^c[n]=k|\mathcal{X}[n-1]) & \text{if } 0 \leq k \leq K-1, \\ \sum_{\ell=K}^{K+\tilde{K}} \Pr(\mathcal{L}_j^c[n]=\ell|\mathcal{X}[n-1]) & \text{otherwise.} \end{cases}$$

Note that in order for this estimation model to work, the knowledge of the initial energy battery level of the cooperating node is needed at the S_2 node. Therefore, we assume that the initial energy battery level of the cooperating node is transmitted to the S_2 node in the first time block. This is equivalent to setting $\tilde{d}^c[0] = 1$. Using the estimation model, the packet delivery ratio Δ_i^c of S_2 is

$$\Delta_i^c = \frac{[\Pr(\tilde{d}_1^c = 1) + \Pr(\tilde{d}_2^c = 1 \cap \tilde{d}_4^c = 1)]N}{\Pr(\mathcal{E}_i = 1)N}, \quad (5.14)$$

$$\Delta_i^c = \Pr(L_i^c \geq \delta_i \cap \hat{L}_j^c < \delta_j) + \Pr(L_i^c \geq \tilde{\delta} \cap L_j^c \geq \delta_j \cap \hat{L}_j^c \geq \delta_j), \quad (5.15)$$

and the packet delivery ratio Δ_j^c of the cooperating node is

$$\Delta_j^c = \frac{\Pr(\tilde{d}_3^c = 1)N}{\Pr(\mathcal{E}_i = 1)N}, \quad (5.16)$$

$$\begin{aligned} \Delta_j^c = & (1 - q_i) \Pr(L_j^c \geq \delta_j) + \Pr(L_i^c < \tilde{\delta} \cap L_j^c \geq \delta_j) + \\ & \Pr(\tilde{\delta} \leq L_i^c < \delta_i \cap L_j^c \geq \delta_j \cap \hat{L}_j^c < \delta_j) - (1 - q_i) \left[\Pr(L_i^c < \tilde{\delta} \cap L_j^c \geq \delta_j) + \right. \\ & \left. \Pr(\tilde{\delta} \leq L_i^c < \delta_i \cap L_j^c \geq \delta_j \cap \hat{L}_j^c < \delta_j) \right]. \end{aligned} \quad (5.17)$$

Here, there is no closed form expression for the joint distribution of L_i^c , L_j^c , and \hat{L}_j^c . Therefore, we use Monte Carlo technique to find the packet delivery ratios in (5.15) and (5.17).

5.3 Relay Mode Statistical Model

As mentioned in Section 4.3.3, the difference between cooperation and relay modes is that in relay mode node N_j operates as a relay, which has no own transmissions. Therefore, the cooperation mode statistical model detailed in Section 5.2 can represent the relay mode statistical model if the superscript c is replaced by r and \tilde{d}_3^r is set to 0. Hence, the packet delivery ratio Δ_i^r of S_2 is

$$\Delta_i^r = \Pr(L_i^r \geq \delta_i \cap \hat{L}_j^r < \delta_j) + \Pr(L_i^r \geq \tilde{\delta} \cap L_j^r \geq \delta_j \cap \hat{L}_j^r \geq \delta_j), \quad (5.18)$$

and the packet delivery ratio of the relay node is $\Delta_j^r = 0$.

5.4 Simulation Results

We simulate the cooperation and relay modes in Sections 4.3.2 and 4.3.3 using the statistical models and the feedback scheme. As stated in Chapter 1, the feedback scheme provides the upper-bound performance as it performs close to the optimal policy. In the simulations, we use the system parameters shown in Figure 4.3. We plot the performance in terms of the packet delivery ratio versus energy harvesting rates \overline{E}_1 and \overline{E}_2 of N_1 and N_2 , respectively.

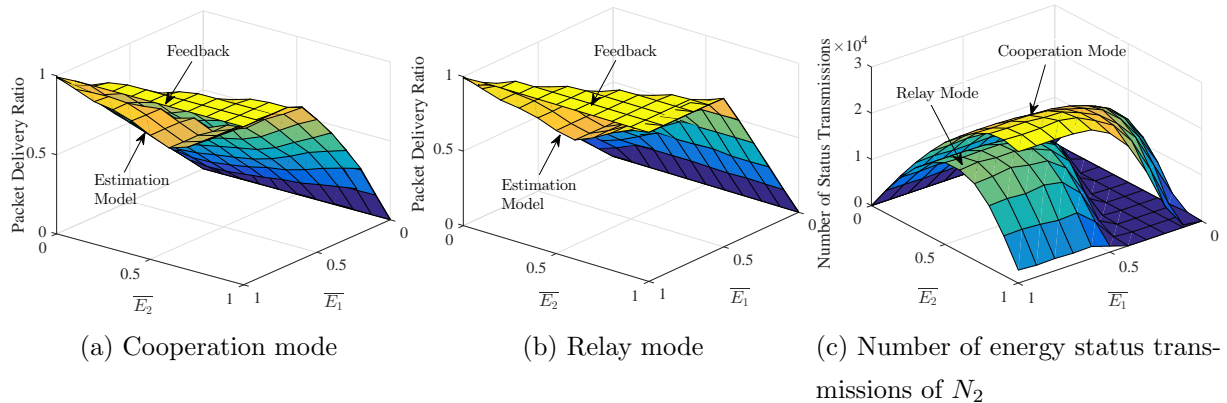


Figure 5.1: Figures (a) and (b) show the performance of N_1 in the cooperation and relay modes using the statistical models compared with the feedback scheme. Figure (c) shows the number of energy status transmissions of N_2 over the N time blocks.

We simulate the case when the energy harvesting processes E_1 and E_2 are independent (uncorrelated) and $\tilde{K} = 1$. So, $\overline{E}_1 = p^{(1)}(1)$ and $\overline{E}_2 = p^{(2)}(1)$, which are the probabilities of harvesting one unit of energy per time block by N_1 and N_2 , respectively. We also simulate the case when E_1 and E_2 are correlated. In this case, we plot the packet delivery ratio versus correlation coefficient ρ assuming that $\tilde{K} = 1$ and $p^{(1)}(1) = p^{(2)}(1) = p$. Given ρ and p , the joint probability $\Pr(E_1 = 1, E_2 = 1) = p^2 + \rho p(1 - p)$. Using p and $\Pr(E_1 = 1, E_2 = 1)$, we calculate the rest of the joint probabilities $P(E_1 = 0, E_2 = 0)$, $P(E_1 = 1, E_2 = 0)$, and $P(E_1 = 0, E_2 = 1)$. Finally, we simulate the FS and CS schemes proposed in the previous chapter using the statistical models for the case when E_1 and E_2 are independent.

5.4.1 Cooperation and relay modes (independent case)

We simulate the cooperation and relay modes using the statistical models when E_1 and E_2 are independent, where in both modes N_1 operates as an S_2 and needs to estimate the energy status of N_2 . Figures 5.1 (a) and (b) illustrate the packet delivery ratio of node N_1 for the cooperation and relay modes, respectively. Figure 5.1 (c) shows the total number of energy status transmitted from N_2 to N_1 in the feedback scheme. From Figures 5.1 (a) and (b) we can notice that in both modes when \overline{E}_1 is high, the gap between the statistical model and feedback scheme increases as \overline{E}_2 moves towards 0.6, at which the uncertainty of

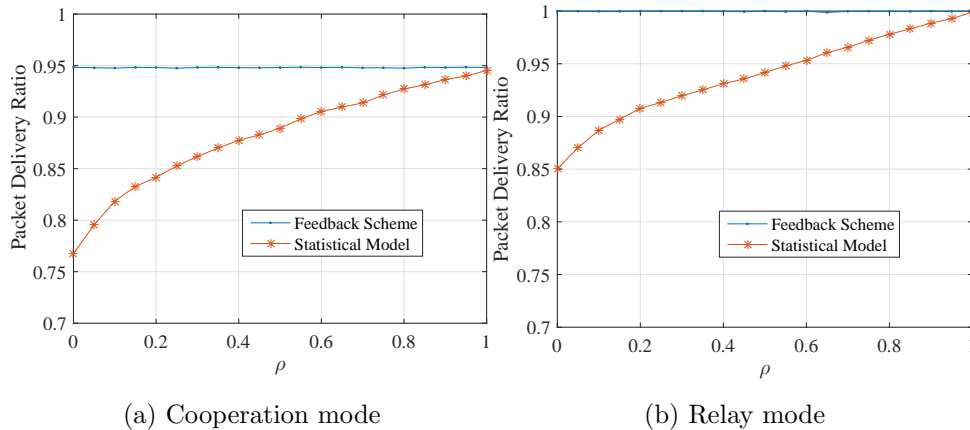


Figure 5.2: Figures (a) and (b) show the packet delivery ratio of N_1 versus correlation coefficient ρ for the cooperation and relay modes, respectively, using the statistical models compared with the feedback scheme.

the energy status of node N_2 is maximized. The fact that the uncertainty is maximized at 0.6 can also be noticed from the feedback scheme in Figure 5.1 (c) if the probability that the energy status changes in each time block is defined as the number of status transmissions over the total number of time blocks. From Figure 5.1 (c), we can observe that the number of energy status transmissions is 0 over some values of \overline{E}_1 and \overline{E}_2 , which means that over these values the energy status of N_2 is constant or deterministic. Therefore, over these values, the statistical model and the feedback scheme perform the same. Hence, we conclude that when the energy status of the cooperating/relay node is deterministic, the feedback scheme will be more energy efficient than the statistical model. Otherwise, the statistical model will be more energy efficient as the energy status transmissions of N_2 could consume a significant amount of energy, especially when using protocols with fixed frame/packet format.

5.4.2 Cooperation and relay modes (correlated case)

Here, we simulate the cooperation and relay modes when the energy harvesting processes E_1 and E_2 are correlated, assuming that $p = 0.7$ and N_1 operates as an S_2 in both modes. Figures 5.2 (a) and (b) show the simulation results in terms of the packet delivery ratio versus correlation coefficient ρ for the cooperation and relay modes, respectively. It can be

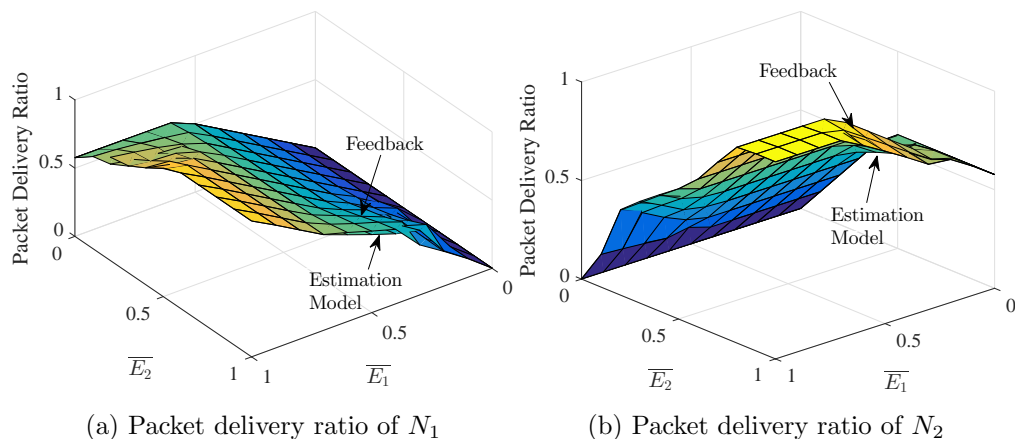


Figure 5.3: Figures (a) and (b) show the packet delivery ratios of N_1 and N_2 , respectively, for the FS scheme when using the statistical models compared with the feedback scheme. We used the same penalty function in Section VI (A) with $\alpha = 3$.

noticed that the performance of the feedback scheme is not affected by ρ because the decision is made based on the actual energy status of node N_2 . In the statistical model, on the other hand, the performance is affected by ρ , where it increases as the correlation between E_1 and E_2 gets stronger until it reaches the performance of the feedback scheme at $\rho = 1$, where the energy status of N_2 becomes actual at N_1 .

5.4.3 FS and CS schemes

We simulate the FS and CS schemes for the same scenarios in Sections 4.5.1 and 4.5.2, respectively, using the statistical models. In the FS scheme, we only simulate the scenario when $\alpha = 3$, and we calculate the value of n^x by (4.26) using the packet delivery ratios derived in Sections 5.2 and 5.3. Due to the imperfect estimation, n^x sometimes comes out as a complex value in the cases when the energy harvesting rate of S_2 is much lower than its event generation rate. In these cases, we just set $n^x = 0$ as it is supposed to be.

Figures 5.3 and 5.4 illustrate the simulation results for the FS and CS schemes, respectively. For the FS scheme, Figure 5.3 shows that the statistical model performs either the same or very close to the feedback scheme. This is because whenever the system operates in the cooperation or relay mode, i.e., whenever x^* is decided to be either c or r in the FS

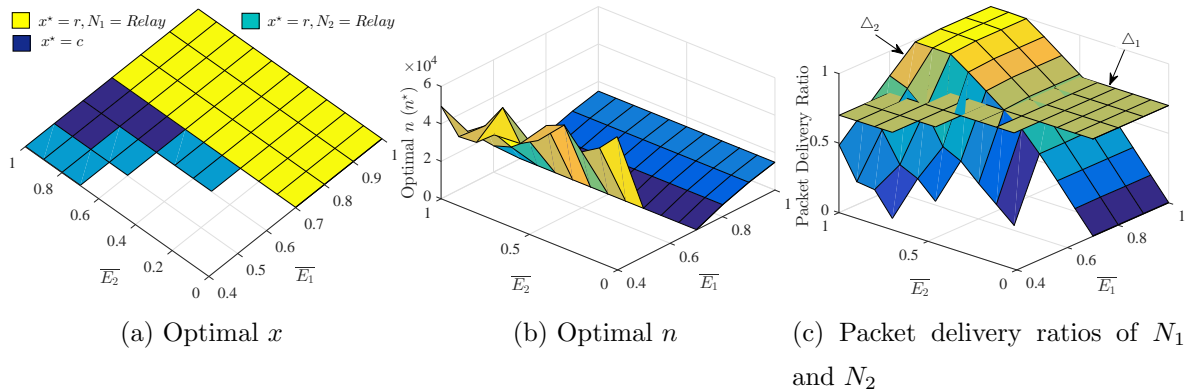


Figure 5.4: Figures (a) and (b) illustrate the optimal x and n provided by the CS scheme using the statistical models in order for node N_1 to achieve the performance $\gamma = 0.7$. Figure (c) shows that node N_1 achieves the performance γ over the values \overline{E}_1 and \overline{E}_2 where the system is feasible.

algorithm, the system operates over the ranges of \overline{E}_1 and \overline{E}_2 where the statistical model and the feedback scheme perform the same or close to each other. As for the CS scheme when using the statistical model, Figure 5.4 shows that the range of \overline{E}_1 and \overline{E}_2 over which N_1 achieves the performance γ by its own stays the same, and the range over which N_1 achieves γ by the help of node N_2 shrinks compared to the feedback scheme shown in Figure 4.7. This is expected because when N_1 achieves the performance γ by its own, it operates as a relay for N_2 over n^r time blocks. After that, it operates as an S_1 to achieve γ over the rest of the time blocks. From (4.28) and because $\Delta_1^r = 0$, n^r will be the same in both the statistical model and feedback scheme, which can also be seen from Figures 5.4 (b) and 4.7 (b). The same value of n^r results in the same range of \overline{E}_1 and \overline{E}_2 over which N_1 achieves γ by its own. In contrast, when N_1 achieves γ by the help of node N_2 , it operates as an S_2 over $n^x, x \in \{c, r\}$ time blocks and then it operates as an S_1 . Here, $\Delta_1^x, x \in \{c, r\}$ in (4.26) is calculated using the statistical model, which results in a lower n^x compared to the feedback scheme due to the imperfect estimation. Thus, the range over which N_1 can achieve γ only by the help of N_2 shrinks compared to the feedback scheme.

5.5 Conclusions

In this chapter, we propose a statistical model that can be used to estimate the energy status of the cooperating/relay node at the source. In the scenarios when the energy status of the cooperating/relay node is certain, i.e., it is either energized or not over the N time blocks, it will be more energy efficient to use the feedback scheme where in these scenarios there will be 0 overhead. Otherwise, it will be more energy efficient to use the statistical model because overhead could consume a significant amount of energy, especially, when using protocols with fixed frame/packet format.

Chapter 6

Scheduling for Throughput Maximization

6.1 Introduction

In this chapter, we address the problem of scheduling for throughput maximization in a wireless energy harvesting uplink. For fairness, we assume that each node's throughput cannot drop below what it achieves by direct transmission to the base station. We tackle this problem by assigning a role to each node in the network, that is either a cooperating node, a Source type 1 (type S_1), or a Source type 2 (S_2). The role assignments of the nodes are optimally done based on the energy harvesting rate of each node compared to its energy depletion rate. Such that, a node of a higher energy harvesting rate is assigned to be a cooperating node of some type S_2 nodes, some nodes of lower energy harvesting rates, if (1) the total number of events that are successfully transmitted from that cooperating node to the base station, including its type S_2 nodes' events, is higher than or equal to the total number of events that are successfully transmitted from the cooperating node and its type S_2 nodes when each transmits its events on its own to the base station, and (2) that cooperating node can forward more events for each one of its type S_2 nodes than any other cooperating node in the network. If a node can neither be a cooperating node nor a type S_2 node, it will be assigned as a type S_1 node, which transmits its events on its own to the base station.

We first analyze the problem for the scenario when the transmit power between the nodes

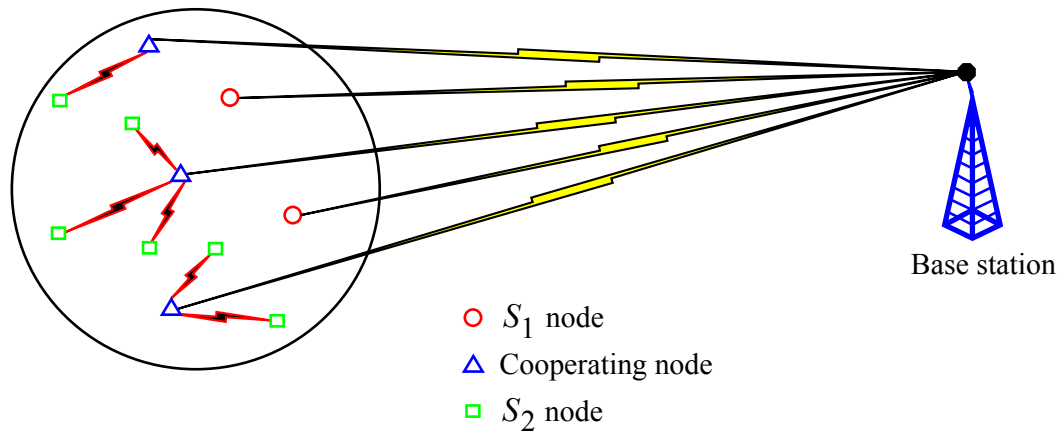


Figure 6.1: A network consists three categories of sensor nodes; type S_1 node which transmits directly to the base station, type S_2 node which transmits to the base station through another node called cooperating node, and cooperating node which transmits its own events as well as it forwards some type S_2 nodes' events to the base station.

is the same. After that, we generalize it for the scenario when the transmit power between the nodes is variable. We first derive the data collection throughput of the network as the summation of the successful transmission probabilities of its sensor nodes to the base station. We then propose a centralized algorithm that maximizes the throughput by optimally assigning a role to each node. The algorithm is run at the base station after receiving the energy harvesting and event generation rates of each node, and then a message that contains the role of each node is broadcasted to the network. We also develop a distributed algorithm for use in networks when central control is not feasible, e.g., when overhead must be kept low or when the base station is also energy-constrained. The results show that the proposed algorithms maximize the throughput with less computation complexity than the brute force approach, where all the possible combinations of nodes' roles that are applicable to the system model are examined. The results also show that our approach, compared with cooperative communication, maximizes the overall throughput of the network such that no node's throughput is adversely affected. Note that, the role assignments of the nodes are quasi-static, in that changes in the network topology or energy harvesting parameters requires that the algorithm run again.

One practical application is bridge health monitoring [66]-[68], where nodes are usually

powered by sunlight and/or vibration. Hence, the nodes that are exposed to sunlight or located along the span are more likely to have a higher energy harvesting rate than their energy depletion rate. Thus, these nodes can relay transmissions of the nodes that are located inside the bridge or away from the span to the base station in order to maximize the network throughput.

6.2 System Model

As shown in Figure 6.1, we consider an uplink wireless energy harvesting sensor network with a set of M sensor nodes, $\mathcal{N} = \{1, 2, \dots, M\}$. We consider a discrete-time model where time is divided into N blocks. In each block, node $i \in \mathcal{N}$ has an event generated (sensed data) $\mathcal{E}_i[n] = 1$ with probability q_i . Each node transmits its events to the base station either directly or through a cooperating node. Therefore, as shown in Figure 6.1, the network contains nodes of three categories; type S_1 nodes which transmit their events directly to the base station, type S_2 nodes which transmit their events to the base station through a cooperating node, and cooperating nodes which transmit their events as well as they forward at least one type S_2 node's events to the base station. We consider a real-time monitoring deployment scenario where events cannot be buffered for a later transmission [53]. We assume the nodes transmit over orthogonal frequency bands.

Each node is assumed to be equipped with energy harvesting devices and a rechargeable battery with capacity K . In the n -th time block, $n \in \{1, 2, \dots, N\}$, node $i \in \mathcal{N}$ harvests $E_i[n] \in \{0, 1, \dots, \tilde{K}\}$ amount of energy with corresponding probabilities $\{p_{i,0}, p_{i,1}, \dots, p_{i,\tilde{K}}\}$, where $\tilde{K} \leq K$ is the maximum amount of energy that can be harvested in one block. We assume that the energy required for a reliable transmission per event from node i to the base station is δ_i , and between the nodes is $\tilde{\delta}$, where δ_i and $\tilde{\delta}$ are integers, and $\tilde{\delta} < \delta_i$ as the distance between the base station and any node is assumed to be larger than the distance between any two nodes.

Let $\mathcal{A}_i \in \{0, 1\}$ be the transmission event of node $i \in \mathcal{N}$ with distribution $\Pr(\mathcal{A}_i = 1) = v_i$. In the n -th time block, if node i has a transmission, i.e., $\mathcal{A}_i[n] = 1$, the node is allowed to transmit only if it is energized, i.e., if its energy battery level $L_i[n] \geq \delta$, where $\delta = \delta_i$ if node

i is a type S_1 or a cooperating node and $\delta = \tilde{\delta}$ if node i is a type S_2 node. At that time block, δ amount of energy will be depleted from its battery, and its transmission will be considered successfully delivered to the base station if node i is a type S_1 node or a cooperating node, or to its cooperating node if node i is a type S_2 node. We denote the successful transmission event of node $i \in \mathcal{N}$ by \mathcal{B}_i . Otherwise, i.e., if $L_i[n] < \delta$, the transmission will be discarded. Consequently, the energy battery level of the $(n+1)$ -th time block of node i is

$$L_i[n+1] = \min\{L_i[n] + E_i[n] - \delta \mathbb{1}_{\{L_i[n] \geq \delta\}} \mathcal{A}_i[n], K\}, \quad (6.1)$$

where $\mathbb{1}_{\{\cdot\}}$ is the indicator function. Because $L_i[n+1]$ depends only on the previous energy battery level $L_i[n]$, it is modeled as a Markov chain with state space $\{0, 1, \dots, K\}$, where the transition between any two states depends on $E_i[n]$ and $\mathcal{A}_i[n]$. Let k and j be the current and the previous states of the energy battery level, respectively, and let $z = k - j$ and $w = k - j + \delta$. Then given v_i and $\mathbf{p}_i = [p_{i,0}, p_{i,1}, \dots, p_{i,\tilde{K}}]^T$, the transition probability $Q_{j,k}^{(i)} = \Pr(L_i[n+1] = k | L_i[n] = j)$ of node $i \in \mathcal{N}$ between any two states $j, k \in \{0, 1, \dots, K\}$ is

$$Q_{j,k}^{(i)} = \begin{cases} p_{i,z} & j < \delta, k < K, \\ p_{i,w}v_i + p_{i,z}(1-v_i) & j \geq \delta, k < K, \\ \sum_{\tilde{k}=z}^{\tilde{K}} p_{i,\tilde{k}} I_1 & j < \delta, k = K, \\ \sum_{\tilde{k}=z}^{w-1} p_{i,\tilde{k}}(1-v_i) I_2 + \sum_{\tilde{k}=w}^{\tilde{K}} p_{i,\tilde{k}} I_3 & j \geq \delta, k = K, \end{cases} \quad (6.2)$$

where $I_1 = \mathbb{1}_{\{z \leq \tilde{K}\}}$, $I_2 = \mathbb{1}_{\{z \leq w-1\}}$, and $I_3 = \mathbb{1}_{\{w \leq \tilde{K}\}}$ are the indicator functions. Let $\mathbf{Q}^{(i)}$ be the transition matrix of the Markov chain whose (j,k) -th element is given by $Q_{j,k}^{(i)}$, and let $\pi_{i,0}, \pi_{i,1}, \dots, \pi_{i,K}$ be its average (steady state) probabilities, where $\pi_{i,k}$, $k = \{0, \dots, K\}$ is the average probability of the k -th energy battery level of node $i \in \mathcal{N}$. Then, the probability that node i is energized is

$$\Delta_i(v_i, \delta, \mathbf{p}_i) = \Pr(L_i \geq \delta) = \sum_{k=\delta}^K \pi_{i,k}, \quad (6.3)$$

and node i has a successful transmission ($\mathcal{B}_i = 1$) is

$$\tau_i(v_i, \delta, \mathbf{p}_i) = v_i \Delta_i(v_i, \delta, \mathbf{p}_i) = v_i \sum_{k=\delta}^K \pi_{i,k}, \quad (6.4)$$

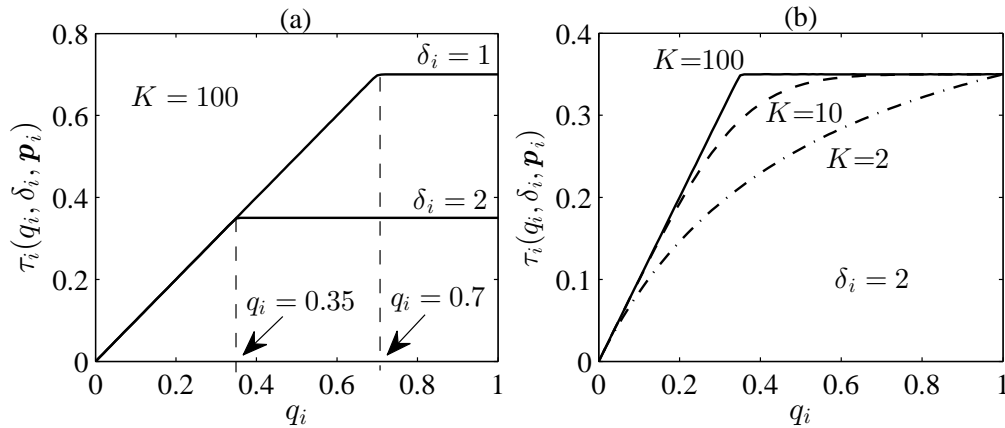


Figure 6.2: Successful transmission probability $\tau_i(q_i, \delta_i, \mathbf{p}_i)$ of node $i \in \mathcal{N}$ versus q_i for different values of δ_i and K , and for $\mathbf{p}_i = [0.3 \ 0.7]$.

where $\pi_{i,0}, \pi_{i,1}, \dots, \pi_{i,K}$ can be obtained using eigen decomposition of $\mathbf{Q}^{(i)} \forall K \geq \delta$ [65]. In the special case when the battery capacity is much greater than δ , i.e., $K \gg \delta$, by following the same derivation of $\sum_{k=\delta}^K \pi_{i,k}$ in [69] where a different problem is considered, we get

$$\Delta_i(v_i, \delta, \mathbf{p}_i) = \begin{cases} 1 & v_i \leq r_i, \\ \frac{\overline{E_i[n]}}{v_i \delta} & v_i > r_i, \end{cases} \quad (6.5)$$

$$\tau_i(v_i, \delta, \mathbf{p}_i) = \begin{cases} v_i & v_i \leq r_i, \\ \frac{\overline{E_i[n]}}{\delta} & v_i > r_i, \end{cases} \quad (6.6)$$

where $\overline{E_i[n]}$ is the average energy harvesting rate of node i , $(v_i \delta)$ is the energy depletion rate, and r_i is the value of v_i at which the energy harvesting rate of the node is equal to its energy depletion rate. r_i can be expressed as

$$r_i = \frac{\overline{E_i[n]}}{\delta}. \quad (6.7)$$

6.3 Successful transmission probability Characterization

Let node $i \in \mathcal{N}$ be a type S_1 node, i.e., $\mathcal{A}_i = \mathcal{E}_i$ and $\delta = \delta_i$. Then, its successful transmission probability $\tau_i(q_i, \delta_i, \mathbf{p}_i)$ over q_i for a given \mathbf{p}_i and different values of δ_i and K

will be as shown in Figure 6.2. From the figure, we notice two key things.

First, we see in Figure 6.2 (a) that when K is much greater than δ_i , i.e., $K \gg \delta_i$, $\tau_i(q_i, \delta_i, \mathbf{p}_i)$ has two regions; linear which is the region over the range of $q_i \leq r_i$, and saturation which is the region over the range of $q_i > r_i$. When $q_i < r_i$, the energy harvesting rate of node i is higher than its depletion rate. If operating in this region, the node will have all of its generated events successfully transmitted, i.e., $\tau_i(q_i, \delta_i, \mathbf{p}_i) = q_i$, and can operate as a cooperating node to successfully forward the fraction $d_i = r_i - q_i$ of events for another node. When $q_i > r_i$, the energy harvesting rate of the node is lower than its depletion rate. If operating in this region, the node will not have all of its generated events successfully transmitted, i.e., $\tau_i(q_i, \delta_i, \mathbf{p}_i) < q_i$, and can operate as a type S_2 node to improve its successful transmission probability. Note that, as δ_i decreases, the linear region increases at the expense of the saturation region, which implies that if $\tau_i(q_i, \delta_i, \mathbf{p}_i) = q_i$, then $\tau_i(q_i, \tilde{\delta}, \mathbf{p}_i) = q_i$ since $\tilde{\delta} < \delta_i$. We need this fact later to prove **Proposition 1**.

Second, we see in Figure 6.2 (b) that when K is close to δ_i and greater, i.e., $K \geq \delta_i$, $\tau_i(q_i, \delta_i, \mathbf{p}_i)$ has an additional region, called transient. The range of this region increases as K gets closer to δ_i , and it reaches the maximum size when $\delta_i = K$. As K gets closer to δ_i , more energy is wasted due to energy overflow, so that lower successful transmission probability is achieved. This wasted energy of node i in this region can be exploited either by operating the node as a type S_2 where it transmits with a lower energy, or by operating the node as a cooperating node where it can successfully forward some events for another node.

In this chapter we consider the first case when $K \gg \delta_i$. The second case when $K \geq \delta_i$ can be considered as a future work.

6.4 Problem Formulation

The goal of this chapter is to maximize the total average of events that are successfully transmitted to the base station from the M nodes over the N time blocks, but without any node dropping below its base performance, defined as the performance obtained through direct transmission of its own events to the base station. As described in Section 6.2, each node in the network acts as either a type S_1 , a type S_2 , or a cooperating node. Thus, the

set \mathcal{N} can be partitioned into three subsets; \mathcal{S} which includes all type S_1 nodes, \mathcal{R} which includes all cooperating nodes, and \mathcal{U} which includes all type S_2 nodes. Hence, $\mathcal{S}, \mathcal{R}, \mathcal{U} \subseteq \mathcal{N}$ and are disjoint.

Let $s \in \mathcal{S}$ be a type S_1 node, $r \in \mathcal{R}$ be a cooperating node, and u be one of the type S_2 nodes that transmits through the cooperating node r , so that $u \in \mathcal{D}(r) \subseteq \mathcal{U}$. The type S_1 node s has a transmission to the base station whenever it has an event generated, and this event is successfully delivered to the base station with probability $\tau_s(q_s, \delta_s, \mathbf{p}_s)$. This holds the same for the type S_2 node u . However, the type S_2 node u transmits its event successfully to its cooperating node with probability $\tau_u(q_u, \tilde{\delta}, \mathbf{p}_u)$. As for the cooperating node r , it has a transmission to the base station not only whenever it has an event generated, but also whenever one of its type S_2 nodes $u \in \mathcal{D}(r)$ has a successful transmission to it. Thus, the cooperating node transmits its event or one of its type S_2 nodes' events successfully to the base station with probability $\tau_r(v_r, \delta_r, \mathbf{p}_r)$, where $v_r = \Pr(\mathcal{E}_r = 1 \cup \bigcup_{u \in \mathcal{D}(r)} \mathcal{B}_u = 1)$ and $\Pr(\mathcal{B}_u = 1) = \tau_u(q_u, \tilde{\delta}, \mathbf{p}_u)$. The cooperating node's event and its type S_2 nodes' events are independent and not mutually exclusive. Therefore, in the same time block, if more than one of them occurs and the cooperating node is energized, only one of them will be considered successfully transmitted, that will be the cooperating node's event if any, or the event of the type S_2 node $u \in \mathcal{D}(r)$ that achieves the smallest successful transmission probability to the base station. Because the base station receives only from type S_1 and cooperating nodes, the total number of the successful received events at the base station over the N time blocks is

$$\mathcal{G} = \Gamma N, \quad (6.8)$$

$$\Gamma = \sum_{s \in \mathcal{S}} \tau_s(q_s, \delta_s, \mathbf{p}_s) + \sum_{r \in \mathcal{R}} \tau_r(v_r, \delta_r, \mathbf{p}_r), \quad (6.9)$$

where Γ is the data collection throughput of the network. In order to maximize (6.8), we maximize Γ by optimizing the sets \mathcal{S} , \mathcal{R} , and $\mathcal{D}(r)$, and these sets can be optimized by optimally assigning each node in \mathcal{N} as either a type S_1 node, a cooperating node, or a type S_2 node of which cooperating node. A node $i \in \mathcal{N}$ is optimally assigned to be a cooperating node of some type S_2 nodes if, 1) the total number of events that are successfully transmitted from that cooperating node to the base station, including its type S_2 nodes' events, is higher

than or equal to the total number of events that are successfully transmitted from that cooperating node and its type S_2 nodes when each one of them transmits its events on its own to the base station, and 2) that relay can forward more events for each one of its type S_2 nodes than any other cooperating node in the network. If node i cannot be a cooperating node or a type S_2 node, then it will be a type S_1 node. Consequently, the optimization problem can be formulated as

$$\begin{aligned}
& \max_{\mathcal{S}, \mathcal{R}, \mathcal{D}(r)} \Gamma \\
\text{s.t.} \quad & \tau_r(v_r, \delta_r, \mathbf{p}_r) \geq \tau_r(q_r, \delta_r, \mathbf{p}_r) + \sum_{u \in \mathcal{D}(r)} \tau_u(q_u, \delta_u, \mathbf{p}_u), \quad \forall r \in \mathcal{R} \\
& \tau_r(v_r, \delta_r, \mathbf{p}_r)|_{u \in \mathcal{D}(r)} - \tau_r(v_r, \delta_r, \mathbf{p}_r)|_{\mathcal{D}(r) \setminus \{u\}} \geq \\
& \quad \tau_j(v_j, \delta_j, \mathbf{p}_j)|_{u \in \mathcal{D}(j)} - \tau_j(v_j, \delta_j, \mathbf{p}_j)|_{\mathcal{D}(j) \setminus \{u\}} \quad \forall r, j \in \mathcal{R} \\
& |\mathcal{S}| + |\mathcal{R}| + \sum_{r \in \mathcal{R}} |\mathcal{D}(r)| = M.
\end{aligned} \tag{6.10}$$

6.5 A brute force approach

In (6.10), the optimal sets \mathcal{S}^* , \mathcal{R}^* , and $\mathcal{D}^*(r)$ can be found by examining all the possible combinations of the nodes in set \mathcal{N} as a type S_1 , a cooperating node, or a type S_2 . To reduce the computation complexity, some of these combinations can be excluded as they do not apply to the system model. In the system model, we have that a cooperating node serves at least one type S_2 node, and a type S_2 node uses only one cooperating node. This implies that the number of type S_2 nodes in the network must be equal to or larger than the number of cooperating nodes. i.e., if the network has $|\mathcal{S}|$ type S_1 nodes, $0 \leq |\mathcal{S}| \leq M$, then the number of cooperating nodes has to be $|\mathcal{R}| \leq \lfloor (M - |\mathcal{S}|)/2 \rfloor$ and the number of type S_2 nodes $|\mathcal{U}| = M - |\mathcal{S}| - |\mathcal{R}|$. Also, this implies that the number of type S_1 nodes cannot be $M - 1$. This is because if the remaining node is categorized as a cooperating node, it will not be associated with a type S_2 node and vice versa. Using these constraints, the number of all possible combinations as a function of M is

$$\mathcal{C} = \left[\sum_{|\mathcal{S}|=1}^{M-2} \sum_{|\mathcal{R}|=1}^{\lfloor (M-|\mathcal{S}|)/2 \rfloor} \binom{|\mathcal{R}| + |\mathcal{U}|}{|\mathcal{R}|} \binom{M}{|\mathcal{S}|} + \sum_{|\mathcal{R}|=1}^{\lfloor M/2 \rfloor} \binom{M}{|\mathcal{R}|} \right] \mathcal{Q} + 1, \tag{6.11}$$

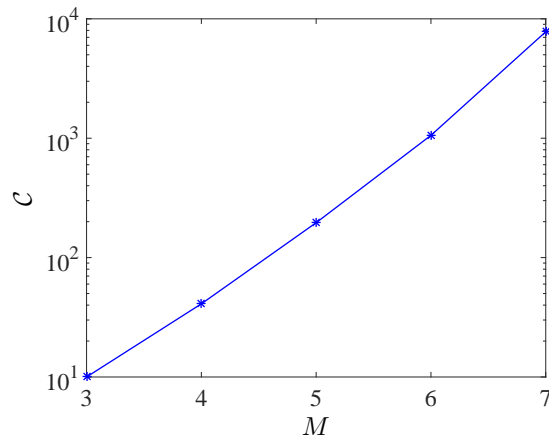


Figure 6.3: The number of all possible combinations increases exponentially with M .

$$\mathcal{Q} = \left(1\mathbb{1}_{(|\mathcal{R}|=1)} + |\mathcal{R}|!\mathbb{1}_{(|\mathcal{R}|=|\mathcal{U}|\neq 1)} + (|\mathcal{R}|^{|\mathcal{U}|} - |\mathcal{R}|)\mathbb{1}_{(1 < |\mathcal{R}| < |\mathcal{U}|)} \right), \quad (6.12)$$

where the first term in (6.11) calculates all the possible combinations when the network has $|\mathcal{S}|$ type S_1 nodes, $0 < |\mathcal{S}| \leq M - 2$, the second term calculates all the possible combinations when the network has only cooperating nodes and type S_2 nodes, i.e., $|\mathcal{S}| = 0$, and the added 1 is for the only combination when all the nodes are type S_1 nodes, i.e., $|\mathcal{S}| = M$. Although the number of the examined combinations is reduced, it is still relatively high. As shown in Figure 6.3, it scales exponentially with M , meaning that the computation complexity of the brute force approach will also scale exponentially. Therefore, we next propose algorithms that finds the optimal Γ with less computation complexity.

6.6 Centralized Algorithm

Algorithm 6.1 illustrates the centralized algorithm that finds the optimal sets \mathcal{S}^* , \mathcal{R}^* , and $\mathcal{D}^*(r)$ that maximizes Γ in (6.10). For a given set of nodes \mathcal{N} , the algorithm initializes two sets \mathcal{Y} and \mathcal{Z} , where $\mathcal{Y}, \mathcal{Z} \subseteq \mathcal{N}$ and $\mathcal{Z} = \mathcal{Y}^c$. Set \mathcal{Y} contains every node in \mathcal{N} that is a candidate to be a cooperating node while set \mathcal{Z} contains every node in \mathcal{N} that is a candidate to be a type S_2 node. A node $i \in \mathcal{N}$ is said to be a cooperating node candidate if its energy harvesting rate is higher than or equal to its energy depletion rate, i.e., $q_i \leq r_i$. Otherwise, the node is said to be a type S_2 candidate. Note that when the node has its energy harvesting rate equal to its energy depletion rate, i.e., $q_i = r_i$, it is still considered

a cooperating node candidate in order to make the algorithm less complex. The algorithm also initializes the sets $\mathcal{R} = \{\emptyset\}$ and $\mathcal{D}(i) = \{\emptyset\} \forall i \in \mathcal{Y}$.

Proposition 1 : If all the nodes are cooperating node candidates, i.e., $q_i \leq r_i \forall i \in \mathcal{N}$, $|\mathcal{Y}| = M$, and $|\mathcal{Z}| = 0$, then the maximum throughput of the network is achieved when all the nodes are type S_1 nodes, i.e., $\mathcal{S}^* = \mathcal{N}$, $\mathcal{R}^* = \mathcal{D}^*(i) = \{\emptyset\} \forall i \in \mathcal{Y}$.

Proof : We have seen in Section 6.3 that $\tau_i(q_i, \delta_i, \mathbf{p}_i) = q_i$ for node $i \in \mathcal{N}$ when $q_i \leq r_i$, and $\tau_i(q_i, \tilde{\delta}, \mathbf{p}_i) = q_i$ if $\tau_i(q_i, \delta_i, \mathbf{p}_i) = q_i$. Given this and assuming that node i is a cooperating node of $|\mathcal{D}(i)|$ type S_2 nodes, the first constraint in (6.10) becomes

$$v_i \Delta_i(v_i, \delta_i, \mathbf{p}_i) \geq q_i + \sum_{u \in \mathcal{D}(i)} q_u. \quad (6.13)$$

Here $v_i = \Pr(\mathcal{E}_i = 1 \cup \bigcup_{u \in \mathcal{D}(i)} \mathcal{E}_u = 1)$. Because the events of the cooperating node and type S_2 nodes are independent and not mutually exclusive, the left-hand-side of (6.13) will be less than its right-hand-side $\forall \Delta_i(v_i, \delta_i, \mathbf{p}_i) \leq 1$. Thus, the constraint in (6.13) will be met only if $\mathcal{D}(i) = \{\emptyset\}$, where in this case both sides of (6.13) will equal to q_i , i.e., node $i \in \mathcal{N}$ will transmit only its events, acting as a type S_1 . When all the nodes are type S_1 , the third constraint in (6.10) will be met, and the second constraint will also be met where both of its sides will be 0.

Proposition 2 : If all the nodes are type S_2 candidates, i.e., $q_i > r_i \forall i \in \mathcal{N}$, $|\mathcal{Y}| = 0$, and $|\mathcal{Z}| = M$, then the maximum throughput is achieved when all the nodes are type S_1 nodes, i.e., $\mathcal{S}^* = \mathcal{N}$, $\mathcal{R}^* = \mathcal{D}^*(i) = \{\emptyset\} \forall i \in \mathcal{Y}$.

Proof : We showed in Section 6.3 that $\tau_i(q_i, \delta_i, \mathbf{p}_i)$ of node $i \in \mathcal{N}$ remains constant $\forall q_i > r_i$. Let node i be a cooperating node of $|\mathcal{D}(i)|$ type S_2 nodes. Because $v_i = \Pr(\mathcal{E}_i = 1 \cup \bigcup_{u \in \mathcal{D}(i)} \mathcal{B}_u = 1) > q_i > r_i$, then $\tau_i(v_i, \delta_i, \mathbf{p}_i) = \tau_i(q_i, \delta_i, \mathbf{p}_i) \forall i \in \mathcal{N}$. Thus, the first constraint in (6.10) becomes

$$\tau_i(q_i, \delta_i, \mathbf{p}_i) \geq \tau_i(q_i, \delta_i, \mathbf{p}_i) + \sum_{u \in \mathcal{D}(i)} \tau_u(q_u, \delta_u, \mathbf{p}_u), \quad (6.14)$$

and it will be met only if $\mathcal{D}(i) = \{\emptyset\}$, i.e., node i transmits only its events, acting as a type S_1 .

If the network has some nodes that are cooperating node candidates and some nodes that are type S_2 candidates, i.e., $|\mathcal{Y}| \neq 0$ and $|\mathcal{Y}| \neq M$, the nodes in \mathcal{Y} will be ordered decreasingly

Algorithm 6.1 Centralized Throughput Maximization Algorithm

- 1: **Inputs:** $q_i, \delta_i, \mathbf{p}_i, \forall i \in \mathcal{N} = \{1, 2, \dots, M\}$, and $\tilde{\delta}$;
 - 2: **Outputs:** $\mathcal{S}^*, \mathcal{R}^*, \mathcal{D}^*(r) \forall r \in \mathcal{R}^*$;
 - 3: **Compute:** r_i using (6.7), $d_i = r_i - q_i$, and $v_i = q_i \forall i \in \mathcal{N}$;
 - 4: **Initialize Sets:** $\mathcal{Y} = \{i : i \in \mathcal{N}, q_i \leq r_i\}$, $\mathcal{Z} = \mathcal{Y}^c$, $\mathcal{R} = \{\emptyset\}$, $\mathcal{D}(i) = \{\emptyset\}, \forall i \in \mathcal{Y}$;
 - 5: Use (6.6) to calculate any $\tau(\cdot)$ that appears below;
 - 6: **if** $|\mathcal{Y}| \neq 0$ AND $|\mathcal{Y}| \neq M$, **then**
 - 7: Order \mathcal{Y} decreasingly based on $d_i, i \in \mathcal{Y}$;
 - 8: Assume d_j of node $j \in \mathcal{Y}$ is the largest;
 - 9: Order \mathcal{Z} increasingly based on $\tau_i(q_i, \delta_i, \mathbf{p}_i), i \in \mathcal{Z}$;
 - 10: Assume $\tau_k(q_k, \delta_k, \mathbf{p}_k)$ of node $k \in \mathcal{Z}$ is the smallest;
 - 11: $h = \tau_j(q_j, \delta_j, \mathbf{p}_j) + \tau_k(q_k, \delta_k, \mathbf{p}_k)$;
 - 12: $v_j = v_j + \tau_k(q_k, \tilde{\delta}, \mathbf{p}_k) - v_j \tau_k(q_k, \tilde{\delta}, \mathbf{p}_k)$;
 - 13: **if** $\tau_j(v_j, \delta_j, \mathbf{p}_j) \geq h$, **then**
 - 14: Node k is a type S_2 of node j ;
 - 15: $\mathcal{D}(j) = \mathcal{D}(j) \cup \{k\}$;
 - 16: $\mathcal{R} = \{\mathcal{R}\} \cup \{j\}$, $\mathcal{Z} = \mathcal{Z} \setminus \{k\}$;
 - 17: **if** $v_j \geq r_j$, **then**
 - 18: $\mathcal{Y} = \mathcal{Y} \setminus \{j\}$;
 - 19: **else;**
 - 20: Update $d_j = r_j - v_j$;
 - 21: **endif;**
 - 22: Go to Step 6;
 - 23: **else**
 - 24: None of the nodes in \mathcal{Z} , including k , can be a type S_2 ;
 - 25: Go to step 28;
 - 26: **endif**
 - 27: **else**
 - 28: $\mathcal{R}^* = \mathcal{R}$, $\mathcal{D}^*(i) = \mathcal{D}(i) \forall i \in \mathcal{Y}$, $\mathcal{S}^* = \mathcal{N} \setminus (\mathcal{R} \cup \bigcup_{i \in \mathcal{Y}} \mathcal{D}(i))$;
 - 29: **endif**
-

based on their fractions of events that they can forward for another node (d). On the other hand, the nodes in \mathcal{Z} will be ordered increasingly based on their successful transmission probabilities to the base station. Ordering these sets will ensure that if the first constraint in (6.10) is met, then the second constraint will also be met. Assume that d_j of node $j \in \mathcal{Y}$ is the largest and $\tau_k(q_k, \delta_k, \mathbf{p}_k)$ of node $k \in \mathcal{Z}$ is the smallest. Then, node k will be tested to be a type S_2 of node j or not by checking the first constraint. If the first constraint is met, then node k will be a type S_2 of node j . After that, node k will be removed from set \mathcal{Z} and added to set $\mathcal{D}(j)$, and node j will be added to the set of cooperating nodes \mathcal{R} . After adding node k to its set, node j will be removed from set \mathcal{Y} only if its energy harvesting rate becomes lower than or equal to its energy depletion rate, i.e., $v_j \geq r_j$. Otherwise, it will remain in the set and its d_j will be updated. After updating and reordering the two sets \mathcal{Y} and \mathcal{Z} , the same procedure will continue with the next nodes in \mathcal{Y} and \mathcal{Z} . If the first constraint is not met, however, node k cannot be a type S_2 of node j , or any of the remaining cooperating node candidates as they have a lower fraction of events that they can forward. This holds the same for the remaining type S_2 candidates as they have higher successful transmission probabilities than node k . And thus the test will terminate.

Note that if two nodes or more in \mathcal{Y} or \mathcal{Z} have the same fraction of events that they can forward or have the same successful transmission probability, respectively, the algorithm will arbitrarily order them. After the test ends or terminates, the sets \mathcal{R} , $\mathcal{D}(i) \forall i \in \mathcal{Y}$, and \mathcal{S} will be optimized. Using these sets, the optimal Γ can be calculated from (6.9). As stated in Section 6.1, the algorithm is run at the base station which broadcasts a message that has the assignment of each node after the test ends. If a node is assigned to be a type S_1 or a cooperating node, then its transmission path is directly to the base station. If it is assigned to be a type S_2 of some cooperating node, then its transmission path to the base station is through that cooperating node.

There is no close form expression for the number of iterations required to find the optimal solution because it depends on the system parameters. However, we can provide an upper-bound expression, which can be derived from the worst scenario, that is when the network has only one cooperating node candidate and the rest of the nodes are type S_2 candidates, and these type S_2 candidates are assigned to be type S_2 nodes of that cooperating node

candidate after running the algorithm. In this scenario, the number of iterations will be the same as the number of type S_2 candidates, which is $M - 1$. Thus, the algorithm's complexity is $\mathcal{O}(M)$, which is linear.

6.7 Distributed Algorithm

Algorithms 6.2 and 6.3 summarize the distributed algorithm that finds the optimal solution for (6.10). Algorithm 6.2 is for node $i \in \mathcal{N}$ if it is a type S_2 candidate, and Algorithm 6.3 is for node $i \in \mathcal{N}$ if it is a cooperating node candidate. Initially, each node $i \in \mathcal{N}$ calculates its r_i using (6.7) when $\delta = \delta_i$, where by comparing q_i with r_i , node i can know if it is a type S_2 candidate or a cooperating node candidate. If node i is a type S_2 candidate, then as illustrated in Algorithm 6.2, the node first calculates its $\tau_i(q_i, \tilde{\delta}, \mathbf{p}_i)$ and $\tau_i(q_i, \delta_i, \mathbf{p}_i)$ using (6.6). And then at the beginning of the time block, the node starts a timer of a duration $t_i = \tau_i(q_i, \delta_i, \mathbf{p}_i)$ time units. The timer is to give priority for the type S_2 candidate that achieves the smallest successful transmission probability to the base station to be assisted first, which is similar to the centralized algorithm where the type S_2 candidates are given priorities by ordering them increasingly based on their successful transmission probabilities. If none of the other type S_2 candidates has broadcasted its successful transmission probabilities before the time t_i ends, which happens only if node i has the shortest timer length, node i will broadcast its $\tau_i(q_i, \tilde{\delta}, \mathbf{p}_i)$ and $\tau_i(q_i, \delta_i, \mathbf{p}_i)$ to the network right after its timer expires, and only the cooperating node candidates will receive them. After that, node i will wait for an ACK from a cooperating node candidate. If the cooperating node candidate $j \in \mathcal{N}$ can be a cooperating node of node i , then it will broadcast an ACK to inform the type S_2 candidates that node i became its type S_2 node. In this case, node i will be a type S_2 of node j and it will terminate the test. If no ACK is received, i.e., none of the cooperating node candidates can be its cooperating node, then node i will be a type S_1 . If one of the other type S_2 candidates has broadcasted its successful transmission probabilities before the time t_i ends, node i will turn off its timer and wait for an ACK from a cooperating node candidate $j \in \mathcal{N}$. If an ACK is received, then the node will wait for the next time block to start the procedure all over again. If not, node i will operate as a type S_1 .

Algorithm 6.2 Distributed Algorithm for a type S_2 Candidate Node $i \in \mathcal{N}$

- 1: **Inputs:** $q_i, \delta_i, \tilde{\delta}, \mathbf{p}_i$;
 - 2: **Outputs:** Category of node i ;
 - 3: **Compute:** $\tau_i(q_i, \tilde{\delta}, \mathbf{p}_i)$ and $\tau_i(q_i, \delta_i, \mathbf{p}_i)$ using (6.6);
 - 4: At the beginning of a time block,
 - 5: Set and start a timer $t_i = \tau_i(q_i, \delta_i, \mathbf{p}_i)$;
 - 6: **if** none of the other type S_2 candidates broadcasted its $\tau(\cdot)$ s, **then**
 - 7: When the timer expires,
 - 8: Broadcast $\tau_i(q_i, \tilde{\delta}, \mathbf{p}_i)$ and $\tau_i(q_i, \delta_i, \mathbf{p}_i)$;
 - 9: Wait for an ACK from a cooperating node candidate $j \in \mathcal{N}$;
 - 10: **if** an ACK received before the end of the time block, **then**
 - 11: Node i is a type S_2 of the cooperating node candidate j ;
 - 12: **else**
 - 13: Node i is a type S_1 ;
 - 14: **endif**
 - 15: **else**
 - 16: Turn off your timer when $\tau(\cdot)$ s are started to be broadcasted;
 - 17: Wait for an ACK from a cooperating node candidate $j \in \mathcal{N}$;
 - 18: **if** an ACK received before the end of the time block, **then**
 - 19: Go to step 4;
 - 20: **else**
 - 21: Node i is a type S_1 ;
 - 22: **endif**
 - 23: **endif**
-

Algorithm 6.3 Distributed Algorithm for a Cooperating Node Candidate $i \in \mathcal{N}$

- 1: **Inputs:** $q_i, \delta_i, \mathbf{p}_i$;
 - 2: **Outputs:** Category of node i ;
 - 3: **Compute:** r_i using (6.7), and $d_i = r_i - q_i$, and set $v_i = q_i$;
 - 4: At the beginning of a time block,
 - 5: Wait for a transmitted $\tau(\cdot)$ s from a type S_2 candidate $j \in \mathcal{N}$;
 - 6: **if** any $\tau(\cdot)$ s received before the end of the time block, **then**
 - 7: Check the first constraint in (6.10) including any previous type S_2 nodes;
 - 8: **if** the constraint is met, **then**
 - 9: Set and start a timer $t_i = (1 - d_i)$;
 - 10: **if** none of the other cooperating node candidates broadcasted ACK, **then**
 - 11: When the timer expires,
 - 12: Broadcast an ACK that node i is a cooperating node of node j ;
 - 13: Calculate $v_i = v_i + \tau_j(q_j, \tilde{\delta}, \mathbf{p}_j) - v_i \tau_j(q_j, \tilde{\delta}, \mathbf{p}_j)$;
 - 14: **if** $v_i < r_i$, **then**
 - 15: Update $d_i = r_i - v_i$, go to step 4;
 - 16: **else**
 - 17: Go to step 31;
 - 18: **endif**
 - 19: **else**
 - 20: Turn off your timer, go to step 4;
 - 21: **endif**
 - 22: **else**
 - 23: **if** the constraint has been met before this time block, **then**
 - 24: Node i is a cooperating node for the nodes that have met the constraint;
 - 25: **else**
 - 26: Node i is a type S_1 ;
 - 27: **endif**
 - 28: **endif**
 - 29: **else**
 - 30: Go to step 23;
 - 31: **endif**
-

If node i is a cooperating node candidate, then as illustrated in Algorithm 6.3, the node first calculates its $d_i = r_i - q_i$ and sets $v_i = q_i$. At the beginning of a time block, node i waits for any broadcasted successful transmission probabilities $\tau(\cdot)$ s from a type S_2 candidate $j \in \mathcal{N}$. If any $\tau(\cdot)$ s are received, node i will first check the first constraint in (6.10). And if the constraint including any previous type S_2 nodes is met, the node will start a timer of a duration $t_i = (1 - d_i)$ time units, where the node of the largest fraction of the extra events that it can forward will assist first. If none of the other cooperating node candidates broadcasted an ACK before the time t_i ends, then node i will broadcast an ACK after the time t_i ends to inform all the type S_2 candidates that node j became its type S_2 node. And then node i will update its v_i and check if its energy harvesting rate is still higher than its energy depletion rate or not. If yes, then it will update its d_i , and then wait for the next time block to start the procedure all over again as it may still be able to assist with the transmissions of another type S_2 candidate. Otherwise, it will terminate the test. If any of the other cooperating node candidates broadcasted an ACK before t_i ends, then node i will turn off its timer and wait for the next time block to start again. On the other hand, at the beginning of a time block, if any $\tau(\cdot)$ s are received and the first constraint is not met, or if no $\tau(\cdot)$ s are received, then node i will be a cooperating node if the constraint has been met with any type S_2 candidates before the current time block. Otherwise, it will be a type S_1 .

In the distributed algorithm, the optimal solution is found in the first time block in which there is no ACK broadcasted. By that time block, each node will already be optimally assigned a role. Note that, if two or more type S_2 candidates or if two or more cooperating node candidates have the same timer length, the priority can be given for the node of the largest ID number. That is, when the type S_2 candidates of the same timer length broadcast their $\tau(\cdot)$ s, the cooperating node candidates of the same timer length each will broadcast an ACK back that has the the largest ID among these type S_2 candidates if the first constraint is met. In turn, the type S_2 candidate of the largest ID number will chose the cooperating node candidate of the largest ID number as a cooperating node, and then broadcast an ACK to inform the cooperating node candidates that the cooperating node candidate of the largest ID number has been chosen to be its cooperating node, and so on.

In the distributed algorithm, the number of iterations required to find the optimal solution

has the same upper-bound as the centralized algorithm. Therefore, the complexity of the distributed algorithm is also linear. Here, the upper-bound of the number of iterations is calculated from Algorithm 6.3 as it is more complex than Algorithm 6.2, and from the same worst scenario discussed in the previous section. Although one of them could save the nodes more energy than the other, both the centralized and distributed algorithms achieve the same throughput over the long term, i.e., when $N \rightarrow \infty$. This is because when $N \rightarrow \infty$, the average probability, given by (6.3), that a node is energized over the N time blocks will be the same regardless of the remaining energy after finding the optimal solution, which is due to the fact that the energy battery level of a node is modeled as a Markov chain. Hence, each node will achieve the same successful transmission probability in (6.4), which will lead to the same network throughput.

6.8 Variable Transmit Power

The centralized and distributed algorithms designed earlier can be adapted for the scenario when the transmit power between the nodes is variable. Here, the transmit power between any two nodes $i, j \in \mathcal{N}$ will be $\delta_{i,j}$ instead of $\tilde{\delta}$. Thus, the successful transmission probability from a type S_2 node u to its cooperating node r will be $\tau_u(q_u, \delta_{u,r}, \mathbf{p}_u)$, which still can be calculated using (6.6).

When the transmit power between the nodes is variable, we cannot guarantee that if the first constraint in (6.10) is met, then the second constraint will also be met. Hence, each type S_2 candidate in \mathcal{Z} has to be tested as a type S_2 of each cooperating node candidate in \mathcal{Y} , which implies that set \mathcal{Y} does not need to be ordered. For this scenario, therefore, we can modify the centralized algorithm illustrated in Algorithm 6.1 as follows. After creating the two sets \mathcal{Z} and \mathcal{Y} , we first order set \mathcal{Z} increasingly. Then, we find the cooperating node candidates that meet the first constraint with the first type S_2 candidate in \mathcal{Z} , and the one that meets the second constraint among these cooperating node candidates will be a cooperating node of that type S_2 candidate. After that, we remove that type S_2 candidate from set \mathcal{Z} , and then update the two sets \mathcal{Z} and \mathcal{Y} . After updating these two sets, we repeat the same steps for the next type S_2 candidate in \mathcal{Z} .

As for the distributed algorithm, a type S_2 candidate will broadcast its $\overline{E[n]}$ and q instead of its $\tau(\cdot)$ s as in the fixed transmit power scenario. Hence, the $\tau(\cdot)$ s will be calculated at the cooperating node candidates in order to reduce the computation complexity. This, however, requires the assumption that each node knows the transmit power between it and any other node in the network. Based on these modifications, Algorithm 6.3 can be changed for the variable transmit power scenario as follows. In each time block, a cooperating node candidate first calculates the $\tau(\cdot)$ s of the type S_2 candidate of the shortest timer length, and then checks the first and the second constraints. After that, it broadcasts an ACK, which will have the number of events that it can forward to that type S_2 candidate without setting any timer. In turn, that type S_2 candidate will select the cooperating node candidate that can forward the largest number of events to it by its ID, and broadcast this in an ACK to the cooperating node candidates. Selecting the cooperating node candidate that can forward the largest number of events as well as broadcasting $\overline{E[n]}$ and q instead of $\tau(\cdot)$ s will be the only change in Algorithm 6.2.

In the adaptive transmit power algorithms, the upper bound of the number of iterations that is required to find the optimal solution is calculated from the worst scenario, that is when M is even, and the half of the nodes are cooperating node candidates and the other half are type S_2 candidates, and each cooperating node candidate still can serve as a cooperating node candidate after it adds a type S_2 to its set. In this scenario, because each type S_2 candidate will be tested as a type S_2 of each cooperating node candidate, the total number of iterations will be $(\frac{M}{2})^2$. Thus, the algorithms' complexity is $\mathcal{O}(M^2)$, which is quadratic.

6.9 Simulation Results

Although the algorithms were designed for an arbitrary number of nodes M , for simplicity, in the simulations we consider a network of three nodes, i.e., $\mathcal{N} = \{1, 2, 3\}$. We use three different sets of parameters. The first set of parameters is $q_1 = q_2 = q_3 = 0.2$, $\mathbf{p}_1 = \mathbf{p}_2 = [0.2 \ 0.8]$, $\mathbf{p}_3 = [0.8 \ 0.2]$, $\tilde{K} = 1$, $K = 100$, $N = 10^5$, $\delta_1 = \delta_2 = \delta_3 = 2$, $\tilde{\delta} = 1$. The second set of parameters is $q_1 = q_2 = q_3 = 0.2$, $\mathbf{p}_1 = \mathbf{p}_2 = \mathbf{p}_3 = [0.2 \ 0.8]$, $\tilde{K} = 1$, $K = 100$, $N = 10^5$, $\delta_1 = \delta_2 = \delta_3 = 2$, $\tilde{\delta} = 1$. The third set of parameters is $q_1 = 0.2$, $q_2 = 0.8$, $q_3 = 0.2$,

Table 6.1: All Possible Scenarios of the Network

Scenario	Node 1	Node 2	Node 3
1	type S_1	type S_1	type S_1
2	type S_1	type S_2	Cooperating node
3	type S_1	Cooperating node	type S_2
4	type S_2	type S_1	Cooperating node
5	Cooperating node	type S_1	type S_2
6	type S_2	Cooperating node	type S_1
7	Cooperating node	type S_2	type S_1
8	Cooperating node	type S_2	type S_1
9	type S_1	Cooperating node	type S_2
10	type S_2	type S_2	Cooperating node

$\mathbf{p}_1 = [0.025 \ 0.025 \ 0.025 \ 0.025 \ 0.1 \ 0.8]$, $\mathbf{p}_2 = [0.2 \ 0.3 \ 0.3 \ 0.2 \ 0 \ 0]$, $\mathbf{p}_3 = [0.1 \ 0.1 \ 0.2 \ 0.3 \ 0.3 \ 0]$, $\tilde{K} = 5$, $K = 100$, $N = 10^5$, $\delta_1 = \delta_2 = \delta_3 = 6$, $\delta_{1,2} = 2$, $\delta_{1,3} = 4$, $\delta_{2,3} = 1$. Each set is contained in its figure's caption.

We simulate both the fixed and variable transmit power scenarios. In these two scenarios, the optimal Γ is calculated using the proposed algorithms and brute force approach. In the brute force approach, using the constraints mentioned in Section 6.5, Table 6.1 shows all the possible scenarios or combinations of the nodes' assignments that were examined. In the same row/scenario of Table 6.1 when there is a type S_2 node and a cooperating node, it means that the type S_2 node is a type S_2 node of that cooperating node. For each scenario, Γ is calculated by simulation using Monte Carlo technique, and analytically using (6.9). In the centralized algorithm, the nodes in \mathcal{Y} or \mathcal{Z} that have the same fraction of events that they can forward or have the same successful transmission probability, respectively, are ordered arbitrarily using a uniform distribution. All the simulations are done using Matlab. We compare our approach with the cooperative transmission scenario discussed in Chapter 2, where each pair of nodes in the network form a three-relay channel with the base station.

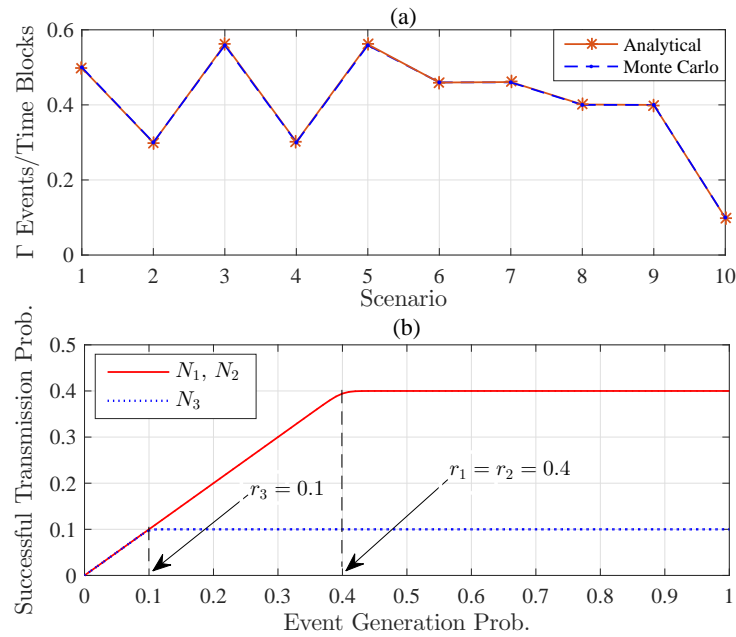


Figure 6.4: Figure (a) shows the network throughput for all the scenarios shown in Table 6.1. Figure (b) shows the successful transmission probability of N_1 , N_2 , and N_3 . Parameters used: $q_1 = q_2 = q_3 = 0.2$, $\mathbf{p}_1 = \mathbf{p}_2 = [0.2 \ 0.8]$, $\mathbf{p}_3 = [0.8 \ 0.2]$, $\tilde{K} = 1$, $K = 100$, $N = 10^5$, $\delta_1 = \delta_2 = \delta_3 = 2$, $\tilde{\delta} = 1$.

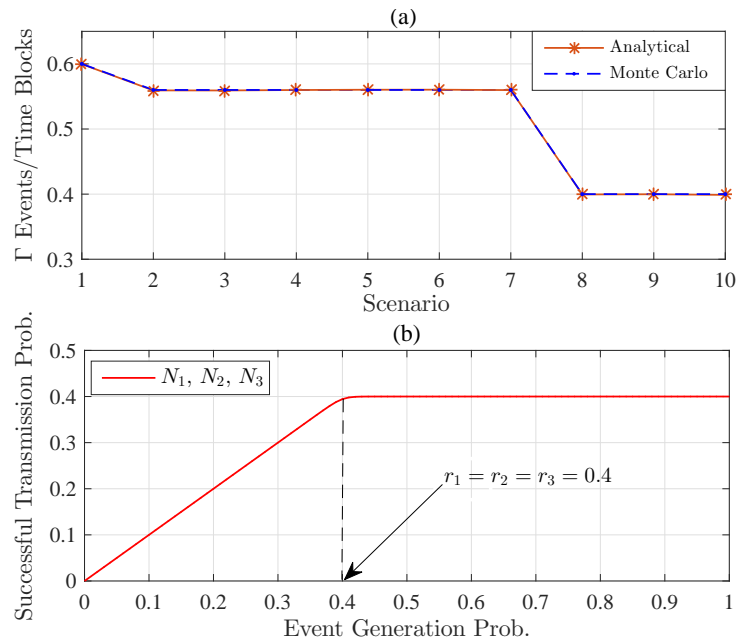


Figure 6.5: Figure (a) shows the network throughput for all the scenarios shown in Table 6.1. Figure (b) shows the successful transmission probability of N_1 , N_2 , and N_3 . Parameters used: $q_1 = q_2 = q_3 = 0.2$, $\mathbf{p}_1 = \mathbf{p}_2 = \mathbf{p}_3 = [0.2 \ 0.8]$, $\tilde{K} = 1$, $K = 100$, $N = 10^5$, $\delta_1 = \delta_2 = \delta_3 = 2$, $\tilde{\delta} = 1$.

6.9.1 Fixed Transmit Power

Using the first set of parameters contained in Figure 6.4, the results of the brute force approach in Figure 6.4 (a) show that Γ is maximized at two scenarios. First, it is maximized at Scenario 3 where node 1 is a type S_1 , node 2 is a cooperating node of node 3. Second, it is maximized at Scenario 5 where node 2 is a type S_1 , node 1 is a cooperating node of node 3. Thus, the optimal solution should be either Scenario 3 or Scenario 5. In the centralized algorithm, from Figure 6.4 (b), we have that $q_1 < r_1$, $q_2 < r_2$, and $q_3 > r_3$, which means that node 1 and node 2 are cooperating node candidates and node 3 is a type S_2 candidate. Because $d_1 = d_2$, in the simulation, node 1 was randomly selected to be ordered ahead of node 2 in the set of cooperating node candidates. And because $\tau_1(v_1, \delta_1, \mathbf{p}_1) \approx 0.36 > q_1 + \tau_3(q_3, \delta_3, \mathbf{p}_3) = 0.3$ events/time blocks, node 3 was assigned to be a type S_2 of node 1, and node 2 was assigned to be a type S_1 , which is the nodes' assignment of Scenario 5. If node 2 was randomly ordered ahead of node 1, then the optimal solution would have been Scenario 3 instead of Scenario 5. In the distributed algorithm, because node 2 is the cooperating node candidate of the largest ID number, the optimal solution was Scenario 3.

Using the second set of parameters contained in Figure 6.5, the brute force approach results in Figure 6.5 (a) show that Γ is maximized at Scenario 1, where all the nodes are type S_1 nodes. In the centralized algorithm, this optimal solution was found without testing any of the nodes since all of them are cooperating node candidates as shown in Figure 6.5 (b). According to **Proposition 1**, if all the nodes are cooperating node candidates, then Γ is maximized when all the nodes are type S_1 nodes. In the distributed algorithm, the optimal solution was found in the first time block because there was no $\tau(\cdot)$ s received at the cooperating node candidates and no ACK was broadcasted.

6.9.2 Variable Transmit Power

Using the third set of parameters shown in Figure 6.6, we simulate the scenario when the transmit power between the nodes is variable using the centralized algorithm. For comparison purposes, we also simulate the scenario when the transmit power is fixed. In the fixed

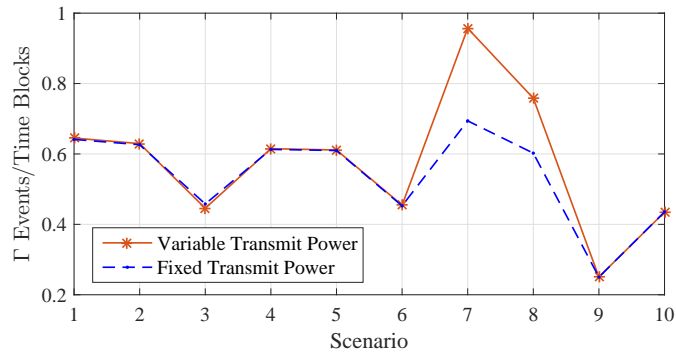


Figure 6.6: The network throughput for each scenario shown in Table 6.1 when the transmit power is variable and fixed. Parameters used: $q_1 = 0.2$, $q_2 = 0.8$, $q_3 = 0.2$, $\mathbf{p}_1 = [0.025 \ 0.025 \ 0.025 \ 0.025 \ 0.1 \ 0.8]$, $\mathbf{p}_2 = [0.2 \ 0.3 \ 0.3 \ 0.2 \ 0 \ 0]$, $\mathbf{p}_3 = [0.1 \ 0.1 \ 0.2 \ 0.3 \ 0.3 \ 0]$, $\tilde{K} = 5$, $K = 100$, $N = 10^5$, $\delta_1 = \delta_2 = \delta_3 = 6$, $\delta_{1,2} = 2$, $\delta_{1,3} = 4$, $\delta_{2,3} = 1$.

transmit power scenario, in order for the nodes to communicate with each other, $\tilde{\delta}$ was set to 4, which is $\delta_{1,3}$, the transmit power between node 1 and node 3. Using the same parameters, we also simulate the two transmit power scenarios using the brute force approach.

The results of the brute force approach in Figure 6.6 show that the network throughput is maximized at Scenario 7, where node 3 is a type S_1 and node 2 is a type S_2 of node 1. Using the centralized algorithm, in the fixed transmit power scenario, this optimal solution was found in one iteration while in the variable transmit power scenario, it was found in two iterations. This is expected because in the variable transmit power scenario, each type S_2 candidate has to be tested as a type S_2 of each cooperating node candidate, and here the number of cooperating node candidates is 2. Also, the results show that the maximum throughput achieved when the transmit power is variable is higher than the maximum throughput achieved when the transmit power is fixed. This is because the transmit power between node 1 and node 2 in the fixed transmit power becomes higher, which results in less number of events that are successfully transmitted from node 2 to node 1, and leads to a lower throughput. Finally, in the variable transmit power scenario, although the transmit power between node 1 and node 2 is higher than the transmit power between node 2 and node 3, node 1 was selected to be a cooperating node of node 2 instead of node 3. This implies that selecting a cooperating node for a node depends only on how many events that cooperating node can forward for that node.

6.9.3 Comparison with Cooperative Transmission

We compare our approach with the cooperative transmission scenario when each pair of nodes in the network form a three-node relay channel with the base station, where one of the pair is a type S_2 node while the other is a cooperating node. We use the first and second sets of parameters shown in Figure 6.4 and Figure 6.5, respectively. Because the network has only three nodes, we consider that two of the nodes form a three-node relay channel with the base station while the third operates as a type S_1 . In both cooperative transmission and our approach, the node that operates as a type S_1 achieves the same performance, which makes the comparison fair.

In cooperative transmission, when using the first set of parameters contained in Figure 6.4, we found that the network throughput is maximized when the nodes' assignment is set as in Scenario 3 or Scenario 5. In these two scenarios, because the type S_2 node always transmits cooperatively using the cooperating node that is always energized, the maximum throughput is the same as in our approach. However, in cooperative transmission, because the cooperating node gives priority for the type S_2 node's transmissions over its own, the cooperating node's throughput drops to 0.16 events/time blocks while the type S_2 node's throughput increases to 0.2 events/time blocks. In our case, the cooperating node's throughput stays the same that is 0.2 events/time blocks while the type S_2 node's throughput increases to 0.16 events/time blocks. This implies that in our approach, the overall throughput of the network is maximized such that no node's throughput is adversely affected.

As for the second set of parameters contained in Figure 6.5, when using cooperative transmission, we found that the network throughput is maximized when the nodes' assignment is set as in one of the scenarios from 2-7. From Figure 6.5 (a), the maximum throughput achieved in each of these scenarios is less than the maximum throughput achieved in our approach, which occurs when all the nodes are type S_1 nodes. The maximum throughput achieved in our approach can be achieved in cooperative transmission without affecting any node's throughput only if in the same time block, the cooperating node is allowed to transmit its own event after it forwards its type S_2 node's event to the base station. However, this will require increasing the length of time blocks, which will increase the overall time required

to collect the same number of events compared to our approach.

6.10 Conclusions

In this chapter, we consider an uplink energy harvesting wireless sensor network. We address the problem of throughput maximization such that each node's throughput cannot drop below what it achieves by direct transmission to the base station. We propose centralized and distributed algorithms, and we consider fixed and variable transmit power scenarios. We conclude that when the transmit power between the nodes is variable, the maximum throughput can sometimes be higher than the maximum throughput achieved when the transmit power is fixed. However, when the transmit power is fixed, the computation complexity is lower. Compared with using cooperative transmission, our approach maximizes the network throughput such that no node's throughput is adversely affected.

Chapter 7

Summary and Future Work

7.1 Summary

In this dissertation, we address the problem of transmission scheduling in cooperative energy harvesting sensor networks. We first consider the problem for a single cooperating node network. We propose a scheduling scheme, called a feedback scheme, that enables the source to decide whether to transmit its events to the destination by its own or by the help of the cooperating node such that the packet delivery ratio of the system is maximized. The feedback scheme can be generalized to any network of many sensor nodes when each group of three nodes in the network form a three-node relay channel. Compared with the-state-of-the-art scheme, the feedback scheme maximizes the packet delivery ratio of the system with no need for optimizing any of the system parameters. And thus, the feedback scheme becomes more practical in networks of unstable parameters and in networks of sensors with large battery capacity.

We then generalize the feedback scheme to include the case of multiple cooperating nodes, and to include one-way and two-way cooperative communications scenarios. The scheme can be extended to three or more hops where in each hop the transmitting node selects a cooperating node from the next hop using the same algorithm. However, this requires some changes in the system model. For example, the number of time slots per a time block would need to be adjusted. We also propose an adaptive method that reduces the overhead caused by transmitting the energy status of the cooperating nodes to the source

in a separate feedback message. In addition, we propose an adaptive scheme that achieves fairness in the performance between the transmitting and cooperating nodes. The adaptive scheme considers only the case of absolute fairness, where the nodes have to achieve the same performance. This could be unreasonable in some scenarios when the penalty on the cooperating node performance has to be high in order to achieve the same performance of the source node. In addition, if the source node achieves higher performance than the cooperating node, the absolute fairness cannot be achieved as each node is fixed and categorized a priori as either a source or a cooperating node. Therefore, we next generalize the system model where each node in the network can be either a source or a cooperating node depending on the system parameters. We then propose a fairness scheduling (FS) scheme that ensures fairness in the performance of the nodes depending on a given penalty function, which fairly determines how much one of the nodes should cooperate with the other. We also propose a constrained scheduling (CS) scheme that constrains one of the transmitting nodes to achieve a certain performance, if possible.

Although the adaptive method reduces the overhead, it is still relatively high which could consume a significant amount of energy resulting in a lower performance of the system. Therefore, we also propose a statistical model that enables the source to estimate the energy status of the cooperating node. In the scenarios when the energy status of the cooperating node is deterministic, e.g., when the cooperating node is always energized, it will be more energy efficient to use the feedback because there will be no overhead. Otherwise, it will be more energy efficient to use the statistical model. We lastly address the problem of throughput maximization in an uplink energy harvesting wireless sensor network. We propose centralized and distributed algorithms that find the optimal role of each node, which is either source, relay, or user, such that the throughput is maximized. We consider fixed and variable transmit power scenarios and address complexity issues. We conclude that when the transmit power between the nodes is variable, the maximum throughput can sometimes be higher than the maximum throughput achieved when the transmit power is fixed. However, when the transmit power is fixed, the computation complexity is lower. Compared with using cooperative transmission, our approach maximizes the network throughput such that none of the nodes' throughputs is adversely affected.

7.2 Future Work

In this section, we provide some interesting issues that can be addressed in the future. For example, in Chapter 4, there are two interesting issues that are described as follows:

1. The proposed schemes in the chapter were designed such that they provide the optimal operating mode for the system that is fixed over the N time blocks. With the assumption that only one event can be reported per time block, in some scenarios, this may lead to energy overflow, which can be exploited to achieve better performance. To avoid energy overflow, the scheduling schemes need to be redesigned such that the operating mode of the system is selected instantaneously at the start of each time block, with the assumption that more than one event can be reported per time block. So that in each time block, each transmitting node can be either a source, a cooperating, or a relay node, and the cooperating node can transmit its own event, if any, after helping with the source's event transmission. In order to implement this new scenario, the joint distribution of the two transmitting nodes energy battery levels in the cooperation mode needs to be reformed under the following assumptions:
 - (a) The events of the two transmitting nodes are not mutually exclusive.
 - (b) If the two transmitting nodes both have an event generated in the same time block, each node transmits its event on its own if each has sufficient energy for direct transmission.
 - (c) If the two transmitting nodes both have an event generated in the same time block, each node transmits its event first, and it then cooperates with the other node if sufficient energy remains and if the other node has energy that is sufficient only for relay transmission.
2. We assume that the length of each time block is sufficient to report only one event. So, if the cooperating/relay node has an event generated, its event will be dropped to assist with the transmission of the other node if it has an event generated. And this may lead to energy overflow. As stated earlier, this could be solved by allowing for

reporting more than one event per time block. However, this might not be the best solution in applications when the time delay in reporting events is intolerated. So another solution is using energy transfer technology. Instead of spending some amount of its collected energy on forwarding another node's transmissions, in this technology, the cooperating/relay node transfers that energy frequently to the other node as a RF signal. Thus, the cooperating node can transmit its events without delay regardless of the source's event status, assuming that the nodes transmit on different frequency bands or orthogonally. To implement this idea, we can assume that the source node $N_i, i \in \{1, 2\}$ collects energy from the cooperating node $N_j, j \in \{1, 2\}, j \neq i$ whenever it transmits to the destination. As in [70], we can assume that the energy transfer efficiency is $0 \leq \eta \leq 1$, i.e., whenever the cooperating node transmits to the destination using δ amount of energy, $(\eta\delta)$ amount of energy enters the source's battery. Based on these assumptions, we reform the distribution of the energy battery levels of the nodes and then we drive their packet delivery ratios. After that, we maximize the sum of the packet delivery ratios of the nodes over δ for the given η such that $\delta_j \leq \delta \leq K$, assuming that δ_j is the minimum amount of transmit energy required to successfully report the event of the cooperating node to the destination.

In Chapter 6, there are also some interesting issues that can be addressed to make the proposed algorithm more general. These issues include:

1. We consider in Chapter 6 the case when $K \gg \delta_i$. The other case when $K \geq \delta_i$ can also be considered in order to include applications when battery capacity of sensor nodes cannot be large. When $K \geq \delta_i$, as shown in Section 6.3, the successful transmission probability has an additional region called transient. When a node operates in this range, it has energy overflow, and this energy can be exploited by operating the node as a type S_2 node so it transmits with lower energy and more events will be transmitted, or as a cooperating node to forward events to some other node/nodes. Thus, the nodes that operate in the transient region can be called cooperating-type S_2 candidates. To solve the problem, we first need to create a new set that includes all cooperating-type S_2 candidates, and then we need to modify the algorithm of the case when $K \gg \delta_i$

such that it tests these nodes as cooperating nodes first and then as type S_2 nodes.

2. The scenario that a node, in each time block, can make an instantaneous decision on its transmission path can be investigated as it may lead to a better throughput.

References

- [1] C. F. Garcia-Hernandez et al., “*Wireless Sensor Networks and Applications: a Survey*,” Int. J. Comput. Sci. Network Security, vol. 7, no. 3, pp. 264–273, Mar. 2007.
- [2] J. Laneman, D. Tse, and G. Wornell, “*Cooperative diversity in wireless networks: Efficient protocols and outage behavior*,” IEEE Trans. Inf. Theory, vol. 50, no. 12, pp. 3062–3080, Dec. 2004.
- [3] M.O. Hasna, and M.S. Alouini, “*End-to-end performance of transmission systems with relays over Rayleigh-fading channels*,” IEEE Transactions on Wireless Communications, vol.2, no.6, pp.1126–1131, Nov. 2003.
- [4] D.S. Michalopoulos, and G.K. Karagiannidis, “*Two-relay distributed switch and stay combining*,” IEEE Transactions on Communications, vol.56, no.11, pp.1790–1794, Nov. 2008.
- [5] E. C. van der Meulen, “*Three-terminal communication channels*,” Adv. Appl. Prob., vol. 3, pp. 120–154, 1971.
- [6] T. Cover, and A. El Gamal, “*Capacity theorems for the relay channel*,” IEEE Trans. Inf. Theory, vol. 25, no. 5, pp. 572–584, Sep. 1979.
- [7] Y. Yao, X. Cai, and G. Giannakis, “*On Energy Efficiency and Optimum Resource Allocation of Relay Transmissions in the Low-Power Regime*,” IEEE Transactions on Wireless Communication., vol. 4, no. 6, Nov. 2005.
- [8] J. A. Paradiso, and T. Starner, “*Energy scavenging for mobile and wireless electronics*,” IEEE Pervasive Computing, vol.4, no.1, pp.18–27, Jan.–Mar. 2005.
- [9] X. Jiang, J. Polastre, and D. Culler, “*Perpetual environmentally powered sensor networks*,” Fourth International Symposium on Information Processing in Sensor Networks, pp.463–468, 15 Apr. 2005.
- [10] W. K. G. Seah, Z. A. Eu, and H. P. Tan, “*Wireless sensor networks powered by ambient energy harvesting (WSN-HEAP) - Survey and challenges*,” 1st International Conference on Wireless Communication, Vehicular Technology, Information Theory and Aerospace and Electronic Systems Technology (Wireless VITAE 2009), Aalborg, pp. 1–5, 2009.

- [11] S. Chalasani, and J. M. Conrad, “A Survey of Energy Harvesting Sources for Embedded Systems,” IEEE SoutheastCon, Huntsville, AL, pp. 442–447, Apr. 2008.
- [12] B. Warneke, B. Atwood, and K. S. J. Pister, “Smart Dust mote forerunners,” Proceedings of 14th Annual International Conference on Microelectromechanical Systems, pp.357–360, 2001.
- [13] N.J. Guilar, T.J. Kleeburg, A. Chen, D.R. Yankelevich, and R. Amirtharajah, “*Integrated Solar Energy Harvesting and Storage*,” IEEE Transactions on Very Large Scale Integration (VLSI) Systems , vol.17, no.5, pp.627–637, May 2009.
- [14] C. Park, and P.H. Chou, “AmbiMax: Autonomous Energy Harvesting Platform for Multi-Supply Wireless Sensor Nodes,” 3rd Annual IEEE Communications Society on Sensor and Ad Hoc Communications and Networks, 2006. SECON '06. pp.168–177, 28 Sep. 2006.
- [15] B.W. Cook, S. Lanzisera; and K.S.J. Pister, “*SoC Issues for RF Smart Dust*,” Proceedings of the IEEE , vol.94, no.6, pp.1177–1196, June 2006.
- [16] P.D. Mitcheson, E.M. Yeatman, G.K. Rao, A.S. Holmes, and T.C. Green, “*Energy Harvesting From Human and Machine Motion for Wireless Electronic Devices*,” Proceedings of the IEEE , vol.96, no.9, pp.1457–1486, Sep. 2008.
- [17] T. Torfs, V. Leonov, C. Van Hoof, and B. Gyselinckx, “Body-Heat Powered Autonomous Pulse Oximeter,” 5th IEEE Conference on Sensors, pp.427–430, 22–25 Oct. 2006.
- [18] S. Sudevalayam, and P. Kulkarni, “*Energy Harvesting Sensor Nodes: Survey and Implications*,” in IEEE Communications Surveys & Tutorials, vol. 13, no. 3, pp. 443–461, Third Quarter 2011.
- [19] H. Tan, P.W.Q. Lee, W.K.-G. Seah, and Z. A. Eu, “Impact of Power Control in Wireless Sensor Networks Powered by Ambient Energy Harvesting (WSN-HEAP) for Railroad Health Monitoring,” International Conference on Advanced Information Networking and Applications Workshops, 2009. WAINA '09. pp.804–809, 26–29 May 2009.
- [20] Z. A. Eu, W. K. G. Seah, and H. P. Tan, “A study of MAC schemes for wireless sensor networks powered by ambient energy harvesting,” Accepted for publication for the 4th Wireless Internet Conference (WICON), Nov. 2008.
- [21] J. Song, and Y. K. Tan, “Energy consumption analysis of ZigBee-based energy harvesting wireless sensor networks,” IEEE International Conference on Communication Systems (ICCS), pp. 468–472, Singapore, 2012.
- [22] X. Fafoutis, T. Sørensen, and J. Madsen, “*Energy Harvesting - Wireless Sensor Networks for Indoors Applications Using IEEE 802.11*”, Procedia Computer Science, Vol. 32, pp. 991–996, ISSN 1877-0509, 2014.

- [23] R. Vaze, "Transmission capacity of wireless ad hoc networks with energy harvesting nodes," IEEE Global Conference on Signal and Information Processing (GlobalSIP), pp. 353–358, Austin, TX, 2013.
- [24] D. Niyato, E. Hossain, and A. Fallahi, "*Sleep and wakeup strategies in solar-powered wireless sensor/mesh networks: Performance analysis and optimization*," IEEE Transaction on Mobile Computation, vol. 6, pp. 221–236, Feb. 2007.
- [25] C. Ok, H. Thadakamalla, U. Raghavan, S. Kumara, S. Kim, X. Zhang; and S. Bukkapatnam, "Optimal Transmission Power in Self-sustainable Sensor Networks for Pipeline Monitoring," IEEE International Conference on Automation Science and Engineering, 2007. CASE 2007. pp.591–596, 22–25 Sept. 2007.
- [26] S. Mao, M. H. Cheung, and V.W.S. Wong, "An optimal energy allocation algorithm for energy harvesting wireless sensor networks," IEEE International Conference on Communications (ICC). pp.265–270, 10–15 June 2012.
- [27] K. Tutuncuoglu, and A. Yener, "*Optimum Transmission Policies for Battery Limited Energy Harvesting Nodes*," IEEE Transactions on Wireless Communications, vol.11, no.3, pp.1180–1189, Mar. 2012.
- [28] K. Tutuncuoglu, and A. Yener, "Short-Term Throughput Maximization for Battery Limited Energy Harvesting Nodes," IEEE International Conference on Communications (ICC), pp.1–5, 5–9 June 2011.
- [29] O. Ozel, K. Tutuncuoglu, J. Yang; S. Ulukus, and A. Yener, "Adaptive transmission policies for energy harvesting wireless nodes in fading channels," 45th Annual Conference on Information Sciences and Systems (CISS), pp.1–6, 23–25 Mar. 2011.
- [30] O. Ozel, K. Tutuncuoglu, J. Yang, S. Ulukus, and A. Yener, "Resource management for fading wireless channels with energy harvesting nodes," Proceedings IEEE INFOCOM, pp.456–460, 10–15 Apr. 2011.
- [31] A. Sendonaris, E. Erkip, and B. Aazhang, "*User cooperation diversity. Part I. System description*," IEEE Transactions on Communications, vol.51, no.11, pp.1927–1938, Nov. 2003.
- [32] J.N. Laneman, W. Wornell, and D.N.C. Tse, "An efficient protocol for realizing cooperative diversity in wireless networks," IEEE International Symposium on Information Theory, pp.294, 2001.
- [33] N. Devroye, P. Mitran, and V. Tarokh, "*Achievable rates in cognitive radio channels*," IEEE Transactions on Information Theory, vol.52, no.5, pp.1813–1827, May 2006.
- [34] T.E. Hunter, and A. Nosratinia, "*Diversity through coded cooperation*," IEEE Transactions on Wireless Communications, vol.5, no.2, pp.283–289, Feb. 2006.

- [35] M. Janani, A. Hedayat, T.E. Hunter, and A. Nosratinia, “*Coded cooperation in wireless communications: space-time transmission and iterative decoding*,” IEEE Transactions on Signal Processing, vol.52, no.2, pp.362–371, Feb. 2004.
- [36] Bin Zhao and M. C. Valenti, “*Practical relay networks: a generalization of hybrid-ARQ*,” in IEEE Journal on Selected Areas in Communications, vol. 23, no. 1, pp. 7–18, Jan. 2005.
- [37] D.N. Nguyen, and M. Krunz, “*Cooperative MIMO in wireless networks: recent developments and challenges*,” IEEE Network, vol.27, no.4, pp. 48–54, July-Aug. 2013.
- [38] S. Shankar N, C. Chou, and M. Ghosh, “Cooperative communication MAC (CMAC) - a new MAC protocol for next generation wireless LANs,” International Conference on Wireless Networks, Communications and Mobile Computing, pp. 1–6, 2005.
- [39] A. Azgin, Y. Altunbasak, and G. AlRegib, “Cooperative MAC and routing protocols for wireless ad hoc networks,” GLOBECOM '05. IEEE Global Telecommunications Conference, 2005., St. Louis, MO, pp. 2854–2859, 2005.
- [40] S. Moh, C. Yu, S. M. Park, H. N. Kim, and J. Park, “CD-MAC: Cooperative Diversity MAC for Robust Communication in Wireless Ad Hoc Networks,” 2007 IEEE International Conference on Communications, pp. 3636–3641, Glasgow, 2007.
- [41] P. Liu, Z. Tao, S. Narayanan, T. Korakis, and S. S. Panwar, “*CoopMAC: A Cooperative MAC for Wireless LANs*,” in IEEE Journal on Selected Areas in Communications, vol. 25, no. 2, pp. 340–354, Feb. 2007.
- [42] S. Gupta, C.M. Vuran, and M.C. Gursoy, “Power efficiency of cooperative communication in wireless sensor networks,” 3rd International Conference on Signal Processing and Communication Systems, 2009. ICSPCS 2009. pp.1-10, 28–30 Sept. 2009.
- [43] Y. Chen, W. Yi, and Y. Yang, “A cross-layer strategy for energy-efficient cooperative communication in wireless sensor networks,” International Conference on Wireless Sensor Network, 2010. IET-WSN. pp.203–208, 15-17 Nov. 2010.
- [44] A. Mehrabi, and K. Kim, “*Maximizing Data Collection Throughput on a Path in Energy Harvesting Sensor Networks Using a Mobile Sink*,” in IEEE Transactions on Mobile Computing, vol. 15, no. 3, pp. 690–704, Mar. 1, 2016.
- [45] X. Ren, W. Liang, and W. Xu, “*Data Collection Maximization in Renewable Sensor Networks via Time-Slot Scheduling*,” in IEEE Transactions on Computers, vol. 64, no. 7, pp. 1870–1883, July 1, 2015.
- [46] X. Ren, and W. Liang, “Delay-tolerant data gathering in energy harvesting sensor networks with a mobile sink,” IEEE Global Communications Conference (GLOBECOM), pp. 93–99, 2012.

- [47] R. S. Liu, K. W. Fan, Z. Zheng, and P. Sinha, “*Perpetual and Fair Data Collection for Environmental Energy Harvesting Sensor Networks*,” in *IEEE/ACM Transactions on Networking*, vol. 19, no. 4, pp. 947–960, Aug. 2011.
- [48] A. B. Sadlapur, and P. V. Pushpa, “Computing optimal data collection rate for energy harvesting sensor networks,” 2013 International Conference on Advances in Computing, Communications and Informatics (ICACCI), pp. 1468–1472, Mysore, 2013.
- [49] N. Dang, M. Roshanaei, E. Bozorgzadeh, and N. Venkatasubramanian, “Adapting data quality with multihop routing for energy harvesting wireless sensor networks,” International Green Computing Conference Proceedings, pp. 1–6, Arlington, VA, 2013.
- [50] X. Wang, V. S. Rao, R. V. Prasad, and I. Niemegeers, “Choose wisely: Topology control in Energy-Harvesting wireless sensor networks,” 13th IEEE Annual Consumer Communications & Networking Conference (CCNC), pp. 1054–1059, Las Vegas, NV, 2016.
- [51] Y. Luo, J. Zhang, and K. B. Letaief, “Throughput maximization for twohop energy harvesting communication systems,” IEEE International Conference on Communications (ICC), pp. 4180–4184, Budapest, 2013.
- [52] B. Varan, and A. Yener, “Two-hop networks with energy harvesting: The (non-)impact of buffer size,” in IEEE Global Conference on Signal and Information Processing (GlobalSIP), pp.399–402, 3-5 Dec. 2013.
- [53] H. Li, N. Jaggi, and B. Sikdar, “An analytical approach towards cooperative relay scheduling under partial state information,” IEEE Proceedings INFOCOM, pp.2666–2670, 25–30 Mar. 2012.
- [54] K. H. Liu, “*Performance Analysis of Relay Selection for Cooperative Relays Based on Wireless Power Transfer With Finite Energy Storage*,” in *IEEE Transactions on Vehicular Technology*, vol. 65, no. 7, pp. 5110–5121, July 2016.
- [55] F. Wang, S. Guo, Y. Yang, and B. Xiao, “*Relay Selection and Power Allocation for Cooperative Communication Networks With Energy Harvesting*,” in *IEEE Systems Journal*, vol.PP, no.99, pp.1–12, 2016.
- [56] K. Liu, “Selection cooperation using RF energy harvesting relays with finite energy buffer,” IEEE Wireless Communications and Networking Conference (WCNC), pp.2156–2161, 6–9 Apr. 2014.
- [57] Y. Luo, J. Zhang, and K.B. Letaief, “Relay selection for energy harvesting cooperative communication systems,” in IEEE Global Communications Conference (GLOBECOM), pp.2514–2519, 9–13 Dec. 2013.
- [58] B. Medepally, and N.B. Mehta, “*Voluntary Energy Harvesting Relays and Selection in Cooperative Wireless Networks*,” *IEEE Transactions on Wireless Communications*, vol.9, no.11, pp.3543–3553, Nov. 2010.

- [59] A.A. Nasir, X. Zhou, S. Durrani, and R.A. Kennedy, “*Relaying Protocols for Wireless Energy Harvesting and Information Processing*,” IEEE Transactions on Wireless Communications, vol.12, no.7, pp.3622–3636, July 2013.
- [60] I. Krikidis, S. Timotheou, and S. Sasaki, “*RF Energy Transfer for Cooperative Networks: Data Relaying or Energy Harvesting?*,” IEEE Communications Letters, vol.16, no.11, pp.1772–1775, Nov. 2012.
- [61] M. Tacca, P. Monti, and A. Fumagalli, “*Cooperative and reliable ARQ protocols for energy harvesting wireless sensor nodes*,” IEEE Transaction on Wireless Communication, vol. 6, no. 7, pp. 2519–2529, July 2007.
- [62] C. Huang, R. Zhang, and S. Cui, “*Throughput Maximization for the Gaussian Relay Channel with Energy Harvesting Constraints*,” in IEEE Journal on Selected Areas in Communications, vol. 31, no. 8, pp. 1469–1479, Aug. 2013.
- [63] N. Ishitani, K. Kobayashi, H. Okada, and M. Katayama, “*Cooperative repeaters to improve data collection in low power generation for solarpowered wireless sensor networks*,” in 12th Annual IEEE Consumer Communications and Networking Conference (CCNC), pp.361–366, 9–12 Jan. 2015.
- [64] S. Gong, L. Duan, and N. Gautam, “*Optimal Scheduling and Beamforming in Relay Networks With Energy Harvesting Constraints*,” in IEEE Transactions on Wireless Communications, vol. 15, no. 2, pp. 1226–1238, Feb. 2016.
- [65] A. Seyedi, and B. Sikdar, “*Modeling and analysis of energy harvesting nodes in wireless sensor networks*,” 46th Annual Allerton Conference on Communication, Control, and Computing, pp.67–71, 23–26 Sept. 2008.
- [66] E. Sazonov, H. Li, D. Curry, and P. Pillay, “*Self-Powered Sensors for Monitoring of Highway Bridges*,” in IEEE Sensors Journal, vol. 9, no. 11, pp. 1422–1429, Nov. 2009.
- [67] D. H. Ha, D. Kim, J. F. Choo, and N. S. Goo, “*Energy harvesting and monitoring using bridge bearing with built-in piezoelectric material*,” The 7th International Conference on Networked Computing (INC), pp. 129–132, Gyeongsangbuk-do, 2011.
- [68] W. Liu, Z. Wang, S. Qu, and R. Luo, “*Vibration energy harvesting and management for wireless sensor networks in bridge structural monitoring*,” IEEE SENSORS, pp. 1–4, Busan, 2015.
- [69] P. Yu, J Lee, T.Q.S. Quek, and Y.-W.P. Hong, “*Energy harvesting personal cells - traffic offloading and network throughput*,” in IEEE International Conference on Communications (ICC), pp.2184–2189, 8–12 June 2015.
- [70] B. Gurakan, O. Ozel, J. Yang, and S. Ulukus, “*Energy cooperation in energy harvesting wireless communications*,” IEEE International Symposium on Information Theory Proceedings (ISIT), pp. 965–969, Cambridge, MA, 2012.

- [71] B. Gurakan, O. Kaya, and S. Ulukus, "Energy harvesting cooperative multiple access channel with data arrivals," IEEE International Conference on Communications (ICC), pp. 1–6, Kuala Lumpur, 2016.